DISSERTATIONES
MEDICINAE
UNIVERSITATIS
TARTUENSIS
241

URVE PAAVER

New perspectives for the amorphization and physical stabilization of poorly water-soluble drugs and understanding their dissolution behavior

DISSERTATIONES MEDICINAE UNIVERSITATIS TARTUENSIS
241

DISSERTATIONES MEDICINAE UNIVERSITATIS TARTUENSIS
241

URVE PAAVER

New perspectives for the amorphization and physical stabilization of poorly water-soluble drugs and understanding their dissolution behavior

UNIVERSITY OF TARTU
PRESS
1632

Department of Pharmacy, Faculty of Medicine, University of Tartu, Estonia

Dissertation is accepted for the commencement of the degree of Doctor of Philosophy (Pharmacy) on September 16, 2015 by the Council of the Faculty of Medicine, University of Tartu, Estonia

Supervisors: Senior Researcher/Associate Professor Karin Kogermann, PhD (Pharm)
Department of Pharmacy, Faculty of Medicine, University of Tartu, Estonia

Professor Jyrki Heinämäki, PhD (Pharm)
Department of Pharmacy, Faculty of Medicine, University of Tartu, Estonia

Reviewers: Professor Aleksandr Žarkovski, MD, PhD, Dr Sci
Department of Pharmacology, Institute of Biomedicine and Translational Medicine, Faculty of Medicine, University of Tartu, Estonia

Professor Ursel Soomets, PhD
Department of Biochemistry, Institute of Biomedicine and Translational Medicine, Faculty of Medicine, University of Tartu, Estonia

Opponent: Kaisa Naelapää, PhD (Pharm)
Team Lead at Novo Nordisk A/S, Copenhagen, Denmark

Commencement: November 20, 2015

Publication of this dissertation is granted by University of Tartu.
This research was supported by the European Social Fund's Doctoral studies and Internationalisation ProgrammeDoRa.

ISSN 1024-395X
ISBN 978-9949-32-970-0 (print)
ISBN 978-9949-32-971-7 (pdf)

University of Tartu Press
www.tyk.ee

CONTENTS

LIST OF ORIGINAL PUBLICATIONS

This thesis is based on the following original papers, which are referred to in the text by the Roman numerals **I–IV**.

I **Paaver, U**., Lust, A., Mirza, S., Rantanen, J., Veski, P., Heinämäki, J., Kogermann, K. Insight into the solubility and dissolution behavior of piroxicam anhydrate and monohydrate forms. *International Journal of Pharmaceutics*, 2012; 431(1–2):111–119. DOI: 10.1016/j.ijpharm.2012.04.042

II **Paaver, U.**, Heinämäki, J., Laidmäe, I., Lust, A., Kozlova, J., Sillaste, E., Kirsimäe, K., Veski, P., Kogermann, K. Electrospun nanofibers as a potential controlled-release solid dispersion system for poorly water-soluble drugs. *International Journal of Pharmaceutics*, 2015; 479(1): 252–260. DOI: 10.1016/j.ijpharm.2014.12.024

III **Paaver, U.**, Heinämäki, J., Kassamakov, I., Hæggström, E., Ylitalo, T., Nolvi, A., Kozlova, J., Laidmäe, I., Kogermann, K., Veski, P. Nanometer depth resolution in 3D topographic analysis of drug-loaded nanofibrous mats without sample preparation. *International Journal of Pharmaceutics*, 2014; 462 (1–2): 29-37. DOI: 10.1016/j.ijpharm.2013.12.041

IV **Paaver, U.**, Tamm, I., Laidmäe, I., Lust, A., Kirsimäe, K., Veski, P., Kogermann, K., Heinämäki, J. Soluplus graft copolymer: potential novel carrier polymer in electrospinning of nanofibrous drug delivery systems for wound therapy. *BioMed Research International*, 2014; 789765. DOI: 0.1155/2014/789765

Contribution of Urve Paaver to original publications (I–IV):

Publication I: Participated in planning the experiments; performed individually all solubility and dissolution tests; carried out partly the data analyses; participated in drafting the manuscript; critically checked and approved the final manuscript.

Publication II: Participated in planning the experiments; performed individually the major part of the electrospinning experiments; coordinated and performed individually solid-state analyses (Raman spectroscopy, XRPD, DSC, SEM) and dissolution tests; participated in drafting the manuscript (including figures); critically checked and submitted the final manuscript.

Publication III: Participated in planning the experiments; performed individually all electrospinning experiments; coordinated and performed solid-state analyses (SWLI, XRPD, SEM); participated in drafting the manuscript (including figures); critically checked and submitted the final manuscript.

Publication IV: Participated in planning the experiments; coordinated and performed electrospinning experiments and solid-state analyses (Raman spectroscopy, XRPD, DSC, SEM) and dissolution tests; performed partly the data analysis; participated in drafting the manuscript (including figures); critically checked and submitted the final manuscript.

LIST OF ABBREVIATIONS

3D	Three-dimensional
AFM	Atomic force microscopy
API	Active pharmaceutical ingredient
BCS	Biopharmaceutics Classification System
CCD	Charge-coupled detector
CR	Controlled-release
CR-SD	Controlled-release solid dispersion
CSD	Cambridge Structural Database
DCM	Dichloromethane
DDS	Drug delivery system
DMF	Dimethyl formamide
DMSO	Dimethyl sulfoxide
DSC	Differential scanning calorimetry
EC	Ethylcellulose
ES	Electrospinning
FESEM	Field emission scanning electron microscopy
FTIR	Fourier transform infrared spectroscopy
GI	Gastrointestinal
HFIP	1,1,1,3,3,3-hexafluoro-2-propanol
HME	Hot-melt extrusion
HPC	Hydroxypropyl cellulose
HPMC	Hydroxypropyl methylcellulose
HPMCP	Hydroxypropyl methylcellulose phthalate
LT	Low temperature
NMR	Nuclear magnetic resonance spectroscopy
PCL	Poly(caprolactone)
PCL-PVAc-PEG	Polyvinyl caprolactam-polyvinyl acetate-polyethylene glycol graft copolymer, Soluplus®
PEG	Polyethylene glycol
PEO	Poly(ethylene oxide)
PEVA	Poly(ethylene-co-vinyl acetate)
PLA	Poly(lactic acid)
PRX	Piroxicam
PRXAH	Piroxicam anhydrate
PRXMH	Piroxicam monohydrate
PVA	Poly(vinyl alcohol)
PVP	Povidone, polyvinylpyrrolidone
PVPP	Polyvinylpolypyrrolidone, crospovidone
PVPVA	Polyvinylpyrrolidone-co-vinylacetate
RT	Room temperature
SCF	Supercritical fluid
SEM	Scanning electron microscopy
SD	Solid dispersion

SLS	Sodium lauryl sulfate
Soluplus®	PCL-PVAc-PEG, polyvinyl caprolactam-polyvinyl acetate-polyethylene glycol graft copolymer
SWLI	Scanning white light interferometry
TEM	Transmission electron microscopy
TFE	2,2,2-trifluoroethanol
THF	Tetrahydrofuran
XRPD	X-ray powder diffraction

I. INTRODUCTION

Since the early 19th century, it has been discovered that many substances could be crystallized into solids having different melting points and crystal habits depending on the conditions of crystallization. The term "polymorphism" is referred to as a phenomenon where a solid substance can exist in structures characterized by different unit cell (i.e., the smallest three-dimensional volume element from which crystals can be built), and where each of the forms (polymorphs) consist of exactly the same elemental composition (Brittain, 2009). Hereby, polymorphs are different crystalline forms of the same pure chemical compound.

Today, an estimated 40% of approved drugs are poorly water-soluble and nearly 90% of developmental pipeline consist of poorly water-soluble molecules (Loftsson and Brewster, 2010). Many poorly water-soluble active pharmaceutical ingredients (APIs) can exist in different polymorphic or solvated crystal forms and also in the amorphous state. Solid-state form and the corresponding transformations of API may have a significant influence on the physicochemical, pharmaceutical and biopharmaceutical properties, e.g. solubility, dissolution rate and bioavailability of API, and this can be a serious problem to achieving the desired concentration of API in systemic circulation after administration for a pharmacological response (Brittain, 2009; Grant, 1999). The amorphous form of API has usually an enhanced dissolution and bioavailability compared to the crystalline state, but this state is the least stable form of API (Vippagunta et al., 2001). It is also well known that amorphous forms of APIs show a strong propensity to crystallize out very quickly (Lohani and Grant, 2006; Yu, 2001).

To improve the stability of amorphous form of API, there are many possibilities. One example is the development of amorphous solid dispersion (SDs) formulations. SDs are mainly two-component API-polymer binary systems. In amorphous SDs usually amorphous drug particles are dispersed in a hydrophilic carrier matrix composed of one or more polymers (Brouwers et al., 2009; Huang and Dai, 2014). SDs are very promising approach to improve the API solubility. But they have some disadvantages, since there is the possibility that during processing (mechanical stress) or storage (temperature and humidity stress), the amorphous state may recrystallize. This may result in decreased solubility and dissolution rate (Vasconcelos et al., 2007).

Electrospinning (ES) is a versatile, reproducible, continuous and scalable technology for the preparation of nanofibers from polymer solution. The major advantages of ES include (1) the capability of producing very thin fibers to the order of few tenths or hundreds nanometers with a large surface area, (2) ease of functionalization for various purposes and (3) superior mechanical properties. The wide variety of used polymers and simplicity of the process makes this technique very attractive for many different applications, including drug delivery (Agarwal et al., 2008; Rošic et al., 2012b). The ES technology combines the SD fabrication technology with the nanotechnology, and hence ES could also be a potential novel technique for stabilizing the amorphous state of API in

a mixture with different polymers. As a versatile process, ES gives us also the possibility to develop both immediate and/or controlled-release (CR) drug delivery systems for poorly water-soluble drugs (Li and Wang, 2013; Wendorff et al., 2012).

The main objectives of this thesis was to gain understanding of the amorphization and physical stabilization of a poorly water-soluble API (piroxicam as a model API), to evaluate the validity of ES as a novel technique in fabricating the high-energy amorphous solid dispersions (SDs) of a poorly water-soluble API, and to gather detailed information on the physicochemical, geometrical and dissolution properties of such nanofibrous SDs.

2. LITERATURE REVIEW

2.1. Solid-state forms

The chemists found already in the 19th century that crystals of the same substance can have different properties, and in the beginning of the 20th century (Groth, 1906–1919) published a five-volume manuscript about such crystals. More than fifty years later, McCrone (1965) and Haleblian & McCrone (1969) first pointed out the importance of polymorphism in chemistry and especially its usefulness in pharmacy.

Pharmaceutical solids (APIs and excipients) can be crystalline or amorphous. In the crystalline state, the constituent molecular units are regularly arranged into a fixed and rigid repeating array in crystal lattice, whereas the amorphous state consists of disordered arrangements of molecules and does not possess a distinguishable crystal lattice (Grant, 1999; Petit and Coquerel, 2006). Crystalline solids can exist in the form of polymorphs, solvates or hydrates. Polymorphism (Greek: *poly* = many; *morphē* = form) is characterized as the ability of an API to exist as two or more crystalline phases (polymorphs) that have different structural arrangements and/or conformations of the molecules in the crystal lattice (Bernstein, 2002; Grant, 1999). Therefore, crystalline polymorphs have the same chemical composition but different internal crystal structure, thus possessing also different physicochemical properties (Vippagunta et al., 2001). Solvates are crystalline forms that include solvent molecules in their crystal structure. If the incorporated solvent is water, then solvates are called as hydrates (Morris, 1999). Solvates and hydrates are also referred as pseudopolymorphs (Bernstein, 2002; Griesser, 2006; Morris, 1999), and more recently also a new term "solvatomorph" has been proposed (Brittain, 2012; Brittain et al., 2009; Seddon, 2004).

Today, we know that polymorphism is very common among APIs, and it is estimated that approximately one-third of organic compounds and about 80% of marketed APIs exhibit polymorphism under experimentally accessible conditions (Lohani and Grant, 2006). Stahli (2007) concluded in his review on polymorphs and co-crystals, that 80–90% of organic compounds can exist in multiple crystalline forms (polymorphs, hydrates, solvates).

Since polymorphs have different internal structure and free energies, they have different physicochemical properties like melting point, solubility, dissolution rate, etc., and those properties can lead to differences in the bioavailability and stability (Grant, 1999). Very often only one polymorph has the lowest free energy and it is thermodynamically the most stable form. The other forms are less stable (also called as metastable forms) and they have a tendency to reduce their free energy by transforming into the stable form, and this can affect the biopharmaceutical performance of the solid dosage form (Grant, 1999; Lohani and Grant, 2006). A well-known example is the case of ritonavir, where the formation (precipitation) of a more stable form resulted in the dissolution test failures of a semisolid formulation (Chemburkar et al., 2000). Sometimes,

however, it is desirable to use a metastable form of an API due to its special properties, such as higher bioavailability, better technological behavior during grinding and compression, or lower hygroscopicity (Lohani and Grant, 2006).

2.2. Amorphous state

The amorphous solid, defined as non-crystalline solid, has a special status in the pharmaceutical drug development, and in the earlier literature it has been considered as one polymorphic form (Haleblian and McCrone, 1969; Petit and Coquerel, 2006). Amorphous state, however, significantly differs from a crystalline state, and thus it is currently classified as a distinct solid-state form. Solid materials can exist intrinsically in the amorphous state or they may be intentionally made amorphous by physical manipulation. The amorphous state lacks a definite three-dimensional long-range order, which is characteristic to a crystalline material, and the position of molecules relative to one another is more random (like in the liquid state). Amorphous solids exhibit typically short-range order over a few molecular dimensions, and consequently, they have quite different physical properties from those of their corresponding crystalline states (Hancock and Zografi, 1997). The importance of amorphous pharmaceutical solids lies in their pharmaceutically useful properties like higher apparent solubility, higher dissolution rate, and sometimes better compression characteristics than the corresponding crystal form. The amorphous solids can be produced by standard pharmaceutical processes, including melt quenching, freeze- and spray-drying, milling, wet granulation, and drying of solvated crystals (Yu, 2001). By using these methods, the amorphous solids produced are generally physically and chemically less stable than the corresponding crystal form of the API (Yu, 2001). Some APIs and excipients are known only or mainly in amorphous form, while others require deliberate prevention of recrystallization to enter and remain in the amorphous state (Petit and Coquerel, 2006).

2.3. Solid-state phase transformations

As discussed previously, the solid-state phase transformations may result in the most stable form with lowest free energy. The solid-state phase transformations including solvated and hydrated phases of APIs may also have a profound impact on the physicochemical, pharmaceutical and biopharmaceutical properties, such as solubility, dissolution rate, chemical stability and bioavailability of API. Since oral bioavailability of many poorly water-soluble APIs depend upon solubility and dissolution rate, the identification and detection of such transformations between polymorphic and/or solvate forms of APIs in bulk state and pharmaceutical formulations, are important (Brouwers et al., 2009; Zimmermann et al., 2009). Several recent reports provide evidence that unexpected solvent-mediated transformations of APIs may be induced especially

during the wet manufacture of pharmaceuticals (Airaksinen et al., 2005; Jørgensen et al., 2002; Savolainen et al., 2009; Zhang et al., 2004). Similarly, during manufacturing process-induced transformations and related precipitation of API may change the expected outcome (Airaksinen et al., 2005; Zimmermann et al., 2009). Furthermore, it has been reported that during dissolution testing the solid-state conversion of APIs (e.g. hydrate formation) may occur and this can be the reason for the misinterpretation of the results (Aaltonen et al., 2006; Koradia et al., 2011).

2.4. Piroxicam and its solid-state forms

Piroxicam (PRX) is a non-steroidal anti-inflammatory drug (NSAID) of the oxicam class that inhibits prostaglandin synthesis. It is widely used to relieve the symptoms of painful, inflammatory conditions like arthritis (Martindale, 2011). Chemically PRX is 4-hydroxy-2-methyl-*N*-(pyridin-2-yl)-2*H*-1,2-benzothiazine-3-carboxamide 1,1-dioxide (**Figure 1**). It is practically insoluble in water, soluble in methylene chloride, slightly soluble in anhydrous ethanol (PhEur, 2015b).

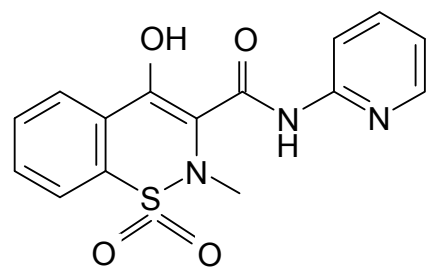

Figure 1. Chemical structure of piroxicam (PRX). Modified from the European Pharmacopoeia 8.0 (PhEur, 2015b).

PRX molecule can exist in different solid-state forms and its polymorphs are well documented in the literature (Kogermann et al., 2007; Naelapää et al., 2012; Nyström et al., 2015; Reck et al., 1988; Sheth et al., 2004a; Vrečer et al., 1991; Vrečer et al., 2003). PRX is a well-known API that has extensively been used as a model substance due its interesting physicochemical properties. PRX is classified as a class II drug in Biopharmaceutics Classification System (BCS) due to its low aqueous solubility and high permeability (Amidon et al., 1995; Gwak et al., 2005; Lombardino and Lowe, 2004). It has a zwitterionic nature and it is known to have two pK_a values (1.86 and 5.46) (Jinno et al., 2000), which contribute to PRX behavior at different pHs (Banerjee et al., 2003). Some studies consider PRX as a weak acid with a pK_a value 5.3 (Okuyama et al., 1999). The degree to which PRX is ionized depends largely on the pH of the

medium. At pH 1.2 PRX exists as a cation and acts as an acid. At pH 5.6 and 7.2 PRX is in a neutral/zwitterionic form and can act as an acid or as a base in a solution. This behavior is obviously due to its oppositely charged -NH_2 and -COOH groups which possesses a large intramolecular multipole moment (Banerjee et al., 2003; Gwak et al., 2005; Jinno et al., 2000). Interestingly, the PRX crystalline forms have also color differences, and hence its structural solid-state changes are easily observed. PRX anhydrate form I (PRXAH) exists as colorless single crystals irrespective of the polymorphic forms. The amorphous form is pale yellow and PRX monohydrate (PRXMH) crystals have rich yellow color (Sheth et al., 2005; Vrečer et al., 1991; Vrečer et al., 2003).

2.5. Solid dispersions

2.5.1. Definition

Today, in pharmaceutical technology the term 'solid dispersion' (SD) is often used to describe all systems in which an API is dispersed in an inert excipient carrier. These systems include also solid solutions where the API exists as a molecular dispersion with no discernible second phase (Miller et al., 2008). The API in SD can be dispersed as separate molecules, amorphous particles, or crystalline particles in the carrier which can be in the amorphous or crystalline state (Miller et al., 2008; Vasconcelos et al., 2007; Vo et al., 2013).

2.5.2. Advantages and disadvantages of solid dispersions in formulating poorly water-soluble drugs

Formulation of SDs is very fruitful approach in improving the release rate and oral bioavailability of poorly water-soluble APIs (Brouwers et al., 2009; Janssens and Van den Mooter, 2009). The first description of SD was published in 1961 by Sekiguchi and Obi, who reported the formation of a solid solute (molecularly dispersed API in a solid solvent). The authors proposed the formation of a eutectic mixture of a poorly water-soluble API and easily water-soluble biologically inert carrier. The eutectic mixture was prepared by melting the physical mixture of the API and carrier, followed by a rapid solidification process. More recently, the eutectic mixtures have been reported to significantly improve the solubility of poorly water-soluble APIs and they have shown an enhanced absorption after oral administration (Sekiguchi and Obi, 1961; Sekiguchi et al., 1964; Serajuddin, 1999; Vasconcelos et al., 2007). The present SD systems are defined in the literature as "the dispersion of one or more active ingredients in an inert carrier matrix at solid state prepared by melting (fusion), solvent, or melting-solvent method"(Chiou and Riegelman, 1971).

The advantages of SDs include reduced particle size (even at the molecular level), enhanced wettability and porosity, and changes in API crystalline state (vitrification to an amorphous state) (Leuner and Dressman, 2000; Vo et al., 2013). The major limitations of SDs are related to the physical stability of API

in SDs and batch variability in manufacturing. During manufacturing process or storage, the amorphous state may recrystallize to different crystal forms. Moreover, the effect of moisture can affect the stability of SD, because most of the polymers used as excipients are hygroscopic and absorb moisture. This in turn may result in a phase separation, crystal growth, conversion from the amorphous to the crystalline state, or conversion of a metastable crystalline form to a more stable form during storage (Chiou and Riegelman, 1971; Prasad et al., 2014; Serajuddin, 1999; Vasconcelos et al., 2007; Wang et al., 2005).

2.5.3. Types of solid dispersions and carrier polymers

Previously, pharmaceutical SDs were produced only by solvent evaporation or melt processing methods, but nowadays supercritical fluid and cryogenic freezing technologies have also been demonstrated to be applicable for fabricating the SDs (Miller et al., 2008; Serajuddin, 1999; Vo et al., 2013). The physical state of the SD will depend on the physicochemical properties of the carrier and API, the API-carrier interactions and the preparation method (Janssens and Van den Mooter, 2009). The first classification system based on the possible physical state of pharmaceutical SDs was introduced by Chiou and Riegelman (1971). Depending on the physical state of the carrier material, the SDs are divided into crystalline SDs and amorphous SDs. The SDs have also been classified into four generations based on their composition (**Figure 2**) (Chiou and Riegelman, 1971; Vo et al., 2013).

Usually the term SD refers to a group of solid products consisting of at least two different components, generally a hydrophilic matrix and a hydrophobic drug. *The first generation* of SDs introduced were eutectic mixtures (also called crystalline SDs), where the crystalline API particles were dispersed in the crystalline matrix (Chiou and Riegelman, 1971; Dhirendra et al., 2009; Sekiguchi and Obi, 1961; Vo et al., 2013). The API in crystalline SD may also exist as amorphous particles or separate molecules (crystalline solid solutions), where the drug molecules can replace the carrier molecule in the crystal lattice (substitutional crystalline solid solutions) or occupy the interstitial spaces between the solvent molecules in the crystal lattice (interstitial crystalline solid solutions) (Chiou and Riegelman, 1971; Leuner and Dressman, 2000; Sekiguchi and Obi, 1961). Crystalline carriers in the 1st generation of SDs comprise of urea (Sekiguchi and Obi, 1961) and sugars as sorbitol and mannitol (Jachowicz, 1987).

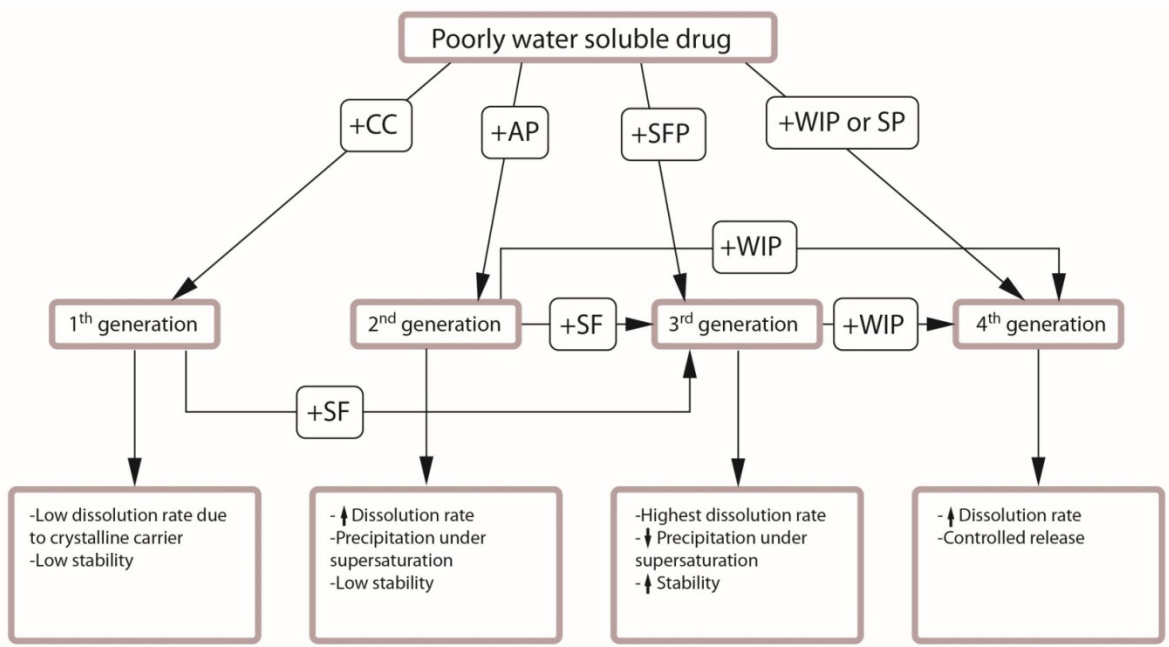

Figure 2. Composition and properties of four generations of SDs. Key: CC = crystalline carrier, AP = amorphous polymer, SFP = surfactant polymer, WIP = water-insoluble polymer, SP = swellable polymer, SF = surfactant, (↑) = increase, (↓) = decrease Modified from Vo et al, 2013.

The second generation of SDs contains amorphous carriers which are mostly polymers (Vo et al., 2013). Amorphous SDs can be classified into fully amorphous solid solutions (glass solutions) and fully amorphous solid suspensions, or combination of these two depending on the physical state of the API (van Drooge et al., 2006). In amorphous solid solution, the API and amorphous carrier are homogeneously dispersed at a molecular level, while amorphous solid suspension consists of two separate phases. Amorphous solid suspensions are formed when the API has limited carrier solubility or a very high melting point. Which one of these two types is obtained depends on the miscibility of API and carrier material and on the preparation method (Chiou and Riegelman, 1971; van Drooge et al., 2006). For formulating the second generation SDs, there are available a great number of different amorphous carrier polymers. They can be divided into full synthetic polymers as povidone or polyvinylpyrrolidone (PVP), polyethylene glycol (PEG), crospovidone (PVPP), polyvinylpyrrolidone-co-vinylacetate (PVPVA) and polymethacrylates, and natural-origin polymers like different cellulose derivatives, starches (potato or corn starch) and sugars (trehalose, sucrose, inulin). Most widely used natural-origin polymers are hydroxypropyl methylcellulose (HPMC), hydroxypropyl cellulose (HPC) and hydroxypropyl methylcellulose phthalate (HPMCP) (van Drooge et al., 2004; Vasconcelos et al., 2007; Vo et al., 2013).

The third generation of SDs contains a surfactant carrier, or a mixture of amorphous polymers and surfactants as carriers (Vo et al., 2013). These SDs are intended to achieve the highest degree of bioavailability for poorly water-soluble drugs, and they avoid such problems as drug precipitation and recrystallization, thus stabilizing the SD (Chiou and Riegelman, 1971; Craig, 2002; Janssens et al., 2007; Karatas et al., 2005; Van den Mooter et al., 2006). The inclusion of surfactants in the formulation with polymeric carrier may help to prevent the precipitation of an API after dissolution *in vivo* and/or protect a fine precipitate from agglomeration into much larger hydrophobic particles (de Waard et al., 2008; Karavas et al., 2007; Pouton, 2006; Yüksel et al., 2003). A lot of different surfactants and emulsifiers are used as additives in the third generation SDs. The most commonly used surfactants and carriers with surface activity are sodium lauryl sulfate (SLS), polysorbates (such as Tween 80 and Tween 20), poloxamers (Brouwers et al., 2009; Vo et al., 2013), cholic acid, bile salts, cholesterol esters and lecithin (Leuner and Dressman, 2000). Recently, Soluplus® graft copolymer has been also shown to be applicable in formulating the third generation SDs (Hughey et al., 2013; Nagy et al., 2012).

The fourth generation of SDs is the recently introduced group of controlled release solid dispersions (CR-SD). Thus, the present SDs are applicable in formulating the poorly water-soluble APIs with a short biological half-life, and they can enhance the solubility of poorly water-soluble drugs and extend the drug release in a controlled manner. The polymers used in CR-SDs are insoluble or dissolve very slowly in water. The conventional polymers applicable in formulating CR-SDs are e.g. ethylcellulose (EC), HPC, some Eudragit®

grades, poly(ethylene oxide) (PEO) and carboxyvinylpolymer (Carbopol®) (Tran et al., 2011; Vo et al., 2013).

2.5.4. Preparation of solid dispersions

All established fabrication methods of SDs are based on two major physical processes – on melting and solvent evaporation.

Melting method

The melting or fusion method was first used by Sekiguchi and Obi (1961) to prepare fast-release SD simple eutectic mixtures. This method is based on melting the API within the carrier above the eutectic point followed by cooling and pulverization of the obtained product (Sekiguchi and Obi, 1961). Cooling leads to supersaturation, but due to solidification the dispersed API becomes trapped within the carrier matrix. The process has an effect on the final dispersion, and for example the cooling rate and proportion of the drug and carrier influence the formation of molecular dispersion (Chiou and Riegelman, 1971; Leuner and Dressman, 2000; Sekiguchi et al., 1964). Different cooling and solidifying methods of melted mixture are described and used in the literature. These processes include, e.g. ice bath agitation (Pokharkar et al., 2006; Sekiguchi et al., 1964; Yoshioka et al., 1994), stainless steel thin layer spreading followed by a cold draught (Chiou and Riegelman, 1969), solidification on petri dishes at room temperature inside a desiccator (Owusu-Ababio et al., 1998; Verheyen et al., 2002), spreading on plates placed over dry ice (Timko and Lordi, 1979), immersion in liquid nitrogen (Yao et al., 2005) and storage in a desiccator (Law et al., 2003; Vippagunta et al., 2007).

One major limitation of melting method is the application of high temperatures, and consequently, many APIs or carrier materials can be degraded by the melting process (Serajuddin, 1999). Another challenge associated with a melting method is the incomplete miscibility of API and carrier polymer in a molten state to obtain a homogenous mixture (Taylor and Zografi, 1997). To avoid the present limitations, some modifications have been introduced to the original method. In recent years, a hot-melt extrusion (HME) has become a common method for fabricating the SDs, since it is a continuous process, thus making it suitable for large-scale production (Crowley et al., 2007; Leuner and Dressman, 2000; Repka et al., 2007; Shah et al., 2013; Vasconcelos et al., 2007; Vo et al., 2013). By HME the API-carrier mixture is simultaneously melted, homogenized, extruded and subsequently shaped for different purposes. An important advantage of a HME method over the other melting methods is the low residence time of the API and carrier at melting temperature in the extruder which reduces the risk of the degradation of thermally labile APIs (Leuner and Dressman, 2000).

The other technologies based on the melting process are melt agglomeration (Seo et al., 2003; Vilhelmsen et al., 2005) and patented Meltrex™ SD manu-

facturing process, where a special twin screw extruder with two independent hoppers (in which the temperature can vary over a broad temperature range), is used (Vasconcelos et al., 2007; Vo et al., 2013; Vynckier et al., 2014). One promising alternative for processing thermolabile APIs is also hot-spin melting, where the API and carrier are melted together over an extremely short time in a high speed mixer and simultaneously in the same apparatus, dispersed in air or an inert gas in a cooling tower (Leuner and Dressman, 2000; Vo et al., 2013).

Solvent evaporation method

A solvent evaporation method consists of the solubilization of the API and carrier in a volatile solvent that is later evaporated (Chiou and Riegelman, 1971). Usually, the resulting films are pulverized and milled. In this method, the main advantage is that the thermal decomposition of APIs or carriers can be prevented, since organic solvent evaporation occurs at low temperature (Leuner and Dressman, 2000; Paudel et al., 2013; Vo et al., 2013). The main disadvantages of this method are mostly connected with the solvent – the price, the difficulty of completely removing liquid solvent, the possibility of drug-solvent chemical interactions and the difficulty of reproducing crystal forms of drugs (Brough and Williams, 2013; Leuner and Dressman, 2000; Paudel et al., 2013; Serajuddin, 1999; Vo et al., 2013).

Tachibana and Nakamura (1965) were the first to dissolve both an API and carrier in a joint solvent and then evaporate the solvent under vacuum that enabled them to produce a solid solution of highly lipophilic β-carotene in PVP. The evaporation method was further developed by Mayersohn and Gibaldi (1966). They dissolved griseofulvin and PVP in chloroform, evaporated the solvent, and then collected the SD with enhanced dissolution, up to 11 times compared to the micronized drug (Mayersohn and Gibaldi, 1966). The term "co-precipitate" for the abovementioned SDs was first used by Bates (1969). For details, how the solvent evaporation process was further developed and why the term "co-precipitate" was later replaced by the term "co-evaporate", see Leuner and Dressman (2000) and some other review articles (Brouwers et al., 2009; Chiou and Riegelman, 1971; Dhirendra et al., 2009; Huang and Dai, 2014; Leuner and Dressman, 2000; Tran et al., 2011; Vasconcelos et al., 2007; Vo et al., 2013).

Today, spray-drying and freeze-drying (lyophilization) are the most commonly used solvent evaporation methods. The first use of product drying in an atomized liquid stream was described in the patent of Percy in 1872 (Paudel et al., 2013). Afterwards the method has been greatly developed. Today, spray-drying involves a solvent evaporation usually by vacuum drying (Karavas et al., 2006; Wagenaar and Müller, 1994; Wang et al., 2005) or spraying the API-carrier-solvent mixture into a stream of heated air flow to remove the solvent (Karavas et al., 2006; Van den Mooter et al., 2006). An alternative method for preparing SDs is to spray an API-carrier-solvent mixture into liquid nitrogen to form a suspension, and the suspension is then lyophilized (Costantino et al., 2002; Leuenberger, 2002; van Drooge et al., 2006). Recently, Paudel et al.

(2013) published an excellent overview about the background and developments of spray drying process.

The basic freeze-drying (lyophilization) process for preparing SDs consists of dissolving the API and carrier in a joint solvent and immersing the mixture in liquid nitrogen until it is completely frozen. The frozen solution is subsequently lyophilized (van Drooge et al., 2006).

Supercritical fluid (SCF) technology provides an interesting new alternative for formulating the SDs of poorly water-soluble APIs. In the SCF, supercritical carbon dioxide is commonly used as a solvent (Muhrer et al., 2006; Sethia and Squillante, 2002) or anti-solvent (Palakodaty and York, 1999; Won et al., 2005; Wu et al., 2009). The use of supercritical carbon dioxide has many advantages since the solvent system is chemically inert, non-toxic and non-flammable. Furthermore, the process temperature and pressure can be kept low, which makes it an attractive for processing heat labile pharmaceuticals (Won et al., 2005).

The electrospinning (ES) technology combines the SD fabrication technology with the nanotechnology. In ES process an API-carrier (usually a polymer) solution is pumped through an orifice and then subjected to an electrical field. When electrical forces overcome the surface tension of the API-polymer solution at the air interface, the fibers with a diameter of micron-, submicron- or nanoscale are formed. The fiber diameter can be adjusted by the surface tension, electrical field, dielectric constant, feeding rate and electric field strength. After rapid evaporation of the solvent, fibers are collected onto a collector plate/ cylinder, and they can be directly used or milled and further processed (Agarwal et al., 2008; Brewster et al., 2004; Rošic et al., 2012b; Sethia and Squillante, 2002; Verreck et al., 2003b). A wide selection of polymers applicable in ES, gives the possibility to fabricate SDs with different properties, e.g. water-soluble polymers for formulating the immediate release dosage forms and water insoluble (biodegradable or non-biodegradable) polymers for controlled release applications (Brouwers et al., 2009).

2.5.5. Characterization of solid dispersions

Many powerful analytical methods are available to characterize the physical solid-state properties, stability and performance of pharmaceutical SDs (Chiou and Riegelman, 1971). The most widely used methods are differential scanning calorimetry (DSC), X-ray powder diffraction (XRPD), Fourier transform infrared spectroscopy (FTIR), scanning electron microscopy (SEM) and the test methods on the release rate of the API (dissolution test) (Chiou and Riegelman, 1971; Leuner and Dressman, 2000; Vo et al., 2013). The other methods are hot stage microscopy, polarization microscopy, the variety of spectroscopic methods, like Raman spectroscopy, etc. However, at least a combination of two or more methods is recommended to study the physical structure correctly (Leuner and Dressman, 2000; Vippagunta et al., 2001). For more details about the analytical methods used for the characterization of pharmaceutical SDs, see the review of Leuner & Dressman (2000).

2.6. Electrospinning

2.6.1. Electrospinning as a method for the fabrication of nanofibers

ES is a rapid and versatile technique to fabricate polymeric nanofibers with a diameter of some tenths nanometers or submicron level and with a large surface to volume ratio (Agarwal et al., 2008; Brewster et al., 2004; Verreck et al., 2003a). The process of ES, also termed as electrostatic spinning, was first introduced by Zeleny in 1914. Later, Formhals introduced many new developments in the ES process and obtained several patents in the 1930's and 1940's (Formhals, 1934, 1939, 1943, 1944). Since then, the ES apparatus and understanding of the process have developed quickly due to the research interest and the potential applications of these nanofibers in various areas. History of the key developments and scientists in brief: Simons patented an apparatus for the production of ultrathin nonwoven fabrics (Simons, 1966), Taylor studied the jet produced from the droplet of a polymer solution (Taylor, 1964, 1969) and Baumgarten (1971) demonstrated that the fiber diameter and the concentration of the solution are directly proportional. Several reviews (Garg and Bowlin, 2011; Hu et al., 2014; Huang et al., 2003; Ignatious et al., 2010; Persano et al., 2013; Schiffman and Schauer, 2008) and books (Li and Wang, 2013; Wendorff et al., 2012) describe the history and developments of ES in details.

The basic idea of ES is that the ultrafine fibers are generated by application of a strong electric field between the droplet of solvated or melted polymer and a grounded target. When the high electrostatic voltage is applied on a drop of polymer solution held by its surface tension at the end of a capillary, then the surface of the liquid distends into a hyperbolic cone known as the Taylor cone (Taylor, 1964, 1969). Once the voltage applied to the spinneret exceeds a critical value (often between 0–30 kV), the electrostatic force overcomes a solution surface tension and the thin jet of solution is drawn from the droplet and whips out towards the grounded collector. Before reaching the collector, the liquid jet elongates, solvent evaporates and ultrafine polymeric fibers are formed and collected on the target (Agarwal et al., 2008; Garg and Bowlin, 2011; Hu et al., 2014; Rošic et al., 2012b; Taylor, 1964; Yu et al., 2009). A schematic setup of the ES process is shown in **Figure 3**.

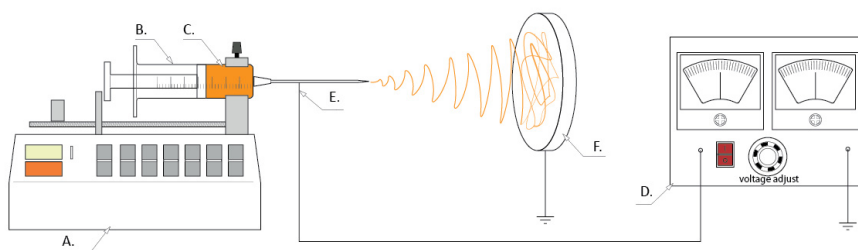

Figure 3. Schematic diagram of an electrospinning setup. Key: A. syringe pump; B. syringe; C. polymer solution; D. high-voltage power supply; E. electrode; F. grounded collector (the figure from the original publication **II**).

2.6.2. Parameters affecting the electrospinning and formation of nanofibers

According to the literature, many parameters can influence the transformation of polymer solutions into nanofibers in the ES process (Bhardwaj and Kundu, 2010; Brewster et al., 2004; Huang et al., 2003; Mit-uppatham et al., 2004; Pelipenko et al., 2012; Rošic et al., 2012a; Rošic et al., 2012b). The parameters can be divided into three different classes: (1) solution-related parameters, (2) process parameters, and (3) ambient parameters. The most important solution properties include e.g. concentration, viscosity, conductivity/ surface charge density, surface tension, molecular weight of polymer, volatility of solvent, and dielectric constant. The major process parameters affecting ES are the applied voltage, feed rate/flow rate, and the distance between a needle tip and collector. The ambient parameters include e.g. humidity and temperature. For details about the critical parameters affecting ES, see the abovementioned references.

2.6.3. Polymers and solvents used for electrospinning

There are hundreds of synthetic and natural polymers that have been processed into nanofibers by ES (Agarwal et al., 2008; Bhardwaj and Kundu, 2010; Chew et al., 2006; Huang et al., 2003; Wendorff et al., 2012). If the ES process conditions and solvent are properly selected (i.e. voltage, distance between the electrodes, flow rate of solution, viscosity, conductivity) virtually all polymers can be electrospun (Agarwal et al., 2008). According to Huang et al. (2003), there are about 44 polymers and solvent systems described in the literature for ES, and additionally 6 melted polymers. The applications for these systems cover e.g. protective clothings, sensors, filters, membranes for the prevention of surface-induced adhesion, conductive fibers, optical sensors, cosmetic uses and medical uses – for wound healing, tissue engineering, hemostatic agents, implantable devices, biomaterial scaffolds and drug delivery systems (DDS) (Huang et al., 2003). Agarwal et al. (2008) described in their review the ES of nanofibers used for biomedical applications – for tissue engineering and DDS applications. To our best knowledge, however, no marketed DDS products are available to date based on nanofibers. Electrospun pharmaceutical nanofibrous dosage forms may be designed to provide rapid, immediate, delayed, sustained or by other way modified dissolution.

The selection of a carrier polymer for ES is crucial since the type of polymer and API-polymer-solvent interactions influence the formation, morphology, mechanical properties and drug release of nanofibrous mat (Bhardwaj and Kundu, 2010; Chronakis, 2005; Huang et al., 2003; Ignatious et al., 2010; Li and Xia, 2004; Teo and Ramakrishna, 2006). For wound healing, natural polymers like chitosan (Bhattarai et al., 2005; Geng et al., 2005; Jayakumar et al., 2010), silk and silk like polymers (Min et al., 2004; Ohgo et al., 2003), collagen, gelatin, elastin and cellulose derivatives (Chew et al., 2006; Wendorff et al., 2012; Zahedi et al., 2010) are preferred. They are commonly blended with

polysynthetic or synthetic polymers, especially with PEO and poly(caprolactone) (PCL) (Chew et al., 2006; Huang et al., 2003). In pharmaceutical development, more suitable polymers for ES would be cellulose derivatives like HPMC, EC, HPC etc., PVP, poly(ethylene-co-vinyl acetate) (PEVA), polyvinyl alcohol (PVA), poly(lactic acid) (PLA), PCL and chitosan (Chew et al., 2006; Huang et al., 2003; Li and Xia, 2004; Teo and Ramakrishna, 2006).

In addition, solvent or solvent system plays a crucial role in fiber formation in an ES process. The solution is spinnable when the solubility of polymer or polymer blend in solvent is optimal. The polymer concentration influences both the viscosity and surface tension of the solution. Important factors are also solvent volatility and solvent conductivity (Sill and von Recum, 2008). The frequently used solvents for nanofiber preparation are chloroform, dichloromethane (DCM), tetrahydrofuran (THF), 2,2,2-trifluoroethanol (TFE), 1,1,1,3,3,3-hexafluoro-2-propanol (HFIP), dimethyl formamide (DMF), dimethyl sulfoxide (DMSO), ethanol, methanol, acetone, acetic acid and distilled water (Bhardwaj and Kundu, 2010; Huang et al., 2003; Kenawy el et al., 2002; Rošic et al., 2012b; Sill and von Recum, 2008; Zahedi et al., 2010). Although distilled water would be a favorable solvent for fabricating nanofibers intended for biomedical and pharmaceutical applications, the polymer solubility often limits the use of it. The addition of a volatile organic solvent increases the solvent evaporation rate and decreases the distance needed between ES needle and collector (Rošic et al., 2012b).

Hydroxypropyl methylcellulose

HPMC or Hypromellose (**Figure 4**) is chemically cellulose hydroxypropyl methyl ether [partly O-methylated and O-(2-hydroxypropylated) cellulose] (PhEur, 2015a) and the variety of different synonyms and trademark names are known like *Benecel MHPC, Methocel, Metolose, Pharmacoat, Tylopur, Tylose MO,* etc. (Rogers, 2009). HPMC is available in several grades that vary in viscosity (2% w/w aqueous solution at 20 °C) and extent of substitution. HPMC is an odorless and tasteless, white or creamy-white fibrous or granular powder with the molecular weight from approximately 10,000 to 1,500,000 Da. It is soluble in cold water giving a colloid solution, and practically insoluble in hot water, acetone, anhydrous ethanol and toluene (PhEur, 2015a; Rogers, 2009). HPMC is widely used in oral, ophthalmic, nasal, and topical pharmaceutical formulations. Depending on the viscosity grade and concentration, HPMC is applicable in formulating the sustained or controlled-release drug products (Dow, 2015b; Leuner and Dressman, 2000; Paudel et al., 2013). Electrospun nanostructures based on cellulose derivatives are potential candidates for several applications within the field of pharmaceuticals and as drug delivery vehicles (Frenot et al., 2007). Verreck et al. (2003) reported on the applications of ES for formulating the nanofibrous DDS of HPMC and poorly water-soluble API, itraconazole. The rate of drug release from the nanofibers was found to be dependent on the API-to-polymer ratio and fiber diameter (Brewster et al., 2004; Verreck et al., 2003a).

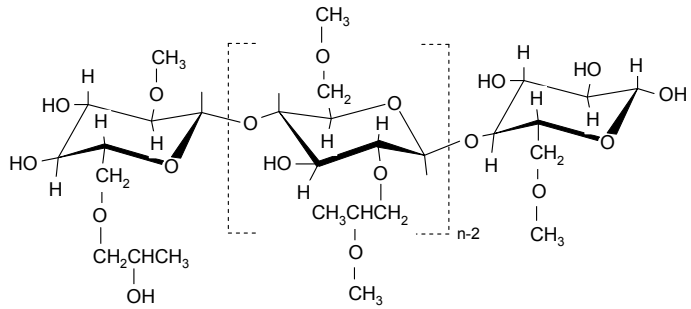

Figure 4. Chemical structure of hydroxypropyl methylcellulose (HPMC). Modified from Dow Product Leaflet, 2015 (Dow, 2015a).

Polyvinyl caprolactam – polyvinyl acetate - polyethylene glycol graft copolymer (Soluplus®)

Soluplus® (PCL-PVAc-PEG graft copolymer) (**Figure 5**) is a new pharmaceutical excipient with an amphiphilic chemical structure, and originally it was designed for preparing the solid solutions of poorly water-soluble APIs by HME technology (Basf, 2010). Soluplus® is a water-soluble copolymer with the average molecular weight ranging from 90,000 to 140,000 Da. It is capable to solubilize poorly water-soluble APIs in aqueous media, and to improve significantly the bioavailability of these APIs (Basf, 2010; Hardung et al., 2010). It has also been used as a binder in wet and dry granulation (Basf, 2010). So far, the use of Soluplus® in ES has been very limited, and only little information is available in the literature. Nagy et al. (2012) compared electrospun and extruded Soluplus®-based oral solid dosage forms for improving the dissolution of a poorly water-soluble APIs. More recently, Stranska et al. patented a new process of manufacturing of drug products using ES technology, and this approach included also Soluplus® graft copolymer combined with *Ticagrelor*, *Telaprevir* or *Aprepitant* as poorly water-soluble APIs to obtain the DDSs with an amorphous API (Stranska et al., 2014).

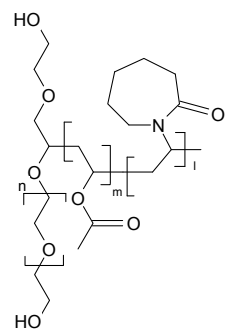

Figure 5. Chemical structure of Soluplus® (polyvinyl caprolactam - polyvinyl acetate - polyethylene glycol graft copolymer, PCL-PVAc-PEG) (**IV**).

2.6.4. Characterization of electrospun nanofibers

The determination of nanofiber morphology and geometric properties such as fiber diameter, diameter distribution, fiber orientation, have been performed with different microscopic techniques and instruments such as SEM, field emission scanning electron microscopy (FESEM), transmission electron microscopy (TEM) and atomic force microscopy (AFM) (Chung et al., 2009; Ding et al., 2002; Huang et al., 2003; Li et al., 2002; Megelski et al., 2002; Pelipenko et al., 2013; Srinivasan and Reneker, 1995; Taepaiboon et al., 2006; Tan and Lim, 2005). There are some problems especially to determine the geometric properties of single nanofibers and the porosity of nanofibrous mats because of the small size and random orientation of the individual fibers. Recently, Janković et al. (2013) evaluated successfully the morphology and mechanical properties of single electrospun nanofibers by means of AFM. The nanofibers were intended for the specific tissue scaffold applications (Janković et al., 2013). Some of the polymer nanofibers, however, are challenging to characterize with respect to their mechanical and geometric properties since mechanical contact or thermal mismatch may lead to the permanent deformation of the fibers (Jayaraman et al., 2004; Naraghi et al., 2007; Tan and Lim, 2006).

The physicochemical characterization of polymeric nanofibers at a molecular level can be performed by FTIR and nuclear magnetic resonance (NMR) spectroscopy techniques (Huang et al., 2003). For solid-state characterization, thermoanalytical methods (such as DSC), XRPD, vibrational spectroscopy (FTIR, Raman), and SEM are known as the most important methods (Brewster et al., 2004; Garg and Bowlin, 2011; Huang et al., 2003; Ignatious et al., 2010; Jannesari et al., 2011; Kenawy et al., 2009; Kenawy el et al., 2002; Nagy et al., 2012; Verreck et al., 2003a).

3. AIMS OF THE STUDY

The overall goal of this thesis was to gain understanding of the amorphization and physical stabilization and dissolution behavior of poorly water-soluble piroxicam (PRX) and its corresponding solid dispersions (SDs) fabricated by means of electrospinning (ES).

The specific aims were:

- to evaluate the validity of ES as a novel technique for preparing high-energy amorphous SDs of a poorly water-soluble drug PRX, and for fabricating the CR-SD nanofibers of PRX and hydrophilic carrier polymers (**II, IV**)
- to evaluate the validity of scanning white light interferometry (SWLI) as a potential novel method for rapid, non-contacting and non-destructive three-dimensional (3D) topographic analysis of electrospun drug-loaded nanofibrous mats without sample preparation (**III**)
- to reveal the effects of hydrophilic carrier polymers, especially a new synthetic graft copolymer PCL-PVAc-PEG (Soluplus®) and solvent systems to the solid-state properties and physical stability of drug-loaded nanofiber systems (**II, IV**)
- to gain understanding of the effect of pH on the solubility and dissolution rate of two solid-state forms of PRX [anhydrate (PRXAH) and monohydrate (PRXMH), respectively] (**I**)
- to gain understanding of the drug release and dissolution behavior of poorly water-soluble PRX from electrospun polymeric nanofibrous mats (**II, IV**)

4. MATERIALS AND METHODS

A more detailed description of materials and methods is given in the original publications which are referred to by their respective Roman numerals (**I–IV**).

4.1. Materials

4.1.1. Raw materials (I–IV)

Piroxicam (anhydrous PRX form I, PRXAH I, Letco Medical, Inc. USA) was used for dissolution experiments and as a poorly water-soluble model drug in electrospun nanofibers (**I–IV**). The carrier polymers used in nanofibers were hydroxypropyl methylcellulose (HPMC) Methocel™ K100M premium CR kindly gifted from The Dow Chemical Company, USA (**II**) or from Colorcon Ltd, U.K. (**III**), and Soluplus® (PCL-PVAc-PEG) kindly gifted from BASF SE Pharma Ingredients & Services, Germany (**III, IV**).

The primary solvents applied in the ES studies were methanol (Sigma-Aldrich C.C., Inc.) ethanol, acetone, 2-propanol and dichloromethane (DMC) (Lach-Ner, s.r.o., Czech Republic) (**II–IV**) and 1,1,1,3,3,3-hexa-fluoro-2-propanol (HFIP) (**II, III**) (≥ 99.0%) (Sigma-Aldrich C.C., Inc.). All other reagents and solvents used were of analytical grade and were used without further purification. Distilled water was used in all dissolution experiments (**I, II, IV**). Materials for buffer solutions (KCl, HCl, Na_2HPO_4, NaH_2PO_4) were obtained from Sigma-Aldrich C.C., Inc. Hard gelatin capsules size 1 (*Elanco* Products Co, Inc.) were manually filled and weighed before and after capsule filling, and subsequently used in the dissolution studies (**I, II, IV**).

4.1.2. Preparation of piroxicam solid-state forms (I)

Prior to dissolution experiments, the initial PRX solid state form was a mixture of PRX forms I and II confirmed by means of XRPD (**I**). Pure anhydrous PRX form I (PRXAH) was prepared by dehydrating PRX monohydrate (PRXMH) at 157 °C. PRXMH was prepared by recrystallization from hot saturated water solution as described by Kogermann et al. (2007). All samples were passed through a 150-μm sieve prior to experiments (**I**).

4.2. Methods

4.2.1. Electrospinning (II–IV)

A schematic diagram of the ES process is shown in **Figure 3**. The automatic syringe pump KdScientific (Model No: KDS-250-CE, Geneq Inc, USA) with a pumping speed from 1 to 2 ml/h, was used for ES (**II–IV**). The high-voltage power supply Gamma High Voltage Research (Model No. ES3OP-10W/ DAM,

USA) was applied for generating the voltage of 7–22 kV used in the experiments. The distance between the spinneret and the fiber collector was in a range of 8–25 cm. For preparing the nanofibers containing HPMC K100M CR as a carrier polymer (0.8% solution) and HFIP as a solvent system, the drug-polymer (PRX/HPMC) ratios (w/w) were 1:1, 2:1 and 4:1 (**II, III**). The levels for the voltage and distance were 7, 9, 10 kV and 8, 10, 12 cm, respectively. For PRX-Soluplus® nanofibers [drug-polymer ratio 1:13 (w/w), 33% (w/v) solution in acetone], the voltage of 9 kV was used (**IV**). The distance between the spinneret and the fiber collector plate was 10 cm. For preparing other nanofibers, the higher operating voltage of 22 kV and distance of 25 cm were applied.

The electrospun nanofibers were investigated immediately after fabrication and within regular time periods during a short-term (until 6-month) aging at a low temperature [6 ± 2 °C / 0% relative humidity (RH)] and room temperature (22 ± 2 °C / 0% RH). In addition, some samples were also stored for up to 2 months at higher temperature and humidity conditions (30 °C / 85% RH) (**II**), and some samples were stored even up to 1 year in room conditions (20–23 °C) and RH 20–50% (unpublished data).

4.2.2. X-ray powder diffraction (I–IV)

The XRPD patterns of all materials and electrospun nanofibers (immediately after fabrication and after a short-term aging) were obtained by using a X-ray diffractometer (D8 Advance, Bruker AXS GmbH, Germany) (**I–IV**). Crystal structures were verified by comparing the experimental results to the theoretical patterns in the Cambridge Structural Database (CSD) or to the diffractograms available in the literature. For PRXAH I and PRXMH, the CSD reference crystal structures under refcode BIYSEH (Reck et al., 1988) and CIDYAP01 (Bordner et al., 1984) were used, respectively. PRXAH forms II and III structures were compared to the diffractograms reported by Kogermann et al. (2011) and Vrečer et al. (2003). The XRPD experiments were carried out in a symmetrical reflection mode (Bragg-Brentano geometry) with CuK_α radiation (1.54 Å). The scattered intensities were measured by using a LynxEye one-dimensional detector with 165 channels. In the original publication **I**, the scanning steps of 0.01° 2θ from 3 to 50° 2θ and a total counting time of 8.8 s per step were used**.** In the other papers (**II–IV**), the angular range was from 5° 2θ to 30° 2θ with the steps of 0.2° 2θ. The operating current and voltage were 40 mA and 40 kV, respectively (**I–IV**).

4.2.3. Raman spectroscopy (I, II, IV)

Raman spectra were collected using a Raman spectrometer equipped with a thermoelectrically cooled charge-coupled detector, CCD (1024×64) and a fiber optic probe (B&W TEK Inc., USA). A 300-mW laser source at 785 nm was used (B&W TEK Inc., USA). Spectra were recorded between 200 and

2200 cm^{-1} with an integration time of 10 s (**I**) and 12 s (**II, IV**), and as the average of three scans. BWTek software (BWTek, Inc., Newark, USA) was used for the collection of Raman spectra. Raman spectra were normalized and a spectral region from 1000 to 1700 cm^{-1} was used for analysis.

In situ Raman spectroscopy was performed using the same Raman spectrometer. The integration time was 1 s. Each spectrum was the average of 3 scans. During the slurry experiments the spectra were collected with an interval of 5 minutes during the time period up to 8 hours (**I**).

4.2.4. Scanning electron microscopy (I–IV)

The morphology and particle size of PRX powder samples and the diameter and surface morphology of nanofibers were investigated with a high-resolution SEM (Helios™ NanoLab 600, FEI Company, USA) (**I–III**). A measurement function of the microscope driving program xT Microscope Control (FEI) was applied for the dimensions measurements (**I–III**). In addition, a high-resolution SEM by Zeiss EVO® 15 MA (Germany) was used to investigate the diameter of fibers and surface morphology of nanofibrous DDSs (**IV**). All samples were mounted on aluminum stubs with silver paint and magnetron sputter coated with a 3-nm gold layer in argon atmosphere prior to microscopy (**I–IV**). The program ImageJ was used for measuring the nanofiber diameter and diameter distribution (**II–IV**).

4.2.5. Scanning white light interferometry (III)

The geometric properties and 3D surface topography of nanofibers and nanomats were characterized by scanning white light interferometry (SWLI). In SWLI, a light beam passes through an interferometric objective (Nikon, Michelson type, magnification 120×) containing a beam splitter that reflects half the incident beam onto a reference surface and that passes the other half onto the test surface (**III**, Fig. 2). Light reflected from the test and reference surfaces recombines and interferes, forming an interferogram. The objective is translated horizontally (scanning) and several interferograms are sequentially imaged. For each camera pixel, the modulation signal is extracted from the intensity signal as the optical path difference seen through the objective's focus varies. The peak of the modulation signal is detected, and a measurement of relative surface height at that point is produced. The modulation signal is periodic for white light sources and is, therefore, not subject to the ambiguity problems that affect phase measurement methods. The technique can measure rough surfaces and several millimeter long steps. The height data are calculated from the interference data with a nanometer resolution. For details about the method and mathematical algorithms used for the data transformation see Larkin (1969), Kassamakov et al. (2007, 2009) and Hanhijärvi et al. (2010). In the current

research we obtained 3D images featuring 29 nm by 29 nm active pixel size from a 55 x 40 μm^2 area.

4.2.6. Differential scanning calorimetry (II, IV)

Thermal properties of the starting materials, their physical mixtures and electrospun nanofibers were studied using a differential scanning calorimeter, DSC (DSC 4000, Perkin Elmer Ltd, Shelton, CT, USA). The DSC system was calibrated for temperature and enthalpy using indium as a standard. Samples of 2–3 mg were sealed in an aluminium pan with 2 pinholes in a lid. In case of pure PRX, the sample size of 0.2 mg was used to be comparable with the other samples tested. A nitrogen purge with a flow rate of 20 ml/min was used in the furnace. The scans were obtained by heating from 30 °C to 220 °C at a rate of 20 °C/min. Each run was performed in triplicate. Temperatures are shown as on-set temperatures of the events unless mentioned otherwise.

4.2.7. Dissolution tests (I, II, IV)

Dissolution tests were carried out in a semi-automated dissolution system (Termostat-Sotax AT7, Sotax, Switzerland) according to United States Pharmacopoeia 28 (USP28-NF23, 2005) basket method (**I, II, IV**). Hard gelatin capsules (size 1) were manually filled with 20 mg of PRX (either PRXAH or PRXMH) (**I**) or with calculated amount of nanofibers (**II, IV**) or with physical mixture of excipients and API for comparison tests (**II, IV**). All capsules were weighed before and after capsule filling. The dissolution studies were also carried out with the nanofibers freely set into the dissolution baskets (**II, IV**). The concentration of PRX in the dissolution medium was measured at 354 nm by using an UV-Vis spectrophotometer (Ultrospec III, Biochrom Ltd, UK). The dissolution medium was 900 ml buffer solution [distilled water, buffers with pH 1.2 (HCl/KCl buffer solution) or pH 7.2 (phosphate buffer solution)] maintained at 37 ± 0.5 °C as described in the USP 28 (**I, II, IV**). The pH of the buffer solutions was confirmed by the pH meter HI 9024 (Hanna Instruments, USA). The dissolution rate of PRXAH and PRXMH was investigated for 10 hours at 50 rpm (**I**). The dissolution rate of HPMC and Soluplus® nanofibers was investigated at similar conditions for up to 6 and 2 hours, respectively (**II, IV**). The samples were filtered through Glass microfibre filters (Whatman® GF/D). An aliquot of the release medium (5 ml) was withdrawn at predetermined time intervals (every 3 minutes). The method reproducibility was verified by investigating six (**I**) or three (**II, IV**) samples during one dissolution test (and two parallels were performed at each dissolution condition). Standard solution was prepared using PRXAH in 0.02 M NaOH solution (**I, II, IV**).

5 RESULTS AND DISCUSSION

5.1. Physical characterization of piroxicam solid-state forms and electrospun nanofibers (I-IV)

5.1.1. Solid-state forms of piroxicam (I)

The SEM micrographs revealed the different particle size and surface properties of the two PRX solid-state forms (**Figure 6**). PRXMH crystals appeared much larger compared to the PRXAH crystals. In addition, PRXMH showed smoother surface of the particles. As expected (Bordner et al., 1984; Reck and Laban, 1990), both solid-state forms showed similar crystal shapes-prisms. The yellow color of PRXMH due to the zwitterionic structure (Sheth et al., 2005), simplified the differentiation of the two PRX solid-state forms.

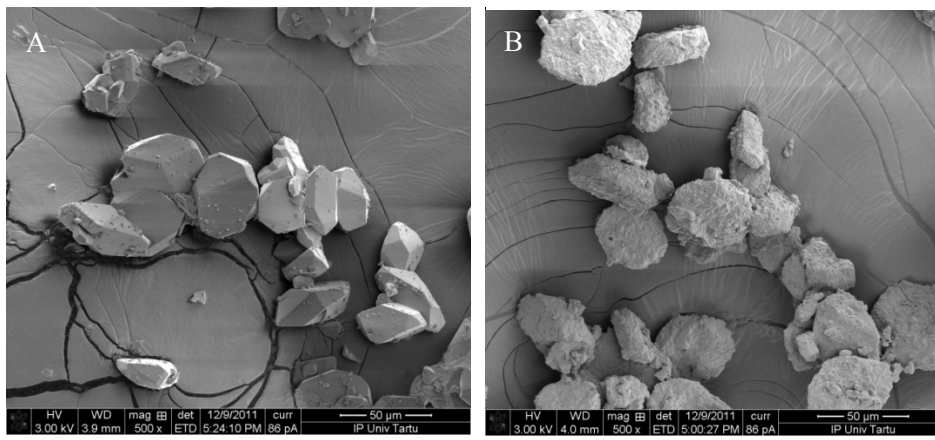

Figure 6. Scanning electron microscopy (SEM) micrographs of: (A) piroxicam monohydrate (PRXMH) and (B) piroxicam anhydrate form I (PRXAH). Magnification of 500×.

The crystal forms of PRX were confirmed by XRPD and Raman spectroscopy (**Figure 7**), and were in good agreement with the theoretical patterns and previously published data (Kogermann et al., 2007).

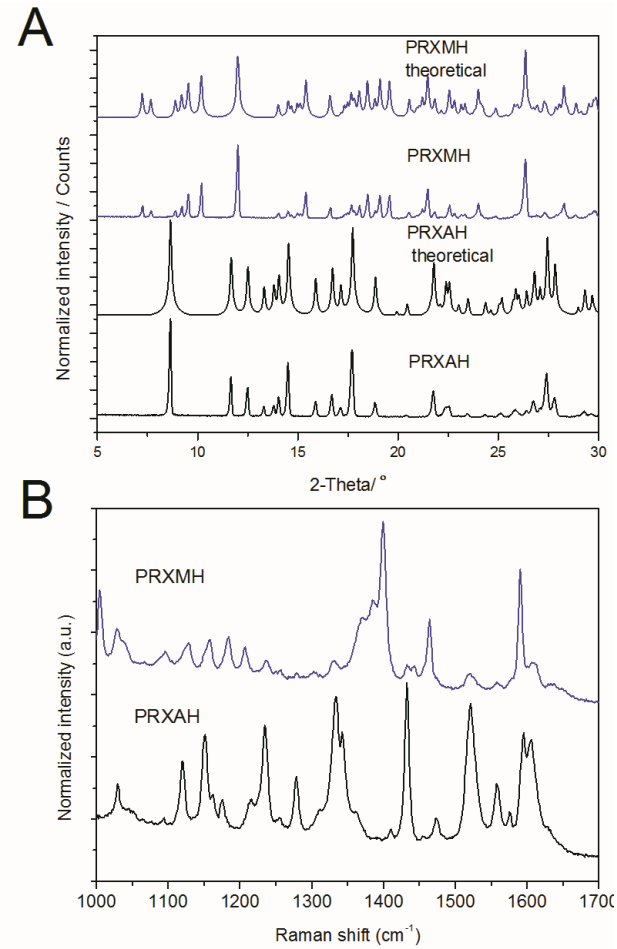

Figure 7. X-ray powder diffraction (XRPD) patterns (A) and Raman spectra (B) of piroxicam monohydrate (PRXMH) and piroxicam anhydrate form I (PRXAH). Theoretical XRPD patterns were obtained from Cambridge Structural Database (CSD), CIDYAP and BIYSEH for PRXMH and PRXAH, respectively. All XRPD patterns and spectra are normalized and offset for clarity.

5.1.2. Solid-state properties of piroxicam incorporated into electrospun nanofibers (II–IV)

To date, the behavior and possible solid-state phase transformations of APIs during ES are not very well known and understood. According to the literature, there are three (Rošic et al., 2012b) or four (Huang et al., 2003) modes how the drug can be incorporated in the electrospun nanofibers (**Figure 8**): (A) The API particles (usually in crystal form) are encapsulated in the carrier polymer; (B) The API particles are homogenously mixed at the molecular level with a carrier polymer to form nanofibers together (solid dispersion, SD); (C) The API is

chemically bond to a carrier polymer; and (D) The API is physically adsorbed onto the surface of polymer nanofibers. If the API-loaded nanofibers are considered as SDs, they can be classified into four generations like established SD systems based on their composition (Chiou and Riegelman, 1971; Vo et al., 2013).

In our experiments (**II–IV**), the drug was simply dissolved in the polymer solution prior to ES, and the amorphization of PRX was aimed to be facilitated by the fast removal of solvent during ES. Consequently, the SD was most likely formed by following the mode "B" described in **Figure 8**. Both polymers used, HPMC (**II, III**) and Soluplus® (**IV**), acted in electrospun formulations as carrier/stabilizer for the amorphization and stabilizer of the supersaturated state upon the release of API.

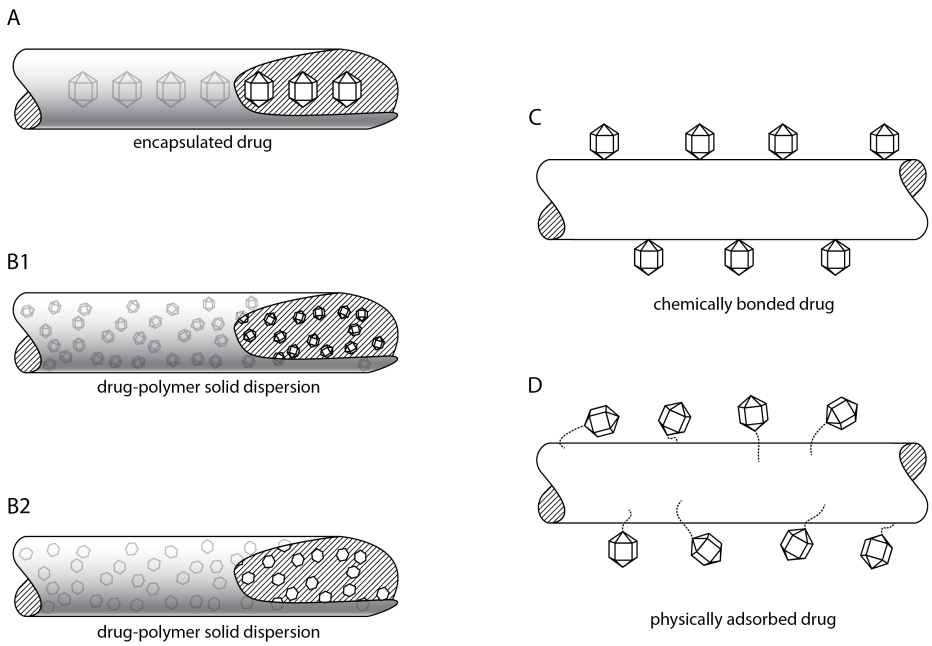

Figure 8. Schematic diagram on the different possibilities of drug loads in/on electrospun nanofibers: (A) encapsulated drug; (B) drug-polymer solid dispersion (SD) (B1 with crystalline drug; B2 with amorphous drug); (C) chemically bonded drug; (D) physically adsorbed drug. Modified from Rošic et al., 2012b and Huang et al., 2003.

Drug solubility and content in the polymer solution have been shown to be important factors affecting the solid-state form and distribution of API in electrospun nanofibers (Meinel et al., 2012; Natu et al., 2010; Rošic et al., 2012b). Since HFIP has high polarity and strong dissolving capability to various polymers and APIs, it was considered as the solvent of choice for dissolving HPMC and PRX for ES applications (**II**). HFIP is also miscible with water and

many organic solvents, it has low surface tension and it is very volatile, thus suggesting applicability in ES (Zhang et al., 2007). PRX was found to be in amorphous form in the electrospun nanofibers (with a drug:polymer ratio 4:1) (**II, III**). Volatile acetone was selected for dissolving Soluplus® graft copolymer, since a quick solvent evaporation is essential for the formation of homogeneous nanofibrous mats. Acetone is also a cheaper and less toxic solvent than HFIP. The amount of PRX dissolved in Soluplus® /acetone solution was many times lower than that used in HPMC/HFIP solutions; the ratio of drug:polymer was in well spinnable solutions only in weight ratio 1:13 (**IV**).

The amorphous form of APIs is physically unstable and has a tendency to spontaneously recrystallize (Hancock and Zografi, 1997). PRX is a polymorphic drug that may exist in different solid state forms, including three anhydrate (I-III), monohydrate and amorphous forms (Sheth et al., 2004a; Vrečer et al., 2003). Recently, a research group from Helsinki found a new, still unidentified form of PRX ("form IV") (Nyström et al., 2015). Therefore, it is very important to analyze in which form PRX actually exists in electrospun nanofibers, and how stable the present solid-state form is, when stored in different environmental conditions. In this study, XRPD and Raman spectroscopy were used for verifying the solid state forms of PRX.

5.1.2.1. X-ray powder diffraction analysis (II–IV)

The XRPD analysis verified that prior ES PRX was present as PRXAH with characteristic XPRD reflections at diffraction angles 2θ of 8.3°, 11.7°, 12.5°, 14.3°, and 17.7° (**I, II, IV**). The cellulose ether polymer (HPMC) and PCL-PVAc-PEG graft copolymer (Soluplus®) were amorphous polymers without any characteristic diffraction reflections in their XRPD pattern (**II–IV**).

In our studies, the amorphous halo in all XRPD patterns indicated the presence of amorphous PRX (**Figure 9 and 10**). Hence, XRPD results revealed that the nanofibers contained PRX in amorphous form immediately after fabrication and after a 3-month (**II**) or 6-month (**IV**) aging period (**Figure 9 and 10**). The samples were stored at low (6–8 °C) and/or room (22 ± 2 °C) temperature and low humidity (RH 0%).

There were no differences between the polymers used and the amount of drug loaded into the nanofibers. The PRX was combined with carrier polymer HPMC at weight ratios of 1:1, 2:1 or 4:1 as described in the original papers (**II, III**). The XRPD diffraction patterns also suggested that PRX existed in amorphous form with no signs of recrystallization or polymorphic solid-state changes during the aging in controlled conditions (temperature, humidity).

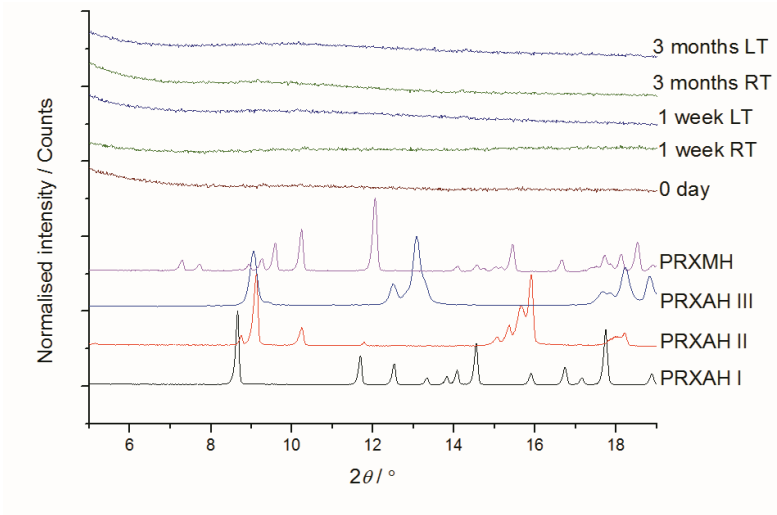

Figure 9. X-ray powder diffraction (XRPD) patterns of piroxicam(PRX)-loaded hydroxypropyl methylcellulose (HPMC) nanofibers (a drug-polymer ratio 1:1 w/w) immediately after fabrication and after a short-term aging of the samples at low (LT 6–8 °C / 0% RH) and room temperature (RT 22 ± 2 °C/0% RH).

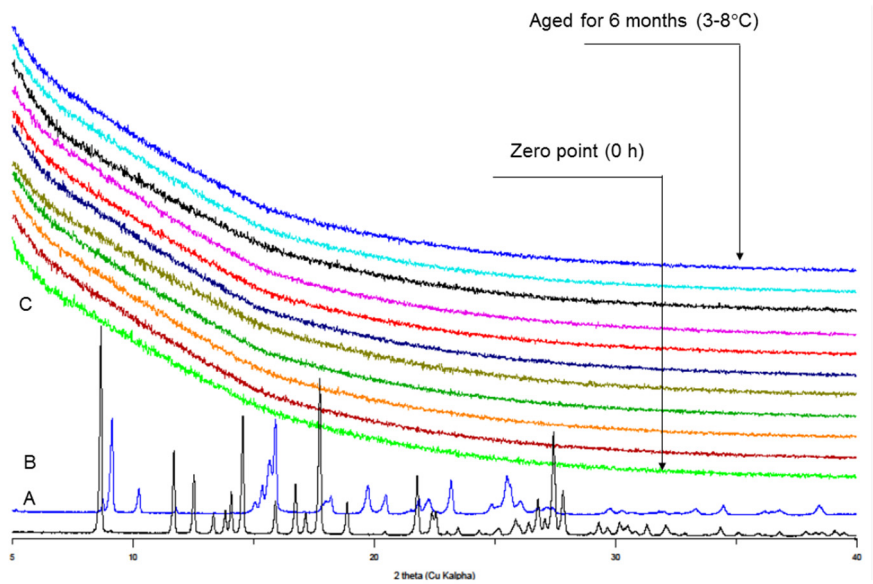

Figure 10. X-ray powder diffraction (XRPD) patterns of crystalline anhydrous piroxicam (PRX) forms and nanofibers of Soluplus® graft copolymer loaded with PRX: (A) PRXAH form I; (B) PRXAH form II; and (C) fresh and aged drug-loaded nanofibers of PRX and Soluplus® (a drug-polymer ratio 1:13 w/w).

According to Kogermann et al. (2011), the spontaneous recrystallization of amorphous PRX starts within few minutes after the amorphous form preparation leading to the formation of PRXAH I. Our results suggest that the ES of PRX with HPMC in HFIP or with Soluplus® in acetone clearly prevents the solid-state transformation (recrystallization) of PRX, and consequently, stabilizes the amorphous form of PRX in the solid formulation. However, it is known that HPMC has the ability to form hydrogen bonds between drug molecules and the polymer, and consequently, to increase the activation energy for crystallization (Brouwers et al., 2009). Soluplus® is a relatively new amphiphilic graft copolymer that has been introduced to the pharmaceutical industry for the purpose of solubilizing poorly water-soluble APIs. This polymer is capable to form SDs with poorly water-soluble APIs and to prevent the rapid hydration of compacts with the tendency to form a strong gel at the surface (Hughey et al., 2013). Soluplus® has shown high affinity or even strong binding with some BCS II class drugs in solid solutions during absorption experiments (Linn et al., 2012). It is evident that the corresponding affinity exists also between PRX and Soluplus® in electrospun nanofibers, thus preventing the recrystallization of amorphous PRX (**II–IV**).

Since the solid-state transformations of drug are dependent on the temperature and humidity, the aging studies of the HPMC-PRX nanofibers were also carried out at elevated temperature and humidity conditions (30 °C / 85% RH) (**II**). The characteristic reflection of PRXAH III at a diffraction angle 2θ of 8.9° suggested partial recrystallization of amorphous PRX already after three-day aging (**Figure 11**) (**II**). When the samples were stored up to 1 year at ambient room temperature (20–23 °C) and RH (2050%), it was found that numerous crystals of PRX forms were formed along the HPMC nanofibers (**Figure 12,** unpublished data).

There are only few reports in the literature on the effects of manufacturing process and storage conditions on the physical solid-state stability of amorphous form of PRX. (Sheth et al., 2004b) reported that by using a cryogenic ball milling some polymorphic memory of PRXAH I could retain in the respective amorphous form of PRX. The amorphous form tends to recrystallize predominantly to PRXAH I, although some PRXAH III character may also be present. Similarly, Naelapää et al. (2012) showed that PRXAH I amorphous samples recrystallized as PRXAH I together with the diffractions of the least stable PRXAH III. Furthermore, the storage conditions have been shown to influence the amorphous state of PRXAH I due to the possible presence of higher residual order in X-ray amorphous PRXAH I samples (Naelapää et al., 2012). Our study reveals that the recrystallization of amorphous PRX was slowed down in controlled conditions (temperature, humidity) by the presence of polymer in the nanofibers. Further solid-state changes were also inhibited (**II**).

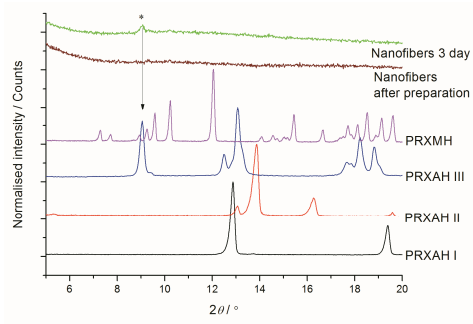

Figure 11. X-ray powder diffraction (XRPD) patterns of piroxicam (PRX) loaded hydroxypropyl methylcellulose (HPMC) nanofibers (a drug-polymer ratio 1:1) immediately after fabrication and after a three-day aging of the samples at elevated temperature and humidity conditions (30 °C/85% RH). The asterisk (*) indicates the main characteristic reflection of PRXAH form III **(II)**.

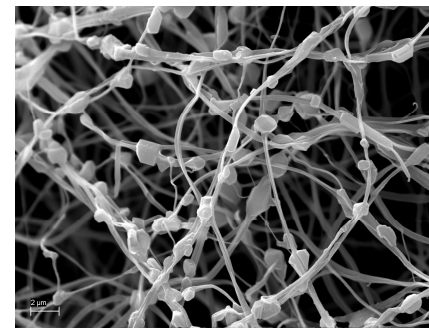

Figure 12. Scanning electron microscopy (SEM) micrograph of piroxicam (PRX) crystals formed inside the hydroxypropyl methylcellulose (HPMC) nanofibers, when the samples were stored for up to 1 year at ambient room temperature (RT 20–23 °C) and relative humidity (RH 20–50%).

5.1.2.2. Raman spectroscopy analysis (II, IV)

The Raman spectra of fresh and aged polymeric PRX and HPMC (1:1) nanofibers were identical, thus indicating that no solid-state transformations occurred during a short-term aging of nanofibers at LT and RT within 3 months (**Figure 13**) (**II**). The joint characteristic peaks for amorphous PRX, are shown at 1159, 1237, 1331, 1365, 1438, 1477, 1531, and 1561 cm^{-1}. The present Raman spectroscopy results were in agreement with the previous Raman spectroscopy results (Kogermann et al., 2011) suggesting the presence of amorphous PRX in the nanofibers.

During ES, a large specific surface area is obtained resulting in a fast and efficient evaporation of organic solvent. Consequently, molecules have no time to (re)crystallize and hence they most likely have an amorphous supermolecular structure (Verreck et al., 2003a; Zong et al., 2002). Moreover, a hydrophilic polymer (like HPMC) with an ability to form hydrogen bonds can prevent the crystal growth of an API by hindering the incorporation of drug molecules into a crystal lattice (Brouwers et al., 2009). It is evident, however, that elevated storage conditions can induce the recrystallization of amorphous PRX, since only three-day aging at 30 °C / 85% RH led to the formation of PRXAH III. Interestingly, both Raman spectroscopy and XRPD analyses revealed (data not shown) that the nanofibers with a higher drug-polymer ratio of 2:1 and 4:1 were amorphous immediately after preparation, but after a two-month aging PRX tended to crystallize out from the nanofibers (unlike with the respective 1:1 samples). This suggests that the amount of HPMC is critical and needs to be

high enough to prevent the recrystallization of PRX through forming hydrogen bonds in the present electrospun nanofibers. These results highlight the importance of proper storage conditions which remarkably can change the solid state stability of amorphous PRX in the electrospun polymeric nanofibers (**II, III**).

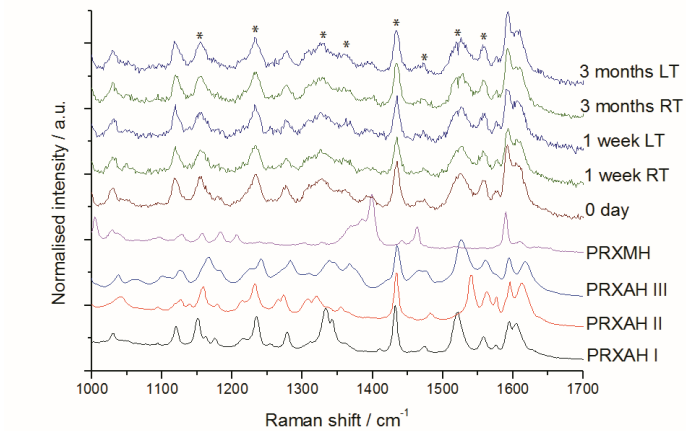

Figure 13. Raman spectra of electrospun piroxicam (PRX) loaded hydroxypropyl methylcellulose (HPMC) nanofibers (a drug-polymer ratio 1:1) immediately after fabrication and after a short-term aging at low (LT 6–8 °C / 0% RH) and room temperature (RT 22 ± 2 °C/0% RH). Key: PRXAH I = PRX anhydrate form I; PRXAH II = PRX anhydrate form II; PRXAH III = PRX anhydrate form III; and PRXMH = PRX monohydrate. The asterisks (*) represent the characteristic peaks for amorphous PRX (**II**).

As seen in **Figure 14**, the electrospun nanofibers of PRX and Soluplus® showed similar characteristic Raman spectroscopy peaks for amorphous PRX as were observed with the PRX and HPMC nanofibers (at 1237, 1477, 1531 and 1561 cm^{-1}). Since the amount of PRX in the Soluplus® nanofibers is much lower than that in the corresponding HPMC nanofibers, only the peaks with higher intensity of amorphous PRX are visible (**IV**).

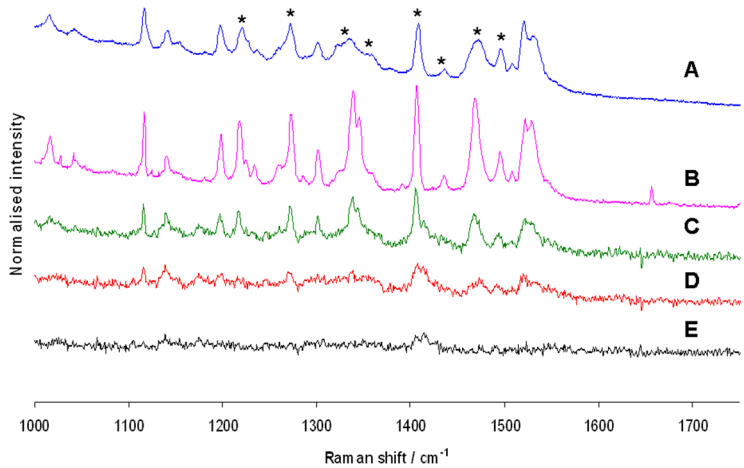

Figure 14. Raman spectra of physical mixture and electrospun nanofibers of piroxicam (PRX) anhydrous form I (PRXAH I) and Soluplus® graft copolymer. Key: (A) amorphous form of PRX (B) pure PRXAH I; (C) physical mixture of PRXAH I and Soluplus® (1:13 w/w); (D) Soluplus® nanofibers loaded with PRX (1:13 w/w drug-polymer ratio); (E) pure Soluplus® graft copolymer nanofibers (**IV**). All spectra are normalized and offset for clarity. The asterisks (*) represent the characteristic peaks for amorphous PRX.

5.1.2.3. Thermal behavior (II, IV)

The DSC thermograms (**Figure 15 and 16**) confirmed the presence of PRX in amorphous form in the electrospun nanofibrous mats immediately after preparation. The DSC thermogram of pure PRXAH I exhibited a single melting endotherm at 204.0 °C (**Figure 15 and 16A**) with the enthalpy of melting (ΔH) 100.8 J/g, which is in good agreement with the values reported in the literature (Stulzer et al., 2008; Wu et al., 2009) (**II, IV**). The pure HPMC and non-drug containing nanofibers showed the thermal behavior of amorphous material without any melting endotherms, just only with small endothermic events in the range of 30–110 °C due to the dehydration of polymers (**Figures 15B and 15C respectively**). The pure Soluplus® graft copolymer showed characteristic endotherm of glass transition temperature (T_g) at 70–80 °C (**Figure 16B**), in agreement with the literature data (Basf, 2010).

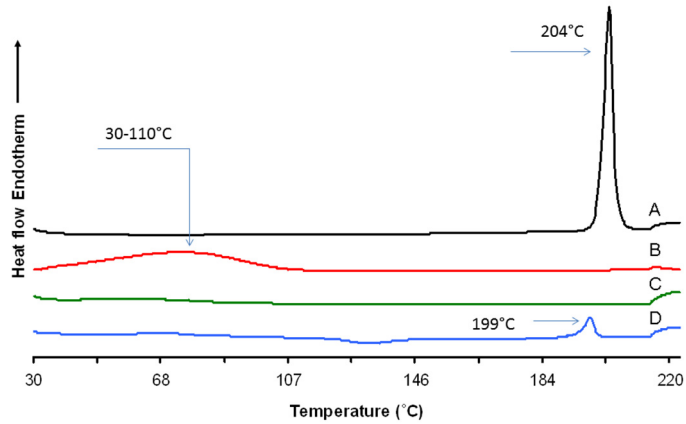

Figure 15. Differential scanning calorimetry (DSC) thermograms. Key: (A) piroxicam (PRX) anhydrate form I (PRXAH I); (B) hydroxypropyl methylcellulose, HPMC (Methocel™ K100M premium CR), (C) electrospun HPMC polymeric nanofibers and (D) electrospun PRX:HPMC nanofibers (a drug-polymer ratio 1:1) (**II**).

In the case of PRX and HPMC nanofibers measured immediately after preparation (**Figure 15D**), the DSC thermograms of electrospun nanofibers showed a weak exothermic event at 131.1 °C (ΔH = -25.1 J/g) suggesting partial (minor) recrystallization of amorphous PRX. This observation was confirmed by the second endotherm at approximately 199.0 °C, most likely corresponding to the PRXAH III melting. In addition, a concomitant reduction in peak size and enthalpy per unit mass of PRX was evident (ΔH of PRX decreased from 100.8 to 50.3 J/g). These results also agree with the XRPD and Raman spectroscopy ones. The recrystallization of PRXAH III from electrospun nanofibers upon heating enlightens the instability of amorphous PRX at higher temperatures **(II)**. The DSC thermographs of PRX-HPMC nanofibers suggest the absence of any solid-state interactions or incompatibility between PRX and HPMC.

As Soluplus® (PCL-PVAc-PEG graft copolymer) has a slightly different thermal behavior (**Figure 16B**), the PRX-loaded polymeric nanofibers presented a broad evaporation endotherm in a range of 30 ºC–110 ºC and exhibited the second (even wider) endotherm ranging from 100 ºC to 220 ºC. This suggests that a physical interaction or fusion of PRX into the Soluplus® had occurred (**IV**). Moreover, no thermal events due to the chemical decomposition were found (**II**). Both DSC thermographs (**Figure 15D and Figure 16D**) supported the XRPD and Raman spectroscopy findings suggesting the presence of amorphous PRX in the nanofibers.

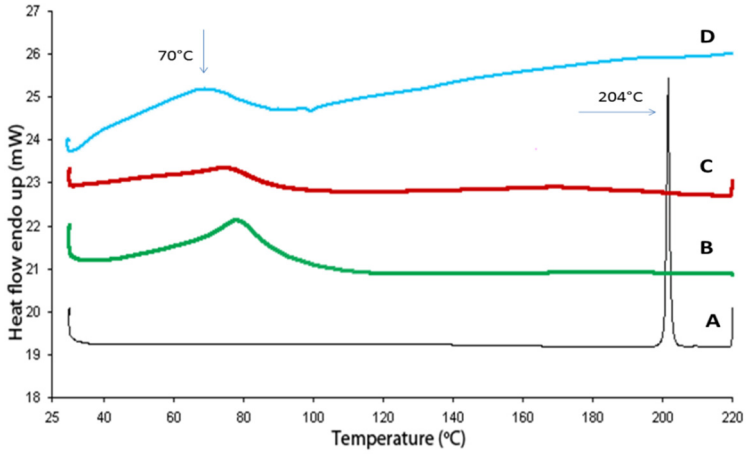

Figure 16. Differential scanning calorimetry (DSC) thermograms of the starting materials, physical mixture with Soluplus® (1:13 w/w), and electrospun nanofibers of PCL-PVAc-PEG graft copolymer (Soluplus®) loaded with and PRX: (A) pure piroxicam (PRX) anhydrous form I (PRXAH I); (B) pure Soluplus® craft copolymer; (C) physical mixture of PRXAH I and Soluplus® (1:13 w/w); (D) drug loaded nanofibers of PRX and Soluplus® (1:13 w/w) (**IV**). The arrows shows the T_g of Soluplus® (70 °C) and the melting point of PRXAH I (204 °C).

5.1.3. Surface morphology, size and size distribution of nanofibers (II–IV)

According to the literature, the morphology and diameter of electrospun nanofibers are dependent on the intrinsic properties of the solution such as the type of polymer, the conformation of polymer chain, viscosity (or concentration), elasticity, electrical conductivity, and the polarity and surface tension of the solvent (Li and Xia, 2004; Lu et al., 2009; Meinel et al., 2012). From the process parameters the most crucial are the applied voltage, the feed rate and the distance to the collector (Rošic et al., 2012b).

In our studies, different polymers and solvent systems were tested to find the most suitable polymer-solvent combinations and optimal process parameters for fabricating the nanofibers (**II, IV**). The morphological properties, size and shape of nanofibers were analyzed by high-resolution SEM. The SWLI 3D topographic analysis was used for the rapid investigation of geometric parameters without any sample preparation.

The drug-loaded nanomats of polymers (HPMC, Soluplus®) and PRX exhibited a 3D layered fiber mesh structure, nonwoven pattern and absence of beads. The representative SEM images of the electrospun nanofibers of PRX and HPMC, and the reference pure polymer nanofibers (without PRX) are shown in **Figure 17** (**II**). The average diameter of the drug-loaded nanofibers was slightly larger (387 ± 125 nm, n = 100) than that of the reference polymeric nanofibers fabricated from the pure polymer-solvent system (195 ± 143 nm, n =

100) (**Figure 17**). The SEM fiber diameter distributions of electrospun nanofibers containing a pure carrier polymer HPMC and HPMC with PRX at weight ratios of 1:1, 1:2 and 1:4, are shown in **Figure 18** (**III**). All types of electrospun nanofibers (with and without PRX) exhibited very uniform thickness forming a homogeneous non-woven nanomat onto a collector plate.

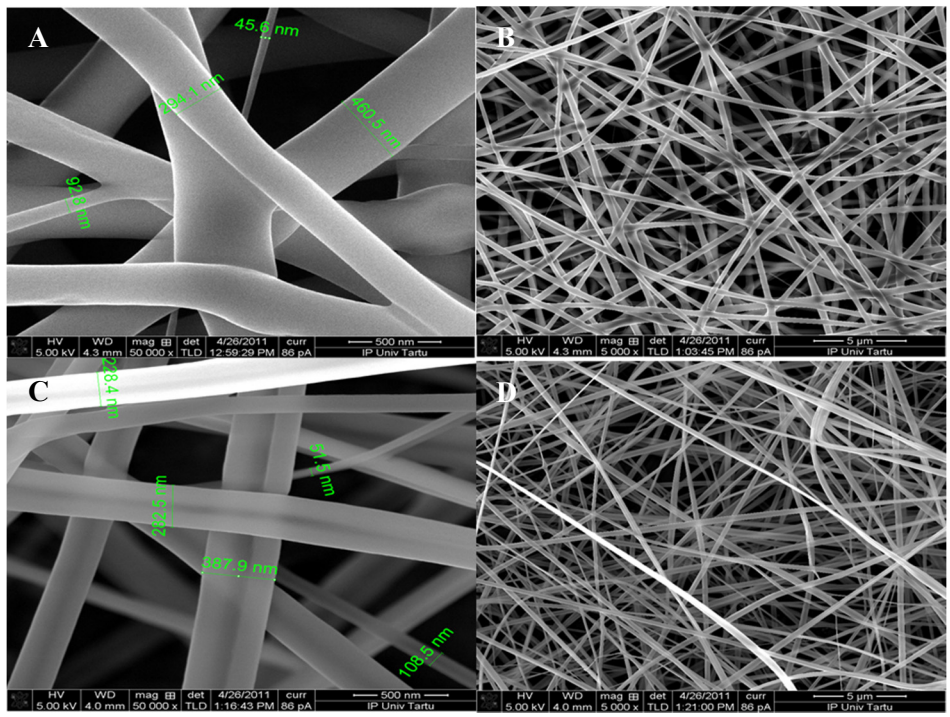

Figure 17. Scanning electron microscopy (SEM) micrographs of electrospun piroxicam (PRX) loaded hydroxypropyl methylcellulose (HPMC) nanofibers (a drug-polymer ratio 1:1) (A, B) and the reference nanofibers of a pure carrier polymer HPMC (C, D). Magnification 50,000× (A, C) or 5,000× (B, D) respectively (**II**).

According to Meinel et al. (2012), blending polymer solutions with drugs can affect the geometric properties of electrospun fibers due to the changes in solution viscosity and electrical conductivity. A decrease in the charge density on the surface of the electrospun jet and an increase in solution viscosity result in larger fiber size.

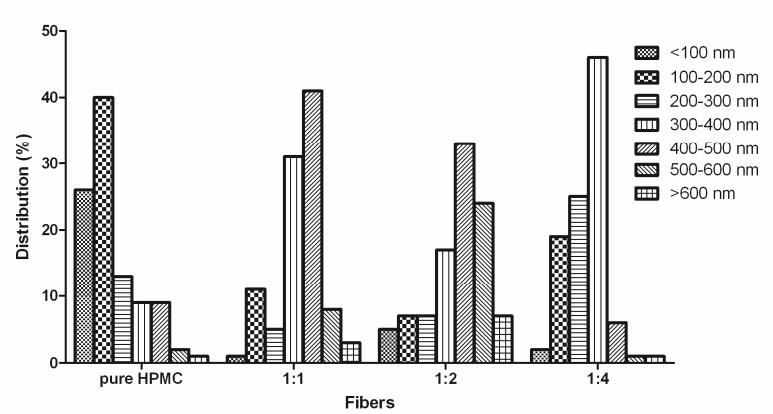

Figure 18. The scanning electron microscopy (SEM) diameter distributions of nanofibers containing a pure carrier polymer HPMC (without drug), and HPMC and a model drug, Piroxicam (PRX) at a ratio of 1:1, 1:2 and 1:4 (**III**).

As seen in **Figure 19** (**IV**), the nanofibers of Soluplus® were circular in cross-section with an average diameter ranging from 500 nm to 2 μm. The formation and presence of defects, such as beads, were not observed suggesting that the viscosity and surface tension of the polymeric solution was suitable for fabricating the drug-loaded nanofiber matrices. Furthermore, the presence of crystallized PRX on the surface of nanofibers was not observed indicating that the drug was in a non-crystalline state in the electrospun nanofibers. The XRPD and Raman spectroscopy data also verified this finding (**II–IV**).

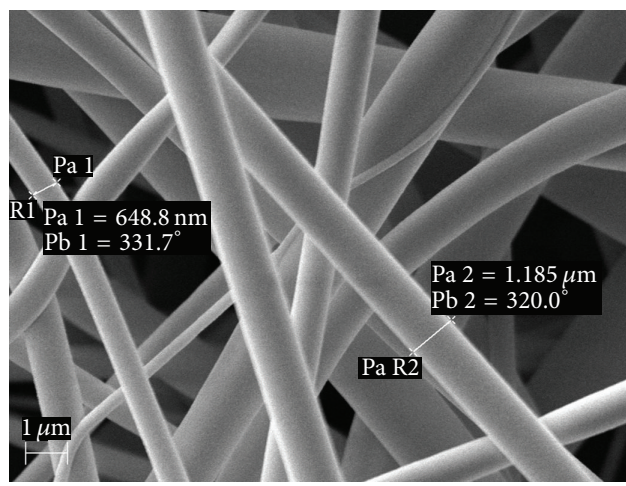

Figure 19. Representative scanning electron microscopy (SEM) micrograph of the electrospun nanofibers of Soluplus® graft copolymer loaded with a model drug, piroxicam (PRX) Magnification 20,000× (**IV**).

Several recent studies have demonstrated that the topography and geometric properties of the polymeric nanofibrous mats are important variables that affect the performance and therapeutic efficiency of the nanomats in pharmaceutical and biomedical applications (Chen et al., 2007; Huang et al., 2012; Leung and Ko, 2011; Lu et al., 2009; Pelipenko et al., 2013). The morphological appearance of the drug-loaded electrospun nanomats has also been reported to be dependent on the material variables, i.e. polymer type, the chemical nature and molecular weight of the drug(s) (Meinel et al., 2012; Taepaiboon et al., 2006). A novel SWLI method (used for the first time for characterizing the nanofibers) provided a nanometer-resolution vertical insight into the internal structure of the polymer nanomats and a quantitative measurement of the thickness of the mats. SEM provided high-quality images of the orientation and size of the individual fibers in the mats but no quantitative measurement related to the vertical fiber layering or thickness of the nanomats. The advantage of SWLI is that the method is rapid, non-destructive, non-contacting and it provides 3D visualization of small samples. Consequently, SWLI has been used e.g. to characterize miniature elements and micro-fluidic devices (Coupland and Lobera, 2010; Kassamakov et al., 2009; Kassamakov et al., 2007; Madani-Grasset et al., 2008). Only few studies report on applying SWLI to characterize pharmaceutical systems. Hanhijärvi et al. (2010) measured the surface roughness of pharmaceutical thin films with SWLI, and more recently Genina et al. (2012) used this method for describing of flexographic coated controlled-release systems.

Characterizing electrospun polymeric nanofibers is challenging since the fibers are small and randomly oriented in the nanomats (usually in a non-woven form). A non-woven form of nanofibrous mats is beneficial in many biomedical applications, such as in wound dressings and nanofibrous scaffolds for cell attachment (Leung and Ko, 2011). We investigated nanofibers with different PRX-HPMC ratios (1:1, 2:1, 4:1) by SWLI and SEM, and compared the methods and results (**III**). The SEM image-based measurements showed that the average fiber diameter (n =100) was independent of the drug-polymer ratio (**Figure 18**). The SWLI measurements revealed that the API-loaded mats were 4.0 µm to 4.5 µm thick (uniformly) regardless of the polymer and PRX ratio. With increasing PRX concentration, the nanomats became sparser and less dense (loose). The diameter and length of individual nanofibers could not be accurately measured with the SWLI. The thickness of the mats was determined by SWLI from the vertical position of the most dense fiber layer. The SWLI thickness of the nanomats was 2.5–3.0 µm (for a PRX and HPMC ratio of 1:1), 2.0–3.0 µm (for a PRX and HPMC ratio of 2:1), and 2.0–2.5 µm (for a PRX and HPMC ratio of 4:1). This suggests that the drug-loaded mats are porous as was also shown with the SWLI 3D topographical maps of the mats. The porosity of the different surface layers is related to the number of layers present in the mat (Ghasemi-Mobarakeh et al., 2007).

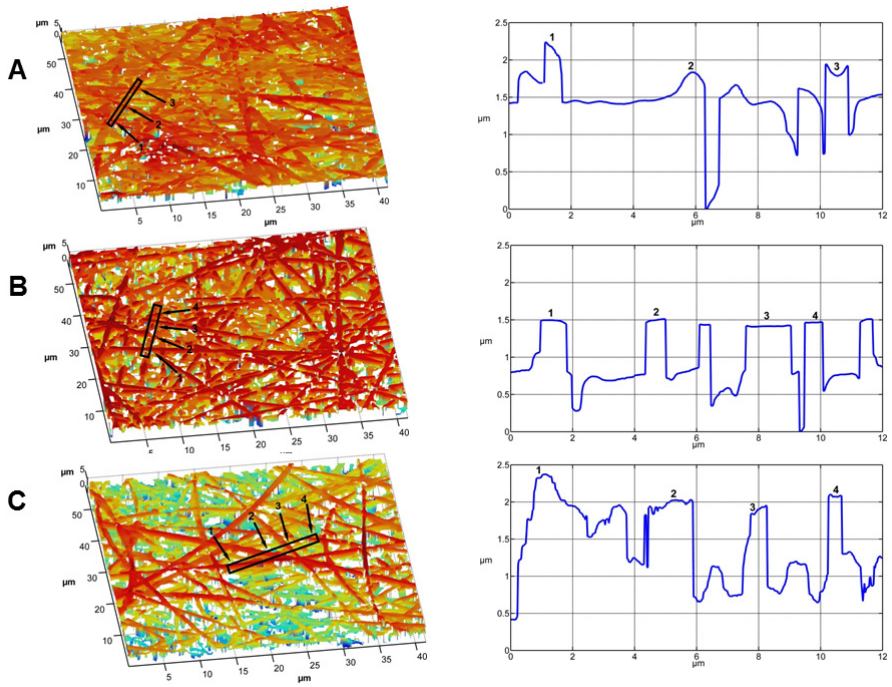

Figure 20. Scanning white light interferometry (SWLI) three-dimensional (3D) images and surface profiles of drug-loaded nanofibrous mats. The model drug piroxicam (PRX) and the carrier polymer HPMC ratios were 1:1 (A), 2:1 (B) and 4:1 (C). The sites that were profiled are indicated with black lines (**III**).

Figure 20 shows the SWLI fiber architecture and surface profiles (roughness) of the API-loaded non-woven nanomats (PRX-HPMC) along randomly selected lines crossing the mat surface (**III**). Cross-over points with individual nanofibers can be clearly distinguished in the SWLI profile. The 3D topographical maps obtained by SWLI show deep porous structures in the non-woven API-loaded nanomats. Our study (**III**) shows usefulness and also some limitations of this method to describe the geometric properties and surface topography of polymeric nanofibers and nanofibrous mats intended for pharmaceutical and/or biomedical applications.

5.2. Dissolution behavior (I, II, IV)

5.2.1. Dissolution of piroxicam solid-state forms (I)

The discussion about maximum solubility of different PRX forms and prediction of solid-state changes during dissolution tests is presented in detail in the original paper **I**. The solubility and dissolution behavior of APIs are the key determinants of drug bioavailability for its intended therapeutic use (Aaltonen et

al., 2006; Javadzadeh et al., 2005). As stated, PRX is a poorly water-soluble, highly permeable class II drug (Amidon et al., 1995), and the rate of oral absorption is mainly controlled by the dissolution rate in the gastrointestinal tract (GI). The solubility and dissolution of PRX depends also greatly on pH, since it has two pK_a values and therefore its solubility and dissolution rate changes at different pH. Solubility is dependent on the degree of ionization, molecular size, interactions of substituted groups with solvent and crystal properties. When the pH of an aqueous solution approaches the pK_a, there is a very pronounced change in the ionization of an API, and consequently in APIs solubility and dissolution.

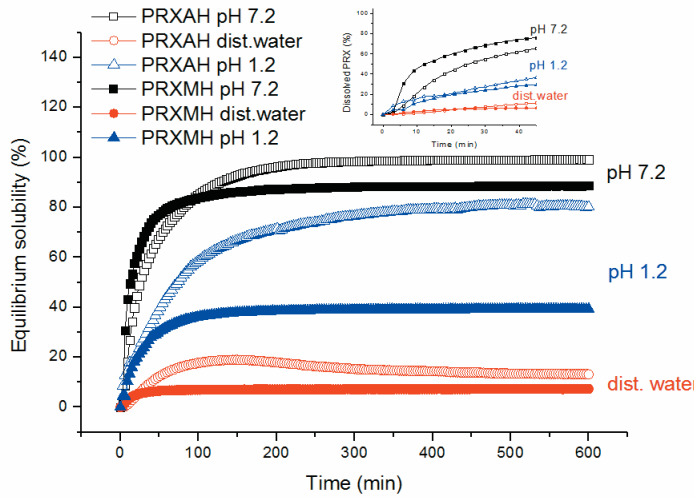

Figure 21. The solubility-time profiles of PRXAH (open symbols) and PRXMH (closed symbols) at pH 7.2 (black squares), distilled water pH 5.6 (red circles), and pH 1.2 (blue triangles) using 200 mg PRX dose. For clarity purposes, the standard deviation is not shown, but for all dissolution results it was below 3.5% (**I**).

To investigate the effects of biorelevant pH on the solubility and dissolution of PRX forms, and consequently, to predict the dissolution behavior in different parts of the GI tract, the *in-vitro* dissolution tests were performed in a simulated gastric fluid (pH 1.2), in distilled water and in a phosphate buffer solution (pH 7.2). According to the results on solubility (**Figure 21**), both PRX forms have the lowest solubility in distilled water (pH 5.6). The highest solubility was observed at pH 7.2 (phosphate buffer solution), and both forms showed mid-solubility values at pH 1.2 (HCl/KCl buffer solution). These results are in agreement with the published findings of Jinno et al. (2000) suggesting that the best solubility of PRX would be in basic environment.

In our dissolution studies (**Figure 22**), the two PRX solid-state forms revealed similar trends and pH dependence as observed in solubility testing. Small differences could be explained by the differences in the amount of PRX

used in the solubility and dissolution tests. As shown in our paper **I**, the solid-state changes during the solubility testing were observed. The PRX transforms to yellow PRXMH during the solubility testing, and this can affect to the solubility of PRX. Since the dissolution tests were performed only for 45 minutes and the amount of used PRX was small (only 20 mg of PRX in capsules) the complete solid-state phase transformation was not observed.

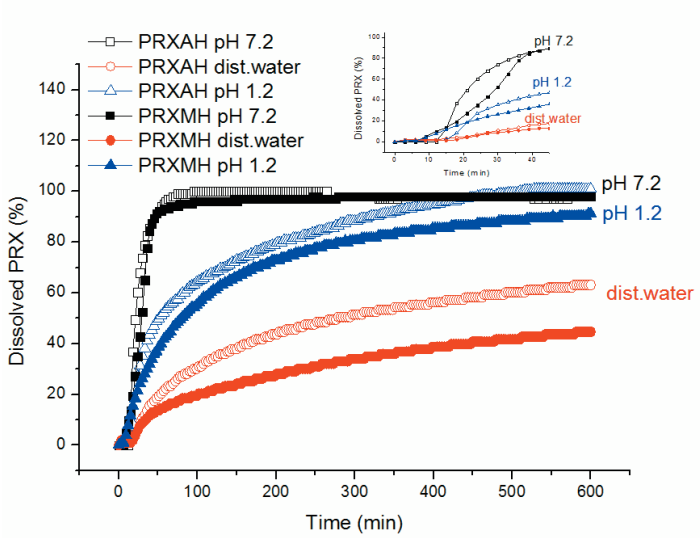

Figure 22. The dissolution profiles of PRXAH (open symbols) and PRXMH (closed symbols) at pH 7.2 (black squares), distilled water pH 5.6 (red circles) and pH 1.2 (blue triangles) using 20 mg PRX dose in capsules. For clarity purposes, the standard deviation is not shown, but for all dissolution results it was below 1.9% (**I**).

5.2.2. Dissolution of electrospun nanofibers (II, IV)

According to the literature, the drug release from electrospun polymeric nanofibers is dependent on several material and process factors including drug molecular weight, loading and state, carrier polymer(s), fiber crystallinity, fiber diameter and porosity, and drug-polymer-ES solvent interactions (Meinel et al., 2012; Natu et al., 2010). The dissolution profiles of PRX loaded in HPMC nanofibers, pure PRX powder and physical mixtures of PRX and HPMC at different pH conditions, are shown in **Figure 23**. The dissolution of pure PRXAH I was dependent on the pH of dissolution media being poorer in the acidic (pH 1.2, **Figure 23A**) than in slightly basic (pH 7.2, **Figure 23B**) dissolution medium. In the case of PRX and HPMC nanofibers, the release rate of PRX shows the controlled release kinetics and interestingly was less dependent on the pH of the dissolution media being only slightly lower at pH 1.2 than pH 7.2. The PRX-HPMC nanofibers behaved as controlled release DDSs, and they showed at least half or even more decrease in the release rate compared to that of pure PRX.

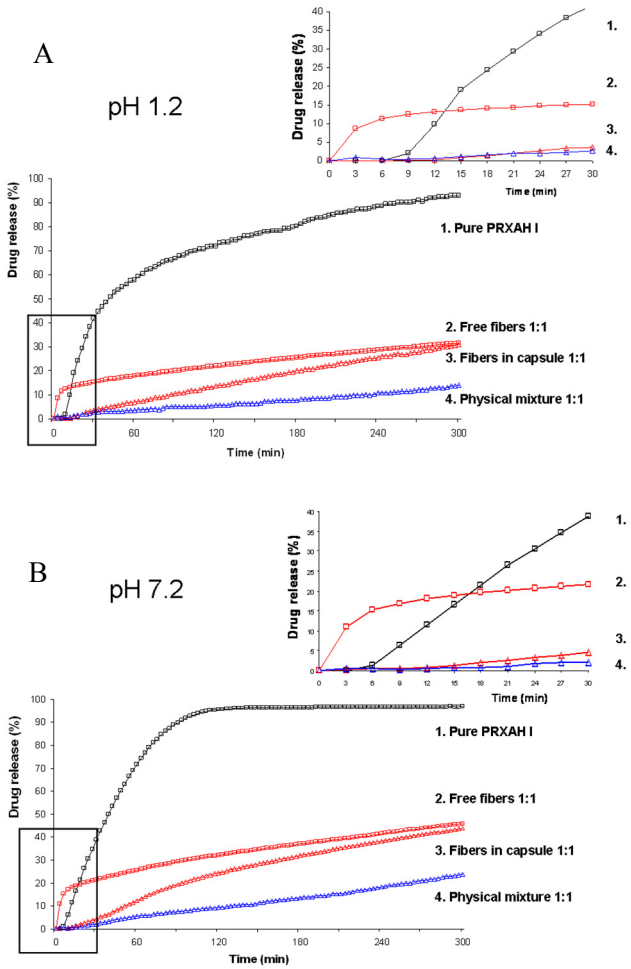

Figure 23. Release profiles of piroxicam (PRX) loaded hydroxypropyl methylcellulose (HPMC) nanofibers at (A) pH 1.2 and (B) pH 7.2 (n = 6). For clarity purposes, the standard deviation is not shown, but for all dissolution results it was below 5.0% (**II**).

As shown in **Figure 23**, the electrospun nanofibers loaded in hard gelatine capsules exhibited a short lag-time (10–15 min), the absence of initial burst release and zero-order linear dissolution kinetics. Sustained-release dissolution of the polymeric nanofibers was attributed to a high-molecular HPMC grade used as a carrier polymer and the formation of a solid matrix inside hard gelatine capsules. According to the literature, the drug release profiles from HPMC containing hydrophilic matrices are generally first-order for highly water-soluble drugs and zero-order for insoluble drugs (Tran et al., 2011). It is evident that the amorphous state of PRX and generation of supersaturated solution associated with the present SD nanofibers, decreased the lag-time for

the drug release *in vitro*. In addition, it is expected that SD nanofibers as a kind of supersaturating DDS could enhance the absorption of a poorly water-soluble drug by reducing the precipitation of drug and thus generating high free drug concentrations, e.g. in the gastrointestinal tract. According to Brouwers et al. (2009), it is possible that the supersaturation plays a role in the absorption process of poorly water-soluble drugs in various solubilizing dosage forms. Such dosage forms can be adjusted into the supersaturated formulations by using a suitable precipitation inhibitor (e.g. HPMC) in the delivery system.

Since our recent study suggests that hard gelatine capsule shells might interact with a carrier polymer (Kogermann et al., 2013), a number of dissolution tests were performed without using hard gelatine capsules (i.e. with free nanofibers in the baskets) (**Figure 23**). The free fibers showed an initial burst release and then almost constant prolonged drug release. This differed from the dissolution behavior of the nanofibers loaded in hard gelatine capsules (a drug-polymer ratio 1:1). **Figure 24** illustrates the effects of drug-polymer ratio on the release profile of PRX loaded nanofibers (free nanofibers in the baskets). The dissolution of amorphous PRX from the nanofibers was a prolonged carrier-polymer controlled process, and the initial dissolution rate of PRX was directly connected with a PRX-polymer ratio. By increasing the drug content in nanofibers, a greater portion of the drug is evidently located near the surface of the nanofibers, and hence initial release of the drug is faster (**Figure 24**).

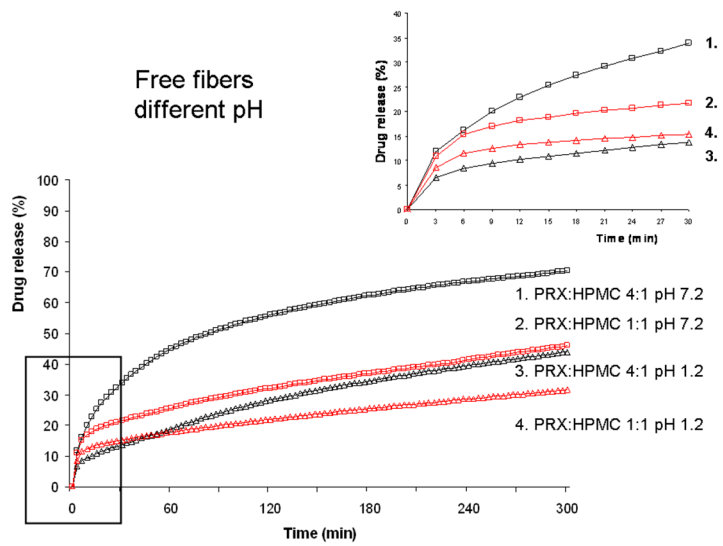

Figure 24. Effects of drug-polymer ratio on the dissolution behavior of piroxicam (PRX) loaded hydroxypropyl methylcellulose (HPMC) nanofibers (n = 6). The dissolution behavior of free nanofibers in baskets (with a drug-polymer ratio 1:1 (red) and 4:1 (blue) w/w) was tested at pH 1.2 (Δ) and 7.2(□). The initial dissolution rate of PRX is shown in the small figure. For clarity purposes, the standard deviation is not shown, but for all dissolution results it was below 5.0% (**II**).

The PRX-Soluplus® nanofibers exhibited completely different dissolution behavior compared to that observed with the PRX-HPMC nanofibers (**Figure 25**) (**IV**). The *in vitro* drug release profiles of PRX-Soluplus® nanofibers were found to be also pH and ionic-strength dependent. Considerable dissolution improvement of PRX was achieved in acidic conditions (pH 1.2), where almost 80% of PRX was released after 30 min (**Figure 25**). Within the corresponding interval, less than 40% of pure PRX was found to be dissolved at pH 7.2. At pH 7.2, the PRX-HPMC nanofibers showed faster dissolution than PRX-Soluplus® nanofibers. With the PRX-Soluplus® nanofibers, the drug release rate was clearly increased when the dissolution medium was changed to distilled water (**Figure 25**). These findings are in agreement with a recent study by Hughey et al. (2013) reporting the effects of kosmotropic salts (anions) on the gel strength and solubility behavior of Soluplus®. The authors stated that at the physiologically relevant temperature of 37 °C, the cloud point of Soluplus® was reached in deionized water and phosphate buffer (pH 6.8) but not in 0.1 N hydrochloric acid (pH 1.2) (Hughey et al., 2013). Obviously, this also explains the prolonged drug release profile of the Soluplus® nanofibrous mats obtained at pH 7.2 (phosphate buffer solution) (**Figure 25**). The dissolution profiles of Soluplus® nanofibers at pH 7.2, however, showed zero-order kinetics and a clear increase in the total time of drug release. This result is in agreement with the behavior of a water-soluble polymer or of a low molecular weight polymer in DDSs, and suggests an erosion-controlled API release mechanism of Soluplus® nanofibrous mats (**IV**).

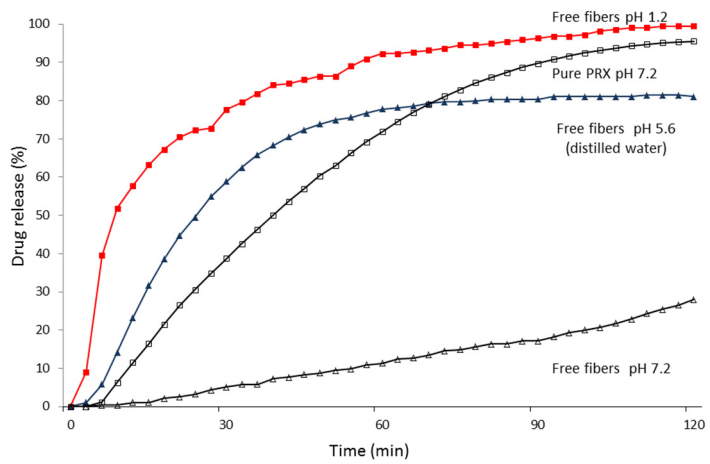

Figure 25. *In vitro* drug release of electrospun non-woven nanomats of PRX and Soluplus® graft copolymer (1:13 w/w ratio) in distilled water, pH 1.2 buffer solution and pH 7.2 phosphate buffer at 37 ± 0.5ºC (n = 5) (**IV**).

6. SUMMARY AND CONCLUSIONS

The main objectives of this thesis were to gain understanding of the amorphization and physical stabilization of a poorly water-soluble API (piroxicam as a model API), to evaluate the validity of ES as a novel technique in fabricating the high-energy amorphous solid dispersions (SDs) of a poorly water-soluble API, and to gather detailed information on the physicochemical, geometrical and dissolution properties of such nanofibrous SDs. The surface morphology, solid state and thermal properties of API and potential solid-state interactions with the polymer(s) were investigated by scanning electron microscopy (SEM), X-ray powder diffraction (XRPD), Raman spectroscopy and differential scanning calorimetry (DSC). Special attention was paid to the geometric properties and surface morphology of drug-loaded nanofibers and nanomats by using scanning white light interferometry (SWLI) for 3D topography analysis. PRX was used as a model poorly water-soluble API, hydroxypropyl methylcellulose (HPMC) and a new synthetic graft copolymer, polyvinyl caprolactam-polyvinyl acetate-polyethylene glycol (PCL-PVAc-PEG, Soluplus®) were investigated as hydrophilic carrier polymers for ES.

ES was found to be applicable for the amorphization of poorly water-soluble PRX and preparing the high-energy amorphous SDs as supersaturated nanofiber matrices. It was possible to reveal the physical stability and dissolution behavior of these electrospun nanofibrous matrices, thus, the fabricated nanofiber matrices showed controlled-release (CR) dissolution behavior. The physicochemical properties, such as stability and dissolution were dependent on the carrier polymer, initial crystalline form of PRX, solvent system and storage conditions applied. HPMC and Soluplus® studied as carrier polymers in ES stabilized the amorphous state of PRX. XRPD and Raman spectroscopy complemented with DSC analysis allowed thorough solid-state characterization of PRX forms and solid-state transformations related to the present nanofibers. SWLI was found to be the method of choice for rapid non-contacting and non-destructive 3D surface topographic analysis of nanofibrous mats. SWLI provided nanometer depth resolution without sample preparation and the method was for the first time used for characterizing the orientation, layer thickness, cross-sectional shape, flattening and the surface morphology of electrospun single nanofibers and nanomats. Such analysis is important because the topography characteristics affect the performance of nanofibrous mats in pharmaceutical and biomedical applications. The two solid-state forms of PRX, anhydrate and monohydrate, showed different solubility and dissolution rate at pH 1.2 (HCl/KCl buffer solution), pH 5.6 (distilled water) and pH 7.2 (phosphate buffer solution). The solubility and dissolution rate of amorphous PRX loaded in electrospun nanofibers were greatly dependent on the physiochemical properties of a carrier polymer.

On the basis of the present results, the following conclusions can be drawn:

1. ES can be used for the amorphization of poorly water-soluble PRX and for fabricating supersaturated CR nanofibrous matrices loaded with PRX. The properties of such CR–SD nanofibers, e.g. the physical stability and dissolution, are dependent on the carrier polymer, initial crystalline form of PRX, solvent system and storage conditions.
2. X-ray powder diffraction (XRPD) and Raman spectroscopy complemented with differential scanning calorimetry (DSC) analysis permit thorough solid-state characterization of PRX forms and its transformations in the electrospun nanofibers. The hydrophilic carrier polymers used in ES are also applicable in stabilizing the amorphous state of PRX in nanofibers.
3. Scanning white light interferometry (SWLI) permits a rapid non-contacting and non-destructive 3D surface topographic analysis of pharmaceutical drug-loaded nanofibrous mats. The method provides nanometer depth resolution without sample preparation. It can be used for characterizing the orientation, layer thickness, cross-sectional shape, flattening and the surface morphology of electrospun single nanofibers and nanomats.
4. The two solid-state forms of PRX, anhydrate and monohydrate, show different solubility and dissolution rate at pH 1.2 (HCl/KCl buffer solution), pH 5.6 (distilled water) and pH 7.2 (phosphate buffer solution). This is due to their different molecular structures and ionization of the molecules.
5. The solubility and dissolution rate of amorphous PRX loaded in electrospun nanofibers are greatly dependent on the physicochemical properties of a carrier polymer.

7. REFERENCES

Aaltonen, J., P. Heinänen, L. Peltonen, H. Kortejärvi, V. P. Tanninen, L. Christiansen, J. Hirvonen, J. Yliruusi, and J. Rantanen, 2006, In situ measurement of solvent-mediated phase transformations during dissolution testing. *J Pharm Sci*, v. 95, p. 2730–2737.

Agarwal, S., J. H. Wendorff, and A. Greiner, 2008, Use of electrospinning technique for biomedical applications. *Polymer*, v. 49, p. 5603–5621.

Airaksinen, S., M. Karjalainen, N. Kivikero, S. Westermarck, A. Shevchenko, J. Rantanen, and J. Yliruusi, 2005, Excipient selection can significantly affect solid-state phase transformation in formulation during wet granulation. *AAPS PharmSciTech*, v. 6, p. E311–322.

Amidon, G. L., H. Lennernas, V. P. Shah, and J. R. Crison, 1995, A theoretical basis for a biopharmaceutic drug classification: the correlation of in vitro drug product dissolution and in vivo bioavailability. *Pharm Res*, v. 12, p. 413–420.

Banerjee, R., H. Chakraborty, and M. Sarkar, 2003, Photophysical studies of oxicam group of NSAIDs: piroxicam, meloxicam and tenoxicam. *Spectrochim Acta A Mol Biomol Spectrosc*, v. 59, p. 1213–1222.

Basf, 2010, Soluplus, Technical Information, p. 1–8.

Bates, T. R., 1969, Dissolution characteristics of reserpine-polyvinylpyrrolidone co-precipitates. *J Pharm Pharmacol*, v. 21, p. 710–712.

Bernstein, J., 2002, *Polymorphism in Molecular Crystals*. IUCr monographs on crystallography. Oxford, New York: Oxford University Press, 428 p.

Bhardwaj, N., and S. C. Kundu, 2010, Electrospinning: A fascinating fiber fabrication technique. *Biotechnol Adv*, v. 28, p. 325–347.

Bhattarai, N., D. Edmondson, O. Veiseh, F. A. Matsen, and M. Zhang, 2005, Electrospun chitosan-based nanofibers and their cellular compatibility. *Biomaterials*, v. 26, p. 6176–6184.

Bordner, J., J. A. Richards, P. Weeks, and E. B. Whipple, 1984, Piroxicam monohydrate: a zwitterionic form, $C_{15}H_{13}N_3O_4S{\cdot}H_2O$. *Acta Crystallogr Sect C: Cryst Struct Commun*, v. 40, p. 989–990.

Brewster, M. E., G. Verreck, I. Chun, J. Rosenblatt, J. Mensch, A. Van Dijck, M. Noppe, A. Ariën, M. Bruining, and J. Peeters, 2004, The use of polymer-based electrospun nanofibers containing amorphous drug dispersions for the delivery of poorly water-soluble pharmaceuticals. *Pharmazie*, v. 59, p. 387–391.

Brittain, H. G., 2009, Theory and Principles of Polymorphic Systems, *in* H. G. Brittain, ed., *Polymorphism in Pharmaceutical Solids*, v. Drugs and the Pharmaceutical Sciences. NY, London: Informa Healthcare, p. 1–23.

Brittain, H. G., 2012, Polymorphism and solvatomorphism 2010. *J Pharm Sci*, v. 101, p. 464–484.

Brittain, H. G., K. R. Morris, and S. X. M. Boerrigter, 2009, Structural Aspects of Solvatomorphic Systems, *in* H. G. Brittan, ed., *Polymorphism in Pharmaceutical Solids*, v. Drugs and the Pharmaceutical Sciences. NY, London: Informa Healthcare, p. 233–280.

Brough, C., and R. O. Williams, 3rd, 2013, Amorphous solid dispersions and nano-crystal technologies for poorly water-soluble drug delivery. *Int J Pharm*, v. 453, p. 157–166.

Brouwers, J., M. E. Brewster, and P. Augustijns, 2009, Supersaturating drug delivery systems: the answer to solubility-limited oral bioavailability?. *J Pharm Sci*, v. 98, p. 2549–2572.

Chemburkar, S. R., J. Bauer, K. Deming, H. Spiwek, K. Patel, J. Morris, R. Henry, S. Spanton, W. Dziki, W. Porter, J. Quick, P. Bauer, J. Donaubauer, B. A. Narayanan, M. Soldani, D. Riley, and K. McFarland, 2000, Dealing with the impact of ritonavir polymorphs on the late stages of bulk drug process development. *Org Process Res Dev*, v. 4, p. 413–417.

Chen, M., P. K. Patra, S. B. Warner, and S. Bhowmick, 2007, Role of fiber diameter in adhesion and proliferation of NIH 3T3 fibroblast on electrospun polycaprolactone scaffolds. *Tissue Eng*, v. 13, p. 579–587.

Chew, S. Y., Y. Wen, Y. Dzenis, and K. W. Leong, 2006, The role of electrospinning in the emerging field of nanomedicine. *Curr Pharm Des*, v. 12, p. 4751–4770.

Chiou, W. L., and S. Riegelman, 1969, Preparation and dissolution characteristics of several fast-release solid dispersions of griseofulvin. *J Pharm Sci*, v. 58, p. 1505–1510.

Chiou, W. L., and S. Riegelman, 1971, Pharmaceutical applications of solid dispersion systems. *J Pharm Sci*, v. 60, p. 1281–1302.

Chronakis, I. S., 2005, Novel nanocomposites and nanoceramics based on polymer nanofibers using electrospinning process – A review. *J Mater Process Technol*, v. 167, p. 283–293.

Chung, S., A. K. Moghe, G. A. Montero, S. H. Kim, and M. W. King, 2009, Nanofibrous scaffolds electrospun from elastomeric biodegradable poly(L-lactide-co-ε-caprolactone) copolymer. *Biomed Mater*, v. 4, p. 015019.

Costantino, H. R., L. Firouzabadian, C. Wu, K. G. Carrasquillo, K. Griebenow, S. E. Zale, and M. A. Tracy, 2002, Protein spray freeze drying. 2. Effect of formulation variables on particle size and stability. *J Pharm Sci*, v. 91, p. 388–395.

Coupland, J. M., and J. Lobera, 2010, Measurement of steep surfaces using white light interferometry. *Strain*, v. 46, p. 69–78.

Craig, D. Q., 2002, The mechanisms of drug release from solid dispersions in water-soluble polymers. *Int J Pharm*, v. 231, p. 131–144.

Crowley, M. M., F. Zhang, M. A. Repka, S. Thumma, S. B. Upadhye, S. K. Battu, J. W. McGinity, and C. Martin, 2007, Pharmaceutical applications of hot-melt extrusion: part I. *Drug Dev Ind Pharm*, v. 33, p. 909–926.

de Waard, H., W. L. Hinrichs, M. R. Visser, C. Bologna, and H. W. Frijlink, 2008, Unexpected differences in dissolution behavior of tablets prepared from solid dispersions with a surfactant physically mixed or incorporated. *Int J Pharm*, v. 349, p. 66–73.

Dhirendra, K., S. Lewis, N. Udupa, and K. Atin, 2009, Solid dispersions: a review. *Pak J Pharm Sci*, v. 22, p. 234–246.

Ding, B., H.-Y. Kim, S.-C. Lee, D.-R. Lee, and K.-J. Choi, 2002, Preparation and characterization of nanoscaled poly(vinyl alcohol) fibers via electrospinning. *Fiber Polymer*, v. 3, p. 73–79.

Dow, 2015a, Hydroxypropyl Methylcellulose, Using METHOCEL cellulose ethers for controlled release of drugs in hydrophilic matrix systems, The Dow Chemical Company.

Dow, 2015b, Using METHOCEL cellulose ethers for controlled release of drugs in hydrophilic matrix systems, Colorcon Inc (US).

Formhals, A., 1934, Process and apparatus for preparing artificial threads, *in* U. S. P. 1975504, ed., http://www.uspto.gov/, USA (July, 2015).
Formhals, A., 1939, Method of producing artificial fibers, *in* U. S. P. 2158415, ed., http://www.uspto.gov/, USA (July, 2015).
Formhals, A., 1943, Production of artificial fibers from fiber forming liquids, *in* U. S. P. 2323025, ed., http://www.uspto.gov/, USA (July, 2015).
Formhals, A., 1944, Method and apparatus for spinning, *in* U. S. P. 234950, ed., http://www.uspto.gov/, USA (July, 2015).
Frenot, A., M. W. Henriksson, and P. Walkenström, 2007, Electrospinning of cellulose-based nanofibers. *J Appl Polym Sci*, v. 103, p. 1473–1482.
Garg, K., and G. L. Bowlin, 2011, Electrospinning jets and nanofibrous structures. *Biomicrofluidics*, v. 5, p. 13403-(1–19).
Geng, X., O. H. Kwon, and J. Jang, 2005, Electrospinning of chitosan dissolved in concentrated acetic acid solution. *Biomaterials*, v. 26, p. 5427–5432.
Genina, N., D. Fors, H. Vakili, P. Ihalainen, L. Pohjala, H. Ehlers, I. Kassamakov, E. Haeggström, P. Vuorela, J. Peltonen, and N. Sandler, 2012, Tailoring controlled-release oral dosage forms by combining inkjet and flexographic printing techniques. *Eu J Pharm Sci*, v. 47, p. 615–623.
Ghasemi-Mobarakeh, L., D. Semnani, and M. Morshed, 2007, A novel method for porosity measurement of various surface layers of nanofibers mat using image analysis for tissue engineering applications. *J Appl Polym Sci*, v. 106, p. 2536–2542.
Grant, D. J. W., 1999, Theory and origin of Polymorphism, *in* H. G. Brittain, ed., *Polymorphism in Pharmaceutical Solids,* v. Drugs and the Pharmaceutical Solids. NY: Marcel Dekker, Inc., p. 1–33.
Griesser, U. J., 2006, The importance of solvates, *in* R. Hilfiker, ed., *Polymorphism: in the pharmaceutical industry*. Weinheim: WILEY-VCH Verlag GmbH & Co. KGaA, p. 211–233.
Groth, P., 1906–1919, *Chemische krystallographie*, Leipzig: Verlag von Wilhelm Engelmann.
Gwak, H. S., J. S. Choi, and H. K. Choi, 2005, Enhanced bioavailability of piroxicam via salt formation with ethanolamines. *Int J Pharm*, v. 297, p. 156–161.
Haleblian, J., and W. McCrone, 1969, Pharmaceutical applications of polymorphism. *J Pharm Sci*, v. 58, p. 911–929.
Hancock, B. C., and G. Zografi, 1997, Characteristics and significance of the amorphous state in pharmaceutical systems. *J Pharm Sci*, v. 86, p. 1–12.
Hanhijärvi, K., T. Majava, I. Kassamakov, J. Heinämäki, J. Aaltonen, J. Haapalainen, E. Haeggström, and J. Yliruusi, 2010, Scratch resistance of plasticized hydroxypropyl methylcellulose (HPMC) films intended for tablet coatings. *Eur J Pharm Biopharm*, v. 74, p. 371–376.
Hardung, H., D. Djuric, and S. Ali, 2010, Combining HME & solubilization: Soluplus® - the solid solution. *Drug Deliv Technol*, v. 10, p. 20–27.
Hu, X., S. Liu, G. Zhou, Y. Huang, Z. Xie, and X. Jing, 2014, Electrospinning of polymeric nanofibers for drug delivery applications. *J Control Release*, v. 185, p. 12–21.
Huang, L. Y., C. Branford-White, X. X. Shen, D. G. Yu, and L. M. Zhu, 2012, Time-engineeringed biphasic drug release by electrospun nanofiber meshes. *Int J Pharm*, v. 436, p. 88–96.
Huang, Y., and W.-G. Dai, 2014, Fundamental aspects of solid dispersion technology for poorly soluble drugs. *Acta Pharm Sinica B*, v. 4, p. 18–25.

Huang, Z.-M., Y.-Z. Zhang, M. Kotaki, and S. Ramakrishna, 2003, A review on polymer nanofibers by electrospinning and their applications in nanocomposites. *Compos Sci Technol*, v. 63, p. 2223–2253.

Hughey, J. R., J. M. Keen, D. A. Miller, K. Kolter, N. Langley, and J. W. McGinity, 2013, The use of inorganic salts to improve the dissolution characteristics of tablets containing Soluplus(R)-based solid dispersions. *Eur J Pharm Sci*, v. 48, p. 758–766.

Ignatious, F., L. Sun, C. P. Lee, and J. Baldoni, 2010, Electrospun nanofibers in oral drug delivery. *Pharm Res*, v. 27, p. 576–588.

Jachowicz, R., 1987, Dissolution rates of partially water-soluble drugs from solid dispersion systems. I. Prednisolone. *Int J Pharm*, v. 35, p. 1–5.

Janković, B., J. Pelipenko, M. Škarabot, I. Muševič, and J. Kristl, 2013, The design trend in tissue-engineering scaffolds based on nanomechanical properties of individual electrospun nanofibers. *Int J Pharm*, v. 455, p. 338–347.

Jannesari, M., J. Varshosaz, M. Morshed, and M. Zamani, 2011, Composite poly(vinyl alcohol)/poly(vinyl acetate) electrospun nanofibrous mats as a novel wound dressing matrix for controlled release of drugs. *Int J Nanomedicine*, v. 6, p. 993–1003.

Janssens, S., H. N. de Armas, J. P. Remon, and G. Van den Mooter, 2007, The use of a new hydrophilic polymer, Kollicoat IR, in the formulation of solid dispersions of Itraconazole. *Eur J Pharm Sci*, v. 30, p. 288–294.

Janssens, S., and G. Van den Mooter, 2009, Review: physical chemistry of solid dispersions. *J Pharm Pharmacol*, v. 61, p. 1571–1586.

Javadzadeh, Y., M. R. Siahi-Shadbad, M. Barzegar-Jalali, and A. Nokhodchi, 2005, Enhancement of dissolution rate of piroxicam using liquisolid compacts. *Farmaco*, v. 60, p. 361–365.

Jayakumar, R., M. Prabaharan, S. V. Nair, and H. Tamura, 2010, Novel chitin and chitosan nanofibers in biomedical applications. *Biotechnol Adv*, v. 28, p. 142–150.

Jayaraman, K., M. Kotaki, Y. Zhang, X. Mo, and S. Ramakrishna, 2004, Recent advances in polymer nanofibers. *J Nanosci Nanotechnol*, v. 4, p. 52–65.

Jinno, J., D. Oh, J. R. Crison, and G. L. Amidon, 2000, Dissolution of ionizable water-insoluble drugs: the combined effect of pH and surfactant. *J Pharm Sci*, v. 89, p. 268–274.

Jørgensen, A., J. Rantanen, M. Karjalainen, L. Khriachtchev, E. Räsänen, and J. Yliruusi, 2002, Hydrate formation during wet granulation studied by spectroscopic methods and multivariate analysis. *Pharm Res*, v. 19, p. 1285–91.

Karatas, A., N. Yuksel, and T. Baykara, 2005, Improved solubility and dissolution rate of piroxicam using gelucire 44/14 and labrasol. *Farmaco*, v. 60, p. 777–782.

Karavas, E., E. Georgarakis, and D. Bikiaris, 2006, Application of PVP/HPMC miscible blends with enhanced mucoadhesive properties for adjusting drug release in predictable pulsatile chronotherapeutics. *Eur J Pharm Biopharm*, v. 64, p. 115–126.

Karavas, E., E. Georgarakis, M. P. Sigalas, K. Avgoustakis, and D. Bikiaris, 2007, Investigation of the release mechanism of a sparingly water-soluble drug from solid dispersions in hydrophilic carriers based on physical state of drug, particle size distribution and drug-polymer interactions. *Eur J Pharm Biopharm*, v. 66, p. 334–347.

Kassamakov, I., K. Hanhijärvi, I. Abbadi, J. Aaltonen, H. Ludvigsen, and E. Haeggström, 2009, Scanning white-light interferometry with a supercontinuum source. *Opt Lett*, v. 34, p. 1582–1584.

Kassamakov, I. V., H. O. Seppänen, M. J. Oinonen, E. O. Hæggström, J. M. Österberg, J. P. Aaltonen, H. Saarikko, and Z. P. Radivojevic, 2007, Scanning white light

interferometry in quality control of single-point tape automated bonding. *Microelectron Eng*, v. 84, p. 114–123.
Kenawy, E.-R., F. Abdel-Hay, M. El-Newehy, and G. E. Wnek, 2009, Processing of polymer nanofibers through electrospinning as drug delivery systems. *Mater Chem Phys*, v. 113, p. 296–302.
Kenawy el, R., G. L. Bowlin, K. Mansfield, J. Layman, D. G. Simpson, E. H. Sanders, and G. E. Wnek, 2002, Release of tetracycline hydrochloride from electrospun poly(ethylene-co-vinylacetate), poly(lactic acid), and a blend. *J Control Release*, v. 81, p. 57–64.
Kogermann, K., J. Aaltonen, C. J. Strachan, K. Pöllänen, P. Veski, J. Heinämäki, J. Yliruusi, and J. Rantanen, 2007, Qualitative in situ analysis of multiple solid-state forms using spectroscopy and partial least squares discriminant modeling. *J Pharm Sci*, v. 96, p. 1802–1820.
Kogermann, K., A. Penkina, K. Predbannikova, K. Jeeger, P. Veski, J. Rantanen, and K. Naelapää, 2013, Dissolution testing of amorphous solid dispersions. *Int J Pharm*, v. 444, p. 40–46.
Kogermann, K., P. Veski, J. Rantanen, and K. Naelapää, 2011, X-ray powder diffractometry in combination with principal component analysis - a tool for monitoring solid state changes. *Eur J Pharm Sci*, v. 43, p. 278–289.
Koradia, V., A. F. de Lemos, M. Alleso, H. L. de Diego, M. Ringkjobing-Elema, A. Müllertz, and J. Rantanen, 2011, Phase transformations of amlodipine besylate solid forms. *J Pharm Sci*, v. 100, p. 2896–2910.
Larkin, K. G., 1996, Efficient nonlinear algorithm for envelope detection in white light interferometry. *J Opt Soc Am A*, v. 13, p. 832–843.
Law, D., W. Wang, E. A. Schmitt, Y. Qiu, S. L. Krill, and J. J. Fort, 2003, Properties of rapidly dissolving eutectic mixtures of poly(ethylene glycol) and fenofibrate: the eutectic microstructure. *J Pharm Sci*, v. 92, p. 505–515.
Leuenberger, H., 2002, Spray Freeze-drying – The Process of Choice for Low Water Soluble Drug. *J Nanoparticle Res*, v. 4, p. 111–119.
Leuner, C., and J. Dressman, 2000, Improving drug solubility for oral delivery using solid dispersions. *Eur J Pharm Biopharm*, v. 50, p. 47–60.
Leung, V., and F. Ko, 2011, Biomedical applications of nanofibers. *Polym Adv Technol*, v. 22, p. 350–365.
Li, D., and Y. Xia, 2004, Electrospinning of nanofibers: reinventing the wheel?. *Adv Mater*, v. 16, p. 1151–1170.
Li, W. J., C. T. Laurencin, E. J. Caterson, R. S. Tuan, and F. K. Ko, 2002, Electrospun nanofibrous structure: a novel scaffold for tissue engineering. *J Biomed Mater Res*, v. 60, p. 613–621.
Li, Z., and C. Wang, 2013, *One-Dimensional nanostructures. Electrospinning Technique and Unique Nanofibers*. SpingerBriefs in Materials. Heidelberg, NY: Springer SBM.
Linn, M., E. M. Collnot, D. Djuric, K. Hempel, E. Fabian, K. Kolter, and C. M. Lehr, 2012, Soluplus® as an effective absorption enhancer of poorly soluble drugs in vitro and in vivo. *Eur J Pharm Sci*, v. 45, p. 336–343.
Loftsson, T., and M. E. Brewster, 2010, Pharmaceutical applications of cyclodextrins: basic science and product development. *J Pharm Pharmacol*, v. 62, p. 1607–1621.
Lohani, S., and D. J. W. Grant, 2006, Thermodynamics of polymorphs, *in* R. Hilfiker, ed., *Polymorphism: in the pharmaceutical industry*. Weinheim: WILEY-VCH Verlag GmbH & Co. KGaA, p. 21–42.

Lombardino, J. G., and J. A. Lowe, 2004, The role of the medicinal chemist in drug discovery-then and now. *Nat Rev Drug Discov*, v. 3, p. 853–862.

Lu, X., C. Wang, and Y. Wei, 2009, One-dimensional composite nanomaterials: synthesis by electrospinning and their applications. *Small*, v. 5, p. 2349–2370.

Madani-Grasset, F., N. T. Pham, E. Glynos, and V. Koutsos, 2008, Imaging thin and ultrathin organic films by scanning white light interferometry. *Mater Sci Eng B*, v. 152, p. 125–131.

Martindale, 2011, Piroxicam, *in* S. C. Sweetman, ed., *Martindale: The complete drug reference*, London. Chicago: Pharmaceutical Press, p. 122–123.

Mayersohn, M., and M. Gibaldi, 1966, New method of solid-state dispersion for increasing dissolution rates. *J Pharm Sci*, v. 55, p. 1323–1324.

McCrone, W. C., 1965, Polymorphism, *in* D. Fox, M. M. Labes, and A. Weissberger, eds., *Physics and chemistry of the organic solid state*, v. 2. NY: Wiley Interscience Inc., p. 725–767.

Megelski, S., J. S. Stephens, D. B. Chase, and J. F. Rabolt, 2002, Micro- and Nanostructured Surface Morphology on Electrospun Polymer Fibers. *Macromolecules*, v. 35, p. 8456–8466.

Meinel, A. J., O. Germershaus, T. Luhmann, H. P. Merkle, and L. Meinel, 2012, Electrospun matrices for localized drug delivery: current technologies and selected biomedical applications. *Eur J Pharm Biopharm*, v. 81, p. 1–13.

Miller, D. A., J. W. McGinity, and R. O. Williams III, 2008, Solid dispersion technologies, *in* R. O. Williams III, D. R. Taft, and J. T. McConville, eds., *Advanced Drug Formulation Design to Optimize Therapeutic Outcomes.* Drugs and the pharmaceutical sciences. NY: Informa Healthcare USA, Inc., p. 451–491.

Min, B. M., G. Lee, S. H. Kim, Y. S. Nam, T. S. Lee, and W. H. Park, 2004, Electrospinning of silk fibroin nanofibers and its effect on the adhesion and spreading of normal human keratinocytes and fibroblasts in vitro. *Biomaterials*, v. 25, p. 1289–1297.

Mit-uppatham, C., M. Nithitanakul, and P. Supaphol, 2004, Ultrafine electrospun polyamide-6 fibers: effect of solution conditions on morphology and average fiber diameter. *Macromol Chem Phys*, v. 205, p. 2327–2338.

Morris, K. R., 1999, Structural aspects of hydrates and solvates, *in* H. G. Brittain, ed., *Polymorphism in Pharmaceutical Solids*. Drugs and the pharmaceutical science: NY: Marcel Dekker, Inc., p. 73–124.

Muhrer, G., U. Meier, F. Fusaro, S. Albano, and M. Mazzotti, 2006, Use of compressed gas precipitation to enhance the dissolution behavior of a poorly water-soluble drug: Generation of drug microparticles and drug–polymer solid dispersions. *Int J Pharm*, v. 308, p. 69–83.

Naelapää, K., J. P. Boetker, P. Veski, J. Rantanen, T. Rades, and K. Kogermann, 2012, Polymorphic form of piroxicam influences the performance of amorphous material prepared by ball-milling. *Int J Pharm*, v. 429, p. 69–77.

Nagy, Z. K., A. Balogh, B. Vajna, A. Farkas, G. Patyi, A. Kramarics, and G. Marosi, 2012, Comparison of electrospun and extruded Soluplus®-based solid dosage forms of improved dissolution. *J Pharm Sci*, v. 101, p. 322–332.

Naraghi, M., I. Chasiotis, H. Kahn, Y. Wen, and Y. Dzenis, 2007, Novel method for mechanical characterization of polymeric nanofibers. *Rev Sci Instrum*, v. 78, p. 085108.

Natu, M. V., H. C. de Sousa, and M. H. Gil, 2010, Effects of drug solubility, state and loading on controlled release in bicomponent electrospun fibers. *Int J Pharm*, v. 397, p. 50–58.

Nyström, M., J. Roine, M. Murtomaa, R. Mohan Sankaran, H. A. Santos, and J. Salonen, 2015, Solid state transformations in consequence of electrospraying - A novel polymorphic form of piroxicam. *Eur J Pharm Biopharm*, v. 89, p. 182–189.

Ohgo, K., C. Zhao, M. Kobayashi, and T. Asakura, 2003, Preparation of non-woven nanofibers of Bombyx mori silk, Samia cynthia ricini silk and recombinant hybrid silk with electrospinning method. *Polymer*, v. 44, p. 841–846.

Okuyama, H., Y. Ikeda, S. Kasai, K. Imamori, K. Takayama, and T. Nagai, 1999, Influence of non-ionic surfactants, pH and propylene glycol on percutaneous absorption of piroxicam from cataplasm. *Int J Pharm*, v. 186, p. 141–148.

Owusu-Ababio, G., N. K. Ebube, R. Reams, and M. Habib, 1998, Comparative dissolution studies for mefenamic acid-polyethylene glycol solid dispersion systems and tablets. *Pharm Dev Technol*, v. 3, p. 405–412.

Palakodaty, S., and P. York, 1999, Phase behavioral effects on particle formation processes using supercritical fluids. *Pharm Res*, v. 16, p. 976–985.

Paudel, A., Z. A. Worku, J. Meeus, S. Guns, and G. Van den Mooter, 2013, Manufacturing of solid dispersions of poorly water soluble drugs by spray drying: Formulation and process considerations. *Int J Pharm*, v. 453, p. 253–284.

Pelipenko, J., P. Kocbek, B. Govedarica, R. Rošic, S. Baumgartner, and J. Kristl, 2013, The topography of electrospun nanofibers and its impact on the growth and mobility of keratinocytes. *Eur J Pharm Biopharm*, v. 84, p. 401–411.

Pelipenko, J., J. Kristl, R. Rosic, S. Baumgartner, and P. Kocbek, 2012, Interfacial rheology: an overview of measuring techniques and its role in dispersions and electrospinning. *Acta Pharm*, v. 62, p. 123–140.

Persano, L., A. Camposeo, C. Tekmen, and D. Pisignano, 2013, Industrial upscaling of electrospinning and applications of polymer nanofibers: a review. *Macromol Mater Eng*, v. 298, p. 504–520.

Petit, S., and G. Coquerel, 2006, The amorphous state, *in* R. Hilfiker, ed., *Polymorphism: in the Pharmaceutical Industry*. Weinheim: WILEY-VCH Verlag GmbH & Co. KGaA, p. 259–285.

PhEur, 2015a, Hypromellose, *European Pharmacopoeia Online 8.5*, Strasbourg: Council of Europe, p. 2466–2468.

PhEur, 2015b, Piroxicam, *European Pharmacopoeia Online 8.5*, p. 3048–3049.

Pokharkar, V. B., L. P. Mandpe, M. N. Padamwar, A. A. Ambike, K. R. Mahadik, and A. Paradkar, 2006, Development, characterization and stabilization of amorphous form of a low T_g drug. *Powder Technol*, v. 167, p. 20–25.

Pouton, C. W., 2006, Formulation of poorly water-soluble drugs for oral administration: Physicochemical and physiological issues and the lipid formulation classification system. *Eur J Pharm Sci*, v. 29, p. 278–287.

Prasad, D., H. Chauhan, and E. Atef, 2014, Amorphous stabilization and dissolution enhancement of amorphous ternary solid dispersions: combination of polymers showing drug–polymer interaction for synergistic effects. *J Pharm Sci*, v. 103, p. 3511–3523.

Reck, G., G. Dietz, G. Laban, W. Günther, G. Bannier, and E. Höhne, 1988, X-ray studies on piroxicam modifications. *Pharmazie*, v. 43, p. 477–481.

Reck, G., and G. Laban, 1990, Prediction and establishment of a new crystalline piroxicam modification. *Pharmazie*, v. 45, p. 257–259.

Repka, M. A., S. K. Battu, S. B. Upadhye, S. Thumma, M. M. Crowley, F. Zhang, C. Martin, and J. W. McGinity, 2007, Pharmaceutical applications of hot-melt extrusion: Part II. *Drug Dev Ind Pharm*, v. 33, p. 1043–1057.

Rogers, T. L., 2009, Hypromellose, *in* R. C. Rowe, P. J. Sheskey, and M. E. Quinn, eds., *Handbook of Pharmaceutical Excipients*. London-Chicago: Pharmaceutical Press, p. 326–329.

Rošic, R., J. Pelipenko, P. Kocbek, S. Baumgartner, M. Bešter-Rogač, and J. Kristl, 2012a, The role of rheology of polymer solutions in predicting nanofiber formation by electrospinning. *Eur Polym J*, v. 48, p. 1374–1384.

Rošic, R., J. Pelipenko, J. Kristl, P. Kocbek, and S. Baumgartner, 2012b, Properties, engineering and applications of polymeric nanofibers: current research and future advances. *Chem Biochem Eng Q*, v. 26, p. 417–425.

Savolainen, M., K. Kogermann, A. Heinz, J. Aaltonen, L. Peltonen, C. Strachan, and J. Yliruusi, 2009, Better understanding of dissolution behaviour of amorphous drugs by in situ solid-state analysis using Raman spectroscopy. *Eur J Pharm Biopharm*, v. 71, p. 71–79.

Schiffman, J. D., and C. L. Schauer, 2008, A Review: electrospinning of biopolymer nanofibers and their applications. *Polym Rev*, v. 48, p. 317–352.

Seddon, K. R., 2004, Pseudopolymorph: A polemic. *Cryst Growth Des*, v. 4, p. 1087–1087.

Sekiguchi, K., and N. Obi, 1961, Stuclies on Absorption of Eutectic Mixture. I. A Comparison of the Behavior of Eutectic Mixture of Sulfathiazol and that of Ordinary Sulfathiazole in Man. *Chem Pharm Bull*, v. 9, p. 866–872.

Sekiguchi, K., N. Obi, and Y. Ueda, 1964, Studies on absorption of eutectic mixture. II. Absorption of fused conglomerates of chloramphenicol and urea in rabbits. *Chem Pharm Bull*, v. 12, p. 134–144.

Seo, A., P. Holm, H. G. Kristensen, and T. Schaefer, 2003, The preparation of agglomerates containing solid dispersions of diazepam by melt agglomeration in a high shear mixer. *Int J Pharm*, v. 259, p. 161–171.

Serajuddin, A. T., 1999, Solid dispersion of poorly water-soluble drugs: early promises, subsequent problems, and recent breakthroughs. *J Pharm Sci*, v. 88, p. 1058–1066.

Sethia, S., and E. Squillante, 2002, Physicochemical characterization of solid dispersions of carbamazepine formulated by supercritical carbon dioxide and conventional solvent evaporation method. *J Pharm Sci*, v. 91, p. 1948–1957.

Shah, S., S. Maddineni, J. Lu, and M. A. Repka, 2013, Melt extrusion with poorly soluble drugs. *Int J Pharm*, v. 453, p. 233–252.

Sheth, A. R., S. Bates, F. X. Muller, and D. J. W. Grant, 2004a, Polymorphism in piroxicam. *Cryst Growth Des*, v. 4, p. 1091–1098.

Sheth, A. R., J. W. Lubach, E. J. Munson, F. X. Muller, and D. J. W. Grant, 2005, Mechanocromism of piroxicam accompanied by intermolecular proton trensfer probed by spectroscopic methods and solid-phase changes. *J Am Chem Soc*, v. 127 (18), p. 6641–6651.

Sheth, A. R., D. Zhou, F. X. Muller, and D. J. Grant, 2004b, Dehydration kinetics of piroxicam monohydrate and relationship to lattice energy and structure. *J Pharm Sci*, v. 93, p. 3013–3026.

Sill, T. J., and H. A. von Recum, 2008, Electrospinning: applications in drug delivery and tissue engineering. *Biomaterials*, v. 29, p. 1989–2006.

Simons, H. L., 1966, Process and apparatus for producing patterned non-woven fabrics, *in A. United States Patent* 3, ed., http://www.uspto.gov/ (July, 2015).

Srinivasan, G., and D. H. Reneker, 1995, Structure and morphology of small diameter electrospun aramid fibers. *Polym Int*, v. 36, p. 195–201.

Stahly, P. G., 2007, Diversity in single- and multiple-component crystals. The search for and prevalence of polymorphs and cocrystals. *Cryst Growth Des*, v. 7(6), p. 1007–1026.

Stranska, D., I. Erlebachova, V. Kral, P. Sebek, J. Beranek, A. Dumicic, G. Sedmak, T. Chvojka, and a. s. Zentiva, 2014, Drug formulation using API in nanofibers, *in* E. P. Office, ed., https://www.google.co.in/patents/EP2813212A1?cl=en (July, 2015).

Stulzer, H. K., M. P. Tagliari, A. P. Cruz, M. A. S. Silva, and M. C. M. Laranjeira, 2008, Compatibility studies between piroxicam and pharmaceutical excipients. *Pharm Chem J*, v. 42, p. 215–219.

Tachibana, T. and A. Nakamura, 1965, A methode for preparing an aqueous colloidal dispersion of organic materials by using water-soluble polymers: dispersion of β-carotene by polyvinylpyrrolidone. *Kolloid-Zeitschrift und Zeitschrift für Polymere*, v.203, p.130-133.

Taepaiboon, P., U. Rungsardthong, and P. Supaphol, 2006, Drug-loaded electrospun mats of poly(vinyl alcohol) fibres and their release characteristics of four model drugs. *Nanotechnology*, v. 17, p. 2317–2329.

Tan, E. P. S., and C. T. Lim, 2005, Nanoindentation study of nanofibers. *Appl Phys Lett*, v. 87, p. 123106.

Tan, E. P. S., and C. T. Lim, 2006, Mechanical characterization of nanofibers – A review. *Comp Sci Technol*, v. 66, p. 1102–1111.

Taylor, G. I., 1964, Disintegration of Water Drops in an Electric Field. *Proceedings of the Royal Society A*, v. 280, p. 383–387.

Taylor, G. I., 1969, Electrically Driven Jets. *Proceedings of the Royal Society A*, v. 313, p. 453–475.

Taylor, L. S., and S. L. Shamblin, 2009, Amorphous solids, *in* H. G. Brittain, ed., *Polymorphism in pharmaceutical solids*. Drugs and the pharmaceutical sciences, NY: Informa Healthcare, p. 587–629.

Taylor, L. S., and G. Zografi, 1997, Spectroscopic characterization of interactions between PVP and indomethacin in amorphous molecular dispersions. *Pharm Res*, v. 14, p. 1691–1698.

Teo, W. E., and S. Ramakrishna, 2006, A review on electrospinning design and nanofibre assemblies. *Nanotechnology*, v. 17, p. R89-R106.

Timko, R. J., and N. G. Lordi, 1979, Thermal characterization of citric acid solid dispersions with benzoic acid and phenobarbital. *J Pharm Sci*, v. 68, p. 601–605.

Tran, P. H., T. T. Tran, J. B. Park, and B. J. Lee, 2011, Controlled release systems containing solid dispersions: strategies and mechanisms. *Pharm Res*, v. 28, p. 2353–2378.

USP28-NF23, 2005, *The United States Pharmacopeia, The National Formulary* (USP28-NF23). Rockville, Md, USA: United States Pharmacopoeial Convention, p. 2412.

Van den Mooter, G., I. Weuts, T. De Ridder, and N. Blaton, 2006, Evaluation of Inutec SP1 as a new carrier in the formulation of solid dispersions for poorly soluble drugs. *Int J Pharm*, v. 316, p. 1–6.

van Drooge, D. J., W. L. Hinrichs, and H. W. Frijlink, 2004, Anomalous dissolution behaviour of tablets prepared from sugar glass-based solid dispersions. *J Control Releas*e, v. 97, p. 441–452.

van Drooge, D. J., W. L. Hinrichs, M. R. Visser, and H. W. Frijlink, 2006, Characterization of the molecular distribution of drugs in glassy solid dispersions at the nano-meter scale, using differential scanning calorimetry and gravimetric water vapour sorption techniques. *Int J Pharm*, v. 310, p. 220–229.

Vasconcelos, T., B. Sarmento, and P. Costa, 2007, Solid dispersions as strategy to improve oral bioavailability of poor water soluble drugs. *Drug Discov Today*, v. 12, p. 1068–1075.

Verheyen, S., N. Blaton, R. Kinget, and G. Van den Mooter, 2002, Mechanism of increased dissolution of diazepam and temazepam from polyethylene glycol 6000 solid dispersions. *Int J Pharm*, v. 249, p. 45–58.

Verreck, G., I. Chun, J. Peeters, J. Rosenblatt, and M. E. Brewster, 2003a, Preparation and characterization of nanofibers containing amorphous drug dispersions generated by electrostatic spinning. *Pharm Res*, v. 20, p. 810–817.

Verreck, G., I. Chun, J. Rosenblatt, J. Peeters, A. V. Dijck, J. Mensch, M. Noppe, and M. E. Brewster, 2003b, Incorporation of drugs in an amorphous state into electrospun nanofibers composed of a water-insoluble, nonbiodegradable polymer. *J Control Release*, v. 92, p. 349–360.

Vilhelmsen, T., H. Eliasen, and T. Schaefer, 2005, Effect of a melt agglomeration process on agglomerates containing solid dispersions. *Int J Pharm*, v. 303, p. 132–142.

Vippagunta, S. R., H. G. Brittain, and D. J. Grant, 2001, Crystalline solids. *Adv Drug Deliv Rev*, v. 48, p. 3–26.

Vippagunta, S. R., Z. Wang, S. Hornung, and S. L. Krill, 2007, Factors affecting the formation of eutectic solid dispersions and their dissolution behavior. *J Pharm Sci*, v. 96, p. 294–304.

Vo, C. L., C. Park, and B. J. Lee, 2013, Current trends and future perspectives of solid dispersions containing poorly water-soluble drugs. *Eur J Pharm Biopharm*, v. 85, p. 799–813.

Vrečer, F., S. Srčič, and J. Šmid-Korbar, 1991, Investigation of piroxicam polymorphism. *Int J Pharm*, v. 68, p. 35–41.

Vrečer, F., M. Vrbinc, and A. Meden, 2003, Characterization of piroxicam crystal modifications. *Int J Pharm*, v. 256, p. 3–15.

Vynckier, A.-K., L. Dierickx, J. Voorspoels, Y. Gonnissen, J. P. Remon, and C. Vervaet, 2014, Hot-melt co-extrusion: requirements, challenges and opportunities for pharmaceutical applications. *J Pharm Pharmacol*, v. 66, p. 167–179.

Wagenaar, B. W., and B. W. Müller, 1994, Piroxicam release from spray-dried biodegradable microspheres. *Biomaterials*, v. 15, p. 49–54.

Wang, X., A. Michoel, and G. Van den Mooter, 2005, Solid state characteristics of ternary solid dispersions composed of PVP VA64, Myrj 52 and itraconazole. *Int J Pharm*, v. 303, p. 54–61.

Wendorff, J. H., S. Agarwal, and A. Greiner, 2012, *Electrospinning: Materials, Processing, and Applications*. Weinheim: Wiley-VCH Verlag GmbH & Co. KGaA, 242 p.

Won, D.-H., M.-S. Kim, S. Lee, J.-S. Park, and S.-J. Hwang, 2005, Improved physicochemical characteristics of felodipine solid dispersion particles by supercritical anti-solvent precipitation process. *Int J Pharm*, v. 301, p. 199–208.

Wu, K., J. Li, W. Wang, and D. A. Winstead, 2009, Formation and characterization of solid dispersions of piroxicam and polyvinylpyrrolidone using spray drying and precipitation with compressed antisolvent. *J Pharm Sci*, v. 98, p. 2422–2431.

Yao, W.-W., T.-C. Bai, J.-P. Sun, C.-W. Zhu, J. Hu, and H.-L. Zhang, 2005, Thermodynamic properties for the system of silybin and poly(ethylene glycol) 6000. *Thermochim Acta*, v. 437, p. 17–20.

Yoshioka, M., B. C. Hancock, and G. Zografi, 1994, Crystallization of indomethacin from the amorphous state below and above its glass transition temperature. *J Pharm Sci*, v. 83, p. 1700–1705.

Yu, D.-G., L.-M. Zhu, K. White, and C. Branford-White, 2009, Electrospun nanofiber-based drug delivery systems. *Health*, v. 1, p. 67–75.

Yu, L., 2001, Amorphous pharmaceutical solids: preparation, characterization and stabilization. *Adv Drug Deliv Rev*, v. 48, p. 27–42.

Yüksel, N., A. Karatas, Y. Ozkan, A. Savaser, S. A. Ozkan, and T. Baykara, 2003, Enhanced bioavailability of piroxicam using Gelucire 44/14 and labrasol: in vitro and in vivo evaluation. *Eur J Pharm Biopharm*, v. 56, p. 453–459.

Zahedi, P., I. Rezaeian, S.-O. Ranaei-Siadat, S.-H. Jafari, and P. Supaphol, 2010, A review on wound dressings with an emphasis on electrospun nanofibrous polymeric bandages. *Polym Adv Technol*, v. 21, p. 77–95.

Zeleny, J., 1914, The electrical discharge from liquid points, and a hydrostatic method of measuring the electric intensity at their surfaces. *Phys Rev*, v. 3, p. 69–91.

Zhang, G. G., D. Law, E. A. Schmitt, and Y. Qiu, 2004, Phase transformation considerations during process development and manufacture of solid oral dosage forms. *Adv Drug Deliv Rev*, v. 56: Netherlands, p. 371–390.

Zhang, Y. Z., B. Su, J. Venugopal, S. Ramakrishna, and C. T. Lim, 2007, Biomimetic and bioactive nanofibrous scaffolds from electrospun composite nanofibers. *Int J Nanomedicine*, v. 2, p. 623–638.

Zimmermann, A., F. Tian, H. Lopez de Diego, M. Ringkjobing Elema, J. Rantanen, A. Müllertz, and L. Hovgaard, 2009, Influence of the solid form of siramesine hydrochloride on its behavior in aqueous environments. *Pharm Res*, v. 26, p. 846–854.

Zong, X., K. Kwangsok, D. Fang, S. Ran, B. S. Hsiao, and B. Chu, 2002, Structure and process relationship of electrospun bioabsorbable nanofiber membranes. *Polymer*, v. 43, p. 4403–4412.

8. SUMMARY IN ESTONIAN

Uued võimalused vees halvasti lahustuvate raviainete amorfse vormi saamiseks ja füüsikaliseks stabiliseerimiseks ning nende lahustumiskäitumise uurimine

Sissejuhatus

Juba XIX sajandil märkasid keemikud, et ühe keemilise aine või ühendi kristallid võivad olla erineva kujuga ja sellest tulenevalt ka erinevate füüsikaliste omadustega (sulamistemperatuur, lahustumiskiirus jm). Nähtust hakati nimetama polümorfismiks ja vastavaid ühendeid polümorfideks (Brittain, 2009; Grant, 1999). Selle nähtuse olulisust keemias ja eriti farmaatsias mõisteti juba XX sajandi keskpaigas (Haleblian and McCrone, 1969; McCrone, 1965). Kui ühe keemilise ühendi struktuuri on kaasatud ka lahusti molekulid, siis nimetatakse selliseid ühendeid solvaatideks ja nähtust solvatomorfismiks. Juhul, kui solvendiks on vesi, siis hüdraatideks (Brittain et al., 2009; Morris, 1999; Seddon, 2004). Paljud raviained võivad eksisteerida erinevates tahketes polümorfsetes või solvaatsetes vormides ja ka amorfses olekus. Kuna kõigil neil vormidel on erinev sisemine kristallstruktuur ja vabaenergia, siis on neil ka erinevad füsikokeemilised omadused, mis mõjutavad oluliselt raviaine käitumist organismis. Neist kõige olulisemad ravimpreparaadi seisukohast on raviaine lahustuvus ja lahustumiskiirus. Tavaliselt on üks polümorf kindla temperatuuri ja rõhu väärtuse juures termodünaamiliselt kõige püsivam ja teised vormid (nimetatud ka metastabiilseteks vormideks) muutuvad vabaenergia vähenemise tõttu aja jooksul kõige stabiilsemaks vormiks. Amorfsed ained on kõige ebastabiilsemad tahke aine vormid ja nende puhul on tegemist mittekristalliliste ainetega, millel puudub kindel kolmedimensionaalne kristallstruktuur ja molekulide järjestatus. Kuigi varasemas kirjanduses on eksitavalt amorfset ainet käsitletud ka kui ühte polümorfset vormi (Haleblian and McCrone, 1969; Petit and Coquerel, 2006). Eristatakse aineid, mis on oma olemuselt amorfsed ja neid, mis on erinevate võtetega amorfsesse olekusse viidud. Neid viimaseid käsitletakse ka tänapäeval siiski tahke aine ühe vormina (Taylor and Shamblin, 2009). Tänu oma kristallvormi puudumisele ja kõrgele siseenergiale lahustub amorfne raviaine kõige kiiremini ja tema lahustuvus on reeglina teistest kristallvormidest suurem. Samuti on amorfse vormi kõrge siseenergia tema suure ebastabiilsuse põhjuseks ning amorfsed ained võivad kergesti rekristalliseeruda. Sellise rekristalliseerumise tagajärjel võib oluliselt muutuda raviaine lahustuvus, lahustumiskiirus ja biosaadavus organismis (Lohani and Grant, 2006). Farmaatsias on kasutusel mitmeid võimalusi amorfsete tahkete ainete saamiseks nagu näiteks külmutus- või pihustuskuivatamine, peenestamine, märg granuleerimine jne, kuid saadud amorfne tahke aine on oluliselt vähem stabiilne, kui tema vastav kristallvorm (Yu, 2001).

Kaasajal omavad ca 80% turul olevatest raviainetest polümorfseid või solvaatvorme (Lohani and Grant, 2006; Stahly, 2007) ja samas sisaldavad

umbes 40% turustatavatest ning ca 90% arendamisel olevatest uutest ravimpreparaatidest vees halvasti lahustuvaid raviaineid (Loftsson and Brewster, 2010). Seega, kuna halb või vähene vesi-lahustuvus on ravimpreparaatide valmistamisel üks võtmeküsimusi, eriti Biofarmatseutilise klassifikatsiooni süsteemi (BSC) II klassi raviainete puhul, kus lahustumiskiirus on imendumist limiteerivaks faktoriks, on raviainete lahustuvuse, lahustumiskiiruse ja seega ka biosaadavuse suurendamine üks olulisi teemasid farmaatsiatööstuse jaoks.

Piroksikaam (PRX) on oksikaamide gruppi kuuluv vees halvasti lahustuv raviaine, mida sageli kasutatakse tema huvitavate füsikokeemiliste omaduste tõttu mudelraviainena teaduslikus uurimistöös. Tema tahke aine erinevad vormid (PRX amorfne vorm ja veevabad kristallvormid I (PRXAH), II, III ning monohüdraatvorm, PRXMH) on kirjanduses hästi dokumenteeritud ning omavad lisaks erinevale kristalli kujule ka erinevat värvust ja seetõttu on tahke aine vormide üleminek ühest vormist teise sageli visuaalselt jälgitav (Kogermann et al., 2007; Nyström et al., 2015; Sheth et al., 2005; Vrečer et al., 2003). PRX kuulub BCS järgi II klassi, kui halvasti lahustuv ja hästi imenduv raviaine (Amidon et al., 1995; Gwak et al., 2005; Lombardino and Lowe, 2004). Et PRX omab kahte pK_a väärtust (1,86 ja 5,46), siis võib ta seetõttu käituda nii happe kui alusena vastavalt keskkonnale (Banerjee et al., 2003; Jinno et al., 2000).

Tahkete dispersioonidena tuntakse täna farmaatsias süsteeme, kus tahke raviaine on dispergeeritud tahkes inertses kandjas, kus pole detekteeritav teine faas. Raviaine võib olla tahkes dispersioonis kas dispergeeritult kandjas molekulaarsel tasemel (tahke lahus) või amorfsete osakestena, või siis kristalliliste osakestena kandjas, mis võib omakorda olla kas kristalliline või amorfne (Miller et al., 2008; Vo et al., 2013). Tahked dispersioonid on osutunud edukaks vees halvasti lahustuvate raviainete lahustuvuse parandamisel ja nende biosaadavuse suurendamisel, kuid endiselt on probleeme raviaine püsivuse tagamisega tahkete dispersioonide tootmisprotsessi jooksul ja säilitamisel ning see võib oluliselt muuta raviaine biosaadavust organismis (Brouwers et al., 2009; Janssens and Van den Mooter, 2009; Leuner and Dressman, 2000; Vo et al., 2013).

Elektrospinnimine (ES) on tahkete polümeersete nanofiibrite valmistamise tehnika, mida tuntakse juba möödunud sajandi algusest (Zeleny, 1914). Kaasajal on tehnikat täiustatud ja ES-l võib saada nanofiibreid peaaegu kõigist polümeeridest, kui valida sobiv solventsüsteem ning ES tingimused. Raviainete viimine ES polümeerilahuste koostisesse on uus võimalus raviainete lahustuvuse ja seega ka biosaadavuse muutmiseks. Moodustuvates tahketes dispersioonides on raviaine sageli dispergeeritud molekulaarsel tasemel või muudab inkorporeerimise protsessi ajal oma tahke aine vormi (Huang and Dai, 2014; Nagy et al., 2012; Rošic et al., 2012b).

Töö eesmärgid

Töö eesmärgiks oli saada teadmisi vees halvasti lahustuva raviaine, piroksikaami (PRX) amorfse vormi tekkest ja stabiilsusest elektrospinnimisel saadud nanofiibrites ning PRX kristallvormide lahustumiskäitumisest.
Täpsemad töö eesmärgid olid:

- kasutada elektrospinnimist kui uut võimalust raviaine kontrollitud vabanemisega tahke amorfse dispersiooni saamiseks halvasti lahustuvast raviainest, PRX ja hüdrofiilsetest polümeeridest;
- kasutada skaneeriva valge valgusega interferomeetriat (SWLI) kui potentsiaalset uut meetodit, mis ei vaja proovi ettevalmistamist, elektrospinnitud raviaine nanofiiber-võrgu pinnaomaduste kiireks, kontaktivabaks ja kahjutuks 3D analüüsimiseks;
- selgitada välja hüdrofiilsete polümeeride, eriti uue sünteetilise pook-kopolümeeri Soluplus® (PCL-PVAc-PEG, polüvinüülkaprolaktaam-polüvinüülatsetaat-polüetüleenglükool pook-kopolümeer) ja solventsüsteemide mõju raviainet sisaldavate nanofiibrite stabiilsusele ja raviaine tahke vormi muutustele neis;
- teha täpsemalt kindlaks pH mõju PRX kahe tahke vormi (veevaba PRXAH ja monohüdraadi PRXMH) lahustuvusele ja lahustumiskiirusele;
- saada teadmisi vees halvasti lahustuva raviaine PRX vabanemis- ja lahustumiskiirusest polümeersetest elektrospinnitud nanofiibritest.

Materjalid Ja meetodid

Uuringus kasutati mudelraviainena vees halvasti lahustuvat piroksikaami, PRX [nii veevaba piroksikaami vorm I (PRXAH I) kui monohüdraatvormi (PRXMH), mis valmistati ise]. Hüdrofiilsete polümeeridena kasutati hüdroksüpropüülmetüültselluloosi (HPMC) keskmise molekulmassiga 100 000 Da (Methocel™ K100M Premium CR) ja pook-kopolümeeri Soluplus® (PCL-PVAc-PEG, polüvinüülkaprolaktaam-polüvinüülatsetaat-polüetüleenglükool pook-kopolümeer). Solventidena elektrospinnimisel kasutati vastavalt 1,1,1,3,3,3-heksafluoro-2-propanooli (HFIP) ja atsetooni.

Uuringus kasutatud meetodite hulka kuulusid elektrospinnimine ning saadud nanofiibrite suuruse ja kuju uurimine skaneeriva elektronmikroskoobi (SEM) ning pinna 3D topograafia uurimine skaneeriva valge valguse interferomeetri (SWLI) abil. Raviaine füsikokeemilisi omadusi ning vormide vahelisi muutusi säilitamisel uuriti kasutades erinevaid meetodeid: Raman spektroskoopiat, pulber-röntgendifraktomeetriat (XRPD) ja diferentsiaalset skaneerivat kalorimeetriat (DSC).

PRX vormide ja PRXi sisaldavate nanofiibrite lahustumiskiiruse uurimiseks kasutati *in vitro* dissolusiooniteste vastavalt USP 28 korvikeste meetodile kasutades kolme erinevat lahustumiskeskkonda: pH 1,2 (HCl/KCl puhverlahus), pH 5,6 (destilleeritud vesi) ja pH 7,2 (fosfaatpuhver). Nanofiiber-võrgustik viidi korvikestesse kas pakitult kõvadesse želatiinkapslitesse või lahtiselt.

Uuringu põhitulemused

Elektrospinnimine sobib vees halvasti lahustuva raviaine, piroksikaami (PRX) amorfse vormi saamiseks. Pulber-röntgendidraktomeetria (XRPD), Raman spektroskoopia ja diferentsiaalse skaneeriva kalorimeetria (DSC) tulemused kinnitasid, et erinevate hüdrofiilsete polümeeridega (HPMC ja Soluplus®) elektrospinnimisel saadud nanofiibrites moodustub üleküllastunud tahke dispersioon, milles PRX püsib amorfses vormis nii külmkapitemperatuuril (LT) 6–8º C kui ka toatemperatuuril (RT) 22±2º C ja 0%-lise suhtelise niiskuse (RH) juures kuni 6 kuud. Moodustunud üleküllastunud tahkete dispersioonide omadused, nagu füüsikaline stabiilsus ja lahustumine, on sõltuvuses nii kasutatud polümeerist, PRX algsest kristallivormist, kasutatud solvendist (solventsüsteemist) ja säilitamistingimustest. Kõrgem temperatuur ja suurem õhuniiskus ning suurem PRX kontsentratsioon nanofiibrites viivad kiirema raviaine kristallvormi muutuseni.

SEM võimaldab saadud SEM piltidelt näha tekkinud nanofiibrite kuju, homogeensust ning mõõta nende diameetrit, kuid hinnata tekkinud nanofiibri pinnastruktuuri ja saada 3D ettekujutust on raskem. Ka vajab SEM uuring proovide ettevalmistamist (kullaga katmist) ning seetõttu on aja- ning töömahukas. SWLI on kiirelt kasutatav ilma eelneva täiendava uuritava proovi ettevalmistuseta, see on kontaktivaba ja kahjutu nanomeeter-skaalas resolutsiooniga meetod pinna kolmedimensionaalseks (3D) topograafiliseks analüüsiks. SWLI meetodit kasutati esmakordselt üksiku elektrospinnitud nanofiibri ja nanofiiber-võrgustiku orientatsiooni, kihi paksuse, ristlõike kuju ja pinna morfoloogia uurimiseks. Selline uuring on oluline, kuna topograafilised omadused mõjutavad nanofiiber-võrgustike kasutatavust farmaatsias ja biomeditsiinis.

PRX-i kaks tahke aine vormi, veevaba vorm (PRXAH) ning PRX monohüdraat vorm (PRXMH), omavad erinevat lahustuvust ning lahustumiskiirust erinevates keskkondades: pH 1,2 (HCl/KCl puhverlahuses), pH 5,6 (destilleeritud vees) ja pH 7,2 (fosfaatpuhvris). PRXAH omab suuremat lahustuvust kõigis uuritud keskkondades võrreldes PRXMH-ga ($p<0,05$), vaid katse alguses pH 7,2 ja pH 1,2 juures oli PRXMH lahustumiskiirus suurem kui PRXAH-l. Elektrospinnitud nanofiibrites oleva PRX amorfse vormi lahustuvus ja lahustumiskiirus on otseses sõltuvuses vastava polümeeri füsikokeemilistest omadustest. Nii on PRX/HPMC nanofiibritest vabaneva PRX lahustumiskiirus vähem sõltuvuses lahustumiskeskkonna pH-st kui puhta PRXAH lahustumise korral, olles pH 1,2 juures vaid veidi väiksem kui pH 7,2 juures. PRX vabaneb HPMC nanofiibritest aeglaselt, mis teeb elektrospinnitud nanofiiber-võrgustiku sobivaks raviainet prolongeeritult (reguleeritult) vabastava ravimvormi valmistamiseks. Ka Soluplus®-i pook-kopolümeerist vabaneb PRX amorfne vorm aeglaselt, kuid erinevalt PRX/HPMC nanofiibritest on PRX/Soluplus® nanofiibritest vabaneva PRX lahustumiskiirus kõige väikesem pH 7,2 juures ning kõige suurem pH 1,2 juures.

Järeldused:

1. Elektrospinnimist saab kasutada vees halvasti lahustuva raviaine, piroksikaami (PRX) amorfse vormi saamiseks. Saadud nanofiiber-võrgustikud on PRX kontrollitult vabastavad üleküllastunud tahked dispersioonid, mille omadused nagu füüsikaline stabiilsus ja lahustumine on sõltuvuses kasutatud polümeerist, PRX algsest kristallvormist, kasutatud solventsüsteemist ja säilitamise tingimustest.
2. Pulber-röntgendifraktomeetriline (XRPD) ja Raman spektroskoopiline ja täiendav diferentsiaalne skaneeriv kalorimeetriline (DSC) analüüs võimaldavad määrata PRX vorme ja nende muutumist elektrospinnitud nanofiibrites. Kasutatud polümeerid stabiliseerivad PRX amorfse oleku nanofiibrites.
3. Skaneeriv valge valguse interferomeetria (SWLI) on kontaktivaba ja kahjutu nanomeeter-skaalas resolutsiooniga meetod pinna kolmemõõtmeliseks (3D) topograafiliseks analüüsiks, mida saab kasutada kiiresti ilma eelneva proovi ettevalmistuseta. SWLI meetodit saab kasutada üksiku elektrospinnitud nanofiibri ja nanofiiber-võrgustiku orientatsiooni, kihi paksuse, ristlõike kuju ja pinna morfoloogia uurimiseks. Selline uuring on oluline, kuna topograafilised omadused mõjutavad nanofiiber-võrgustike kasutatavust farmaatsias ja biomeditsiinis.
4. PRX-i kaks kristallivormi, veevaba vorm I ning monohüdraat, omavad erinevat lahustuvust ning lahustumiskiirust pH 1,2 (HCl/KCl puhverlahuses), pH 5,6 (destilleeritud vees) ja pH 7,2 (fosfaatpuhvris) oma erineva molekulaarse struktuuri ja ionisatsiooni tõttu.
5. Elektrospinnitud nanofiibrites oleva amorfse PRX lahustuvus ja lahustumiskiirus on otseses sõltuvuses kasutatud polümeeri omadustest.

ACKNOWLEDGEMENTS

This work was mainly carried out at the Department of Pharmacy, Faculty of Medicine, University of Tartu, Estonia during the years 2011–2015. Some additional experiments were performed at the Division of Pharmaceutical Chemistry and Technology, Faculty of Pharmacy, and the Electronics Laboratory, Department of Physics, University of Helsinki. The XRPD and SEM experiments were conducted at the Department of Geology, University of Tartu and at the Institute of Physics, University of Tartu, respectively.

The work was part of the targeted financing project no SF0180042s09 and ETF project no 7980. The work was partially supported by the Institutional Research Funding (IUT 34–18). I would like to acknowledge the Estonian Science Foundation and the Estonian Ministry of Education and Research, the NordForsk, the European Social Fund's Doctoral Studies and Internationalization Program DoRa for financial support.

I wish to thank all the persons that were involved with this study at the University of Tartu, Estonia and at the University of Helsinki, Finland.

I wish to express my sincere and deepest gratitude to:

- Associate Professor Karin Kogermann and Professor Jyrki Heinämäki, the supervisors of this thesis, for their time, excellent guidance and encouragement. Their supervision, patience and warm support made my PhD journey easier.
- Professor Peep Veski, who sadly passed away, for his continuous support, inspiration, knowledge, he shared with me during fruitful discussions, professional advices, and motivating in critical times.
- Professor Aleksandr Žarkovski and Professor Ursel Soomets for reviewing the thesis.
- All my co-authors and co-workers from Tartu:
  - Prof. V. Sammelselg and PhD student J. Kozlova from the Institute of Physics, University of Tartu for help in SEM studies;
  - Mr P. Paaver from the Institute of Ecology and Earth Sciences, University of Tartu, who taught me to use SEM myself;
  - Prof. K. Kirsimäe and Mr J. Aruväli from the Institute of Ecology and Earth Sciences, University of Tartu for their help with XRPD studies;
  - Dr. A. Lust, Dr. A. Klugman, Dr. I Laidmäe and M.Sc (Pharm) I. Tamm for fruitful discussions, help and support;
  - Mrs K. Kustavus for her assistance in drawing structural formulas of chemicals;
  - My students E. Sillaste, P. Mägar for participating in lab experiments.
- All my co-authors from Helsinki, Copenhagen, and Cambridge:
  - Prof. E. Hæggström, Dr. I. Kassamakov, T. Ylitalo and A.Nolvi from the Department of Physics, University of Helsinki for SWLI experiments.
  - Prof. J. Rantanen from the Department of Pharmaceutics and Analytical Chemistry, University of Copenhagen, Denmark

- Dr. S. Mirza from the School of Engeneering and Applied Sciences at Harvard University, Cambridge, MA, USA
- All my friends, for their support.

Finally, I wish to express my love to my family, my children Triin, Jaanus and Andres, for supporting me always, for their patience and understanding.

Urve Paaver,
Tartu 2015

PUBLICATIONS

CURRICULUM VITAE

Name: Urve Paaver
Date of birth: September 21, 1958, Tartu, Estonia
Citizenship: Estonian
Address: Department of Pharmacy, University of Tartu
Nooruse 1, 50411, Tartu, Estonia
Phone: +372 737 5282
E-mail: urve.paaver@ut.ee

Education:

1965–1975	Tartu 5th Secondary School
1976–1981	University of Tartu, Faculty of Medicine, Department of Pharmacy, pharmacist
2006–2006	University of Tartu, Faculty of Physics and Chemistry, Institute of Organic and Bioorganic Chemistry (MSc)
2012–2015	University of Tartu, Faculty of Medicine, PhD studies, extern

Professional employment:

2011–…	University of Tartu, Faculty of Medicine, Department of Pharmacy, lecturer of pharmaceutical technology
2007–2011	University of Tartu, Faculty of Medicine, Department of Pharmacy, Chair of Pharmacognosy and Pharmaceutical Management, lecturer
2006–2007	University of Tartu, Faculty of Medicine, Department of Pharmacy, Chair of Pharmacognosy and Pharmaceutical Management, researcher
1988–2006	University of Tartu, Faculty of Medicine, Department of Pharmacy, Chair of Pharmacognosy and Pharmaceutical Management, assistant
1981–1988	University of Tartu, Faculty of Medicine, Department of Pharmacy, Chair of Pharmacognosy and Pharmaceutical Management, senior engineer-botanist

Research interest:

The design and quality assessment of multifunctional nanomedicines.
Solid state properties of pharmaceuticals and their modification possibilities.
The functionality related characteristics of excipients for pharmaceutical dosage forms.

I have 10 scientific publications and more than 60 presentations at international scientific conferences.

Publications:

Heinämäki, J.; Halenius, A.; Paavo, M.; Alakurtti, S.; Pitkänen, P.; Pirttimaa, M.; **Paaver, U.**; Kirsimäe, K.; Kogermann, K.; Yliruusi, J. (2015). Suberin fatty acids isolated from outer birch bark improve moisture barrier properties of cellulose ether films intended for tablet coatings. International Journal of Pharmaceutics, 489, 91–99.

Paaver, U.; Heinämäki, J.; Laidmäe, I.; Lust, A.; Kozlova, J.; Sillaste, E.; Kirsimäe, K.; Veski, P.; Kogermann, K. (2015). Electrospun nanofibers as a potential controlled-release solid dispersion system for poorly water-soluble drugs. International Journal of Pharmaceutics, 479(1), 252–260.

Paaver, U.; Heinämäki, J.; Kassamakov, I.; Hæggström, E.; Ylitalo, T.; Nolvi, A.; Kozlova, J.; Laidmäe, I.; Kogermann, K.; Veski, P. (2014). Nanometer depth resolution in 3D topographic analysis of drug-loaded nanofibrous mats without sample preparation. International Journal of Pharmaceutics, 462(1–2), 29–37.

Paaver, U.; Tamm, I.; Laidmäe, I.; Lust, A.; Kirsimäe, K.; Veski, P.; Kogermann, K.; Heinämäki, J. (2014). Soluplus Graft Copolymer: Potential Novel Carrier Polymer in Electrospinning of Nanofibrous Drug Delivery Systems for Wound Therapy. BioMed Research International, 2014(ID 789765), 1–7.

Paaver, U.; Lust, A.; Mirza, S.; Rantanen, J.; Veski, P.; Heinämäki, J.; Kogermann, K. (2012). Insight into the solubility and dissolution behavior of piroxicam anhydrate and monohydrate forms. International Journal of Pharmaceutics, 431(1-2), 111–119.

Penkina, A.; Hakola, M.; **Paaver, U.**; Vuorinen, S.; Kirsimäe, K.; Kogermann, K.; Veski, P.; Yliruusi, J.; Repo, T.; Heinämäki, J. (2012). Solid-state properties of softwood lignin and cellulose isolated by a new acid precipitation method. International Journal of Biological Macromolecules, 51(5), 939–945.

Paaver, U.; Matto, V.; Raal, A. (2010). Total tannin content in distinct Quercus robur L. galls. Journal of Medicinal Plants Research, 4(8), 702–705.

Paaver, U.; Orav, A.; Arak, E.; Mäeorg, U.; Raal, A. (2008). Phytochemical analysis of the essential oil of Thymus serpyllum L. growing wild in Estonia. Natural Product Research, 22(2), 108–115.

Ivask, K.; Orav, A.; Kailas, T.; Raal, A.; Arak, E.; **Paaver, U.** (2005). Com–position of the essential oil from wild marjoram (Origanum vulgare L.ssp vulgare) cultivated in Estonia. Journal of Essential Oil Research, 17(4), 384–387.

Raal, A., **Paaver, U**.; Arak, E., Orav, A. (2004). Content and composition of the essential oil of Thymus serpyllum L. growing wild in Estonia. Medicina (Kaunas), 40(8), 795–800.

ELULOOKIRJELDUS

Nimi: Urve Paaver
Sünniaeg: 21. september, 1958
Kodakondsus: eesti
Aadress: TÜ Farmaatsia instituut
Nooruse 1, 50411, Tartu, Eesti
Telefon: +372 737 5282
E-mail: urve.paaver@ut.ee

Haridus:

1965–1976	Tartu V Keskkool
1976–1981	Tartu Riiklik Ülikool, Arstiteaduskond, proviisori õppekava, proviisor
2006–2006	Tartu Ülikool, magistri õppekava orgaanilise keemia erialal, MSc
2012–2015	Tartu Ülikool, Arstiteaduskond, doktorant-ekstern farmaatsia erialal

Teenistuskäik:

2011–...	Tartu Ülikool; Arstiteaduskond, farmaatsia instituut, farmatseutilise tehnoloogia vanemassistent
2007–2011	Tartu Ülikool, Arstiteaduskond, farmaatsia instituut, farmakognoosia ja farmaatsia organisatsiooni õppetool; farmakognoosia vanemassistent
2006–2007	Tartu Ülikool, Arstiteaduskond, farmaatsia instituut, Farmakognoosia ja farmaatsia organisatsiooni õppetool; teadur
2004–2006	Tartu Ülikool, Arstiteaduskond, farmaatsia instituut, farmakognoosia ja farmaatsia organisatsiooni õppetool; assistent
1988–2004	Tartu Ülikool, Arstiteaduskond, farmaatsia instituut, farmakognoosia ja farmaatsia organisatsiooni õppetool; assistent
1981–1988	Tartu Ülikool, Arstiteaduskond, farmaatsia instituut, farmakognoosia ja farmaatsia organisatsiooni õppetool; vaneminsener-botaanik

Peamised uurimisvaldkonnad:
Multifunktsionaalsete nanomeditsiiniliste süsteemide väljatöötamine ja kvaliteedi hindamine.

Tahkete raviainete füsikokeemilised omadused ja nende modifitseerimise võimalused.

Abiainete funktsionaalsusega seotud omaduste iseloomustamine farmatseutiliste ravimvormide valmistamiseks.

Rahvusvahelistes teadusajakirjades on ilmunud 10 publikatsiooni ja enam kui 60 konverentsiettekannet.

Publikatsioonid:

Heinämäki, J.; Halenius, A.; Paavo, M.; Alakurtti, S.; Pitkänen, P.; Pirttimaa, M.; **Paaver, U.**; Kirsimäe, K.; Kogermann, K.; Yliruusi, J. (2015). Suberin fatty acids isolated from outer birch bark improve moisture barrier properties of cellulose ether films intended for tablet coatings. International Journal of Pharmaceutics, 489, 91–99.

Paaver, U.; Heinämäki, J.; Laidmäe, I.; Lust, A.; Kozlova, J.; Sillaste, E.; Kirsimäe, K.; Veski, P.; Kogermann, K. (2015). Electrospun nanofibers as a potential controlled-release solid dispersion system for poorly water-soluble drugs. International Journal of Pharmaceutics, 479(1), 252–260.

Paaver, U.; Heinämäki, J.; Kassamakov, I.; Hæggström, E.; Ylitalo, T.; Nolvi, A.; Kozlova, J.; Laidmäe, I.; Kogermann, K.; Veski, P. (2014). Nanometer depth resolution in 3D topographic analysis of drug-loaded nanofibrous mats without sample preparation. International Journal of Pharmaceutics, 462(1–2), 29–37.

Paaver, U.; Tamm, I.; Laidmäe, I.; Lust, A.; Kirsimäe, K.; Veski, P.; Kogermann, K.; Heinämäki, J. (2014). Soluplus Graft Copolymer: Potential Novel Carrier Polymer in Electrospinning of Nanofibrous Drug Delivery Systems for Wound Therapy. BioMed Research International, 2014(ID 789765), 1–7.

Paaver, U.; Lust, A.; Mirza, S.; Rantanen, J.; Veski, P.; Heinämäki, J.; Kogermann, K. (2012). Insight into the solubility and dissolution behavior of piroxicam anhydrate and monohydrate forms. International Journal of Pharmaceutics, 431(1–2), 111–119.

Penkina, A.; Hakola, M.; **Paaver, U.**; Vuorinen, S.; Kirsimäe, K.; Kogermann, K.; Veski, P.; Yliruusi, J.; Repo, T.; Heinämäki, J. (2012). Solid-state properties of softwood lignin and cellulose isolated by a new acid precipitation method. International Journal of Biological Macromolecules, 51(5), 939–945.

Paaver, U.; Matto, V.; Raal, A. (2010). Total tannin content in distinct Quercus robur L. galls. Journal of Medicinal Plants Research, 4(8), 702–705.

Paaver, U.; Orav, A.; Arak, E.; Mäeorg, U.; Raal, A. (2008). Phytochemical analysis of the essential oil of Thymus serpyllum L. growing wild in Estonia. Natural Product Research, 22(2), 108–115.

Ivask, K.; Orav, A.; Kailas, T.; Raal, A.; Arak, E.; **Paaver, U.** (2005). Composition of the essential oil from wild marjoram (Origanum vulgare L.ssp vulgare) cultivated in Estonia. Journal of Essential Oil Research, 17(4), 384–387.

Raal, A., **Paaver, U**.; Arak, E., Orav, A. (2004). Content and composition of the essential oil of Thymus serpyllum L. growing wild in Estonia. Medicina (Kaunas), 40(8), 795–800.

DISSERTATIONES MEDICINAE UNIVERSITATIS TARTUENSIS

1. **Heidi-Ingrid Maaroos.** The natural course of gastric ulcer in connection with chronic gastritis and *Helicobacter pylori*. Tartu, 1991.
2. **Mihkel Zilmer.** Na-pump in normal and tumorous brain tissues: Structural, functional and tumorigenesis aspects. Tartu, 1991.
3. **Eero Vasar.** Role of cholecystokinin receptors in the regulation of behaviour and in the action of haloperidol and diazepam. Tartu, 1992.
4. **Tiina Talvik.** Hypoxic-ischaemic brain damage in neonates (clinical, biochemical and brain computed tomographical investigation). Tartu, 1992.
5. **Ants Peetsalu.** Vagotomy in duodenal ulcer disease: A study of gastric acidity, serum pepsinogen I, gastric mucosal histology and *Helicobacter pylori*. Tartu, 1992.
6. **Marika Mikelsaar.** Evaluation of the gastrointestinal microbial ecosystem in health and disease. Tartu, 1992.
7. **Hele Everaus.** Immuno-hormonal interactions in chronic lymphocytic leukaemia and multiple myeloma. Tartu, 1993.
8. **Ruth Mikelsaar.** Etiological factors of diseases in genetically consulted children and newborn screening: dissertation for the commencement of the degree of doctor of medical sciences. Tartu, 1993.
9. **Agu Tamm.** On metabolic action of intestinal microflora: clinical aspects. Tartu, 1993.
10. **Katrin Gross.** Multiple sclerosis in South-Estonia (epidemiological and computed tomographical investigations). Tartu, 1993.
11. **Oivi Uibo.** Childhood coeliac disease in Estonia: occurrence, screening, diagnosis and clinical characterization. Tartu, 1994.
12. **Viiu Tuulik.** The functional disorders of central nervous system of chemistry workers. Tartu, 1994.
13. **Margus Viigimaa.** Primary haemostasis, antiaggregative and anticoagulant treatment of acute myocardial infarction. Tartu, 1994.
14. **Rein Kolk.** Atrial versus ventricular pacing in patients with sick sinus syndrome. Tartu, 1994.
15. **Toomas Podar.** Incidence of childhood onset type 1 diabetes mellitus in Estonia. Tartu, 1994.
16. **Kiira Subi.** The laboratory surveillance of the acute respiratory viral infections in Estonia. Tartu, 1995.
17. **Irja Lutsar.** Infections of the central nervous system in children (epidemiologic, diagnostic and therapeutic aspects, long term outcome). Tartu, 1995.
18. **Aavo Lang.** The role of dopamine, 5-hydroxytryptamine, sigma and NMDA receptors in the action of antipsychotic drugs. Tartu, 1995.
19. **Andrus Arak.** Factors influencing the survival of patients after radical surgery for gastric cancer. Tartu, 1996.

20. **Tõnis Karki.** Quantitative composition of the human lactoflora and method for its examination. Tartu, 1996.
21. **Reet Mändar.** Vaginal microflora during pregnancy and its transmission to newborn. Tartu, 1996.
22. **Triin Remmel.** Primary biliary cirrhosis in Estonia: epidemiology, clinical characterization and prognostication of the course of the disease. Tartu, 1996.
23. **Toomas Kivastik.** Mechanisms of drug addiction: focus on positive reinforcing properties of morphine. Tartu, 1996.
24. **Paavo Pokk.** Stress due to sleep deprivation: focus on $GABA_A$ receptor-chloride ionophore complex. Tartu, 1996.
25. **Kristina Allikmets.** Renin system activity in essential hypertension. Associations with atherothrombogenic cardiovascular risk factors and with the efficacy of calcium antagonist treatment. Tartu, 1996.
26. **Triin Parik.** Oxidative stress in essential hypertension: Associations with metabolic disturbances and the effects of calcium antagonist treatment. Tartu, 1996.
27. **Svetlana Päi.** Factors promoting heterogeneity of the course of rheumatoid arthritis. Tartu, 1997.
28. **Maarike Sallo.** Studies on habitual physical activity and aerobic fitness in 4 to 10 years old children. Tartu, 1997.
29. **Paul Naaber.** *Clostridium difficile* infection and intestinal microbial ecology. Tartu, 1997.
30. **Rein Pähkla.** Studies in pinoline pharmacology. Tartu, 1997.
31. **Andrus Juhan Voitk.** Outpatient laparoscopic cholecystectomy. Tartu, 1997.
32. **Joel Starkopf.** Oxidative stress and ischaemia-reperfusion of the heart. Tartu, 1997.
33. **Janika Kõrv.** Incidence, case-fatality and outcome of stroke. Tartu, 1998.
34. **Ülla Linnamägi.** Changes in local cerebral blood flow and lipid peroxidation following lead exposure in experiment. Tartu, 1998.
35. **Ave Minajeva.** Sarcoplasmic reticulum function: comparison of atrial and ventricular myocardium. Tartu, 1998.
36. **Oleg Milenin.** Reconstruction of cervical part of esophagus by revascularised ileal autografts in dogs. A new complex multistage method. Tartu, 1998.
37. **Sergei Pakriev.** Prevalence of depression, harmful use of alcohol and alcohol dependence among rural population in Udmurtia. Tartu, 1998.
38. **Allen Kaasik.** Thyroid hormone control over β-adrenergic signalling system in rat atria. Tartu, 1998.
39. **Vallo Matto.** Pharmacological studies on anxiogenic and antiaggressive properties of antidepressants. Tartu, 1998.
40. **Maire Vasar.** Allergic diseases and bronchial hyperreactivity in Estonian children in relation to environmental influences. Tartu, 1998.
41. **Kaja Julge.** Humoral immune responses to allergens in early childhood. Tartu, 1998.

42. **Heli Grünberg.** The cardiovascular risk of Estonian schoolchildren. A cross-sectional study of 9-, 12- and 15-year-old children. Tartu, 1998.
43. **Epp Sepp.** Formation of intestinal microbial ecosystem in children. Tartu, 1998.
44. **Mai Ots.** Characteristics of the progression of human and experimental glomerulopathies. Tartu, 1998.
45. **Tiina Ristimäe.** Heart rate variability in patients with coronary artery disease. Tartu, 1998.
46. **Leho Kõiv.** Reaction of the sympatho-adrenal and hypothalamo-pituitary-adrenocortical system in the acute stage of head injury. Tartu, 1998.
47. **Bela Adojaan.** Immune and genetic factors of childhood onset IDDM in Estonia. An epidemiological study. Tartu, 1999.
48. **Jakov Shlik.** Psychophysiological effects of cholecystokinin in humans. Tartu, 1999.
49. **Kai Kisand.** Autoantibodies against dehydrogenases of α-ketoacids. Tartu, 1999.
50. **Toomas Marandi.** Drug treatment of depression in Estonia. Tartu, 1999.
51. **Ants Kask.** Behavioural studies on neuropeptide Y. Tartu, 1999.
52. **Ello-Rahel Karelson.** Modulation of adenylate cyclase activity in the rat hippocampus by neuropeptide galanin and its chimeric analogs. Tartu, 1999.
53. **Tanel Laisaar.** Treatment of pleural empyema — special reference to intrapleural therapy with streptokinase and surgical treatment modalities. Tartu, 1999.
54. **Eve Pihl.** Cardiovascular risk factors in middle-aged former athletes. Tartu, 1999.
55. **Katrin Õunap.** Phenylketonuria in Estonia: incidence, newborn screening, diagnosis, clinical characterization and genotype/phenotype correlation. Tartu, 1999.
56. **Siiri Kõljalg.** *Acinetobacter* – an important nosocomial pathogen. Tartu, 1999.
57. **Helle Karro.** Reproductive health and pregnancy outcome in Estonia: association with different factors. Tartu, 1999.
58. **Heili Varendi.** Behavioral effects observed in human newborns during exposure to naturally occurring odors. Tartu, 1999.
59. **Anneli Beilmann.** Epidemiology of epilepsy in children and adolescents in Estonia. Prevalence, incidence, and clinical characteristics. Tartu, 1999.
60. **Vallo Volke.** Pharmacological and biochemical studies on nitric oxide in the regulation of behaviour. Tartu, 1999.
61. **Pilvi Ilves.** Hypoxic-ischaemic encephalopathy in asphyxiated term infants. A prospective clinical, biochemical, ultrasonographical study. Tartu, 1999.
62. **Anti Kalda.** Oxygen-glucose deprivation-induced neuronal death and its pharmacological prevention in cerebellar granule cells. Tartu, 1999.
63. **Eve-Irene Lepist.** Oral peptide prodrugs – studies on stability and absorption. Tartu, 2000.

64. **Jana Kivastik.** Lung function in Estonian schoolchildren: relationship with anthropometric indices and respiratory symptomas, reference values for dynamic spirometry. Tartu, 2000.
65. **Karin Kull.** Inflammatory bowel disease: an immunogenetic study. Tartu, 2000.
66. **Kaire Innos.** Epidemiological resources in Estonia: data sources, their quality and feasibility of cohort studies. Tartu, 2000.
67. **Tamara Vorobjova.** Immune response to *Helicobacter pylori* and its association with dynamics of chronic gastritis and epithelial cell turnover in antrum and corpus. Tartu, 2001.
68. **Ruth Kalda.** Structure and outcome of family practice quality in the changing health care system of Estonia. Tartu, 2001.
69. **Annika Krüüner.** *Mycobacterium tuberculosis* – spread and drug resistance in Estonia. Tartu, 2001.
70. **Marlit Veldi.** Obstructive Sleep Apnoea: Computerized Endopharyngeal Myotonometry of the Soft Palate and Lingual Musculature. Tartu, 2001.
71. **Anneli Uusküla.** Epidemiology of sexually transmitted diseases in Estonia in 1990–2000. Tartu, 2001.
72. **Ade Kallas.** Characterization of antibodies to coagulation factor VIII. Tartu, 2002.
73. **Heidi Annuk.** Selection of medicinal plants and intestinal lactobacilli as antimicrobil components for functional foods. Tartu, 2002.
74. **Aet Lukmann**. Early rehabilitation of patients with ischaemic heart disease after surgical revascularization of the myocardium: assessment of health-related quality of life, cardiopulmonary reserve and oxidative stress. A clinical study. Tartu, 2002.
75. **Maigi Eisen.** Pathogenesis of Contact Dermatitis: participation of Oxidative Stress. A clinical – biochemical study. Tartu, 2002.
76. **Piret Hussar.** Histology of the post-traumatic bone repair in rats. Elaboration and use of a new standardized experimental model – bicortical perforation of tibia compared to internal fracture and resection osteotomy. Tartu, 2002.
77. **Tõnu Rätsep.** Aneurysmal subarachnoid haemorrhage: Noninvasive monitoring of cerebral haemodynamics. Tartu, 2002.
78. **Marju Herodes.** Quality of life of people with epilepsy in Estonia. Tartu, 2003.
79. **Katre Maasalu.** Changes in bone quality due to age and genetic disorders and their clinical expressions in Estonia. Tartu, 2003.
80. **Toomas Sillakivi.** Perforated peptic ulcer in Estonia: epidemiology, risk factors and relations with *Helicobacter pylori*. Tartu, 2003.
81. **Leena Puksa.** Late responses in motor nerve conduction studies. F and A waves in normal subjects and patients with neuropathies. Tartu, 2003.
82. **Krista Lõivukene**. *Helicobacter pylori* in gastric microbial ecology and its antimicrobial susceptibility pattern. Tartu, 2003.

83. **Helgi Kolk.** Dyspepsia and *Helicobacter pylori* infection: the diagnostic value of symptoms, treatment and follow-up of patients referred for upper gastrointestinal endoscopy by family physicians. Tartu, 2003.
84. **Helena Soomer.** Validation of identification and age estimation methods in forensic odontology. Tartu, 2003.
85. **Kersti Oselin.** Studies on the human MDR1, MRP1, and MRP2 ABC transporters: functional relevance of the genetic polymorphisms in the *MDR1* and *MRP1* gene. Tartu, 2003.
86. **Jaan Soplepmann.** Peptic ulcer haemorrhage in Estonia: epidemiology, prognostic factors, treatment and outcome. Tartu, 2003.
87. **Margot Peetsalu.** Long-term follow-up after vagotomy in duodenal ulcer disease: recurrent ulcer, changes in the function, morphology and *Helicobacter pylori* colonisation of the gastric mucosa. Tartu, 2003.
88. **Kersti Klaamas.** Humoral immune response to *Helicobacter pylori* a study of host-dependent and microbial factors. Tartu, 2003.
89. **Pille Taba.** Epidemiology of Parkinson's disease in Tartu, Estonia. Prevalence, incidence, clinical characteristics, and pharmacoepidemiology. Tartu, 2003.
90. **Alar Veraksitš**. Characterization of behavioural and biochemical phenotype of cholecystokinin-2 receptor deficient mice: changes in the function of the dopamine and endopioidergic system. Tartu, 2003.
91. **Ingrid Kalev.** CC-chemokine receptor 5 (CCR5) gene polymorphism in Estonians and in patients with Type I and Type II diabetes mellitus. Tartu, 2003.
92. **Lumme Kadaja.** Molecular approach to the regulation of mitochondrial function in oxidative muscle cells. Tartu, 2003.
93. **Aive Liigant**. Epidemiology of primary central nervous system tumours in Estonia from 1986 to 1996. Clinical characteristics, incidence, survival and prognostic factors. Tartu, 2004.
94. **Andres, Kulla.** Molecular characteristics of mesenchymal stroma in human astrocytic gliomas. Tartu, 2004.
95. **Mari Järvelaid.** Health damaging risk behaviours in adolescence. Tartu, 2004.
96. **Ülle Pechter.** Progression prevention strategies in chronic renal failure and hypertension. An experimental and clinical study. Tartu, 2004.
97. **Gunnar Tasa.** Polymorphic glutathione S-transferases – biology and role in modifying genetic susceptibility to senile cataract and primary open angle glaucoma. Tartu, 2004.
98. **Tuuli Käämbre.** Intracellular energetic unit: structural and functional aspects. Tartu, 2004.
99. **Vitali Vassiljev.** Influence of nitric oxide syntase inhibitors on the effects of ethanol after acute and chronic ethanol administration and withdrawal. Tartu, 2004.

100. **Aune Rehema.** Assessment of nonhaem ferrous iron and glutathione redox ratio as markers of pathogeneticity of oxidative stress in different clinical groups. Tartu, 2004.
101. **Evelin Seppet.** Interaction of mitochondria and ATPases in oxidative muscle cells in normal and pathological conditions. Tartu, 2004.
102. **Eduard Maron.** Serotonin function in panic disorder: from clinical experiments to brain imaging and genetics. Tartu, 2004.
103. **Marje Oona.** *Helicobacter pylori* infection in children: epidemiological and therapeutic aspects. Tartu, 2004.
104. **Kersti Kokk.** Regulation of active and passive molecular transport in the testis. Tartu, 2005.
105. **Vladimir Järv.** Cross-sectional imaging for pretreatment evaluation and follow-up of pelvic malignant tumours. Tartu, 2005.
106. **Andre Õun.** Epidemiology of adult epilepsy in Tartu, Estonia. Incidence, prevalence and medical treatment. Tartu, 2005.
107. **Piibe Muda.** Homocysteine and hypertension: associations between homocysteine and essential hypertension in treated and untreated hypertensive patients with and without coronary artery disease. Tartu, 2005.
108. **Külli Kingo.** The interleukin-10 family cytokines gene polymorphisms in plaque psoriasis. Tartu, 2005.
109. **Mati Merila.** Anatomy and clinical relevance of the glenohumeral joint capsule and ligaments. Tartu, 2005.
110. **Epp Songisepp**. Evaluation of technological and functional properties of the new probiotic *Lactobacillus fermentum* ME-3. Tartu, 2005.
111. **Tiia Ainla.** Acute myocardial infarction in Estonia: clinical characteristics, management and outcome. Tartu, 2005.
112. **Andres Sell.** Determining the minimum local anaesthetic requirements for hip replacement surgery under spinal anaesthesia – a study employing a spinal catheter. Tartu, 2005.
113. **Tiia Tamme.** Epidemiology of odontogenic tumours in Estonia. Pathogenesis and clinical behaviour of ameloblastoma. Tartu, 2005.
114. **Triine Annus**. Allergy in Estonian schoolchildren: time trends and characteristics. Tartu, 2005.
115. **Tiia Voor.** Microorganisms in infancy and development of allergy: comparison of Estonian and Swedish children. Tartu, 2005.
116. **Priit Kasenõmm.** Indicators for tonsillectomy in adults with recurrent tonsillitis – clinical, microbiological and pathomorphological investigations. Tartu, 2005.
117. **Eva Zusinaite.** Hepatitis C virus: genotype identification and interactions between viral proteases. Tartu, 2005.
118. **Piret Kõll.** Oral lactoflora in chronic periodontitis and periodontal health. Tartu, 2006.
119. **Tiina Stelmach.** Epidemiology of cerebral palsy and unfavourable neurodevelopmental outcome in child population of Tartu city and county, Estonia Prevalence, clinical features and risk factors. Tartu, 2006.

120. **Katrin Pudersell.** Tropane alkaloid production and riboflavine excretion in the field and tissue cultures of henbane (*Hyoscyamus niger* L.). Tartu, 2006.
121. **Külli Jaako.** Studies on the role of neurogenesis in brain plasticity. Tartu, 2006.
122. **Aare Märtson.** Lower limb lengthening: experimental studies of bone regeneration and long-term clinical results. Tartu, 2006.
123. **Heli Tähepõld.** Patient consultation in family medicine. Tartu, 2006.
124. **Stanislav Liskmann.** Peri-implant disease: pathogenesis, diagnosis and treatment in view of both inflammation and oxidative stress profiling. Tartu, 2006.
125. **Ruth Rudissaar.** Neuropharmacology of atypical antipsychotics and an animal model of psychosis. Tartu, 2006.
126. **Helena Andreson.** Diversity of *Helicobacter pylori* genotypes in Estonian patients with chronic inflammatory gastric diseases. Tartu, 2006.
127. **Katrin Pruus.** Mechanism of action of antidepressants: aspects of serotoninergic system and its interaction with glutamate. Tartu, 2006.
128. **Priit Põder.** Clinical and experimental investigation: relationship of ischaemia/reperfusion injury with oxidative stress in abdominal aortic aneurysm repair and in extracranial brain artery endarterectomy and possibilities of protection against ischaemia using a glutathione analogue in a rat model of global brain ischaemia. Tartu, 2006.
129. **Marika Tammaru.** Patient-reported outcome measurement in rheumatoid arthritis. Tartu, 2006.
130. **Tiia Reimand.** Down syndrome in Estonia. Tartu, 2006.
131. **Diva Eensoo.** Risk-taking in traffic and Markers of Risk-Taking Behaviour in Schoolchildren and Car Drivers. Tartu, 2007.
132. **Riina Vibo.** The third stroke registry in Tartu, Estonia from 2001 to 2003: incidence, case-fatality, risk factors and long-term outcome. Tartu, 2007.
133. **Chris Pruunsild.** Juvenile idiopathic arthritis in children in Estonia. Tartu, 2007.
134. **Eve Õiglane-Šlik.** Angelman and Prader-Willi syndromes in Estonia. Tartu, 2007.
135. **Kadri Haller.** Antibodies to follicle stimulating hormone. Significance in female infertility. Tartu, 2007.
136. **Pille Ööpik.** Management of depression in family medicine. Tartu, 2007.
137. **Jaak Kals.** Endothelial function and arterial stiffness in patients with atherosclerosis and in healthy subjects. Tartu, 2007.
138. **Priit Kampus.** Impact of inflammation, oxidative stress and age on arterial stiffness and carotid artery intima-media thickness. Tartu, 2007.
139. **Margus Punab.** Male fertility and its risk factors in Estonia. Tartu, 2007.
140. **Alar Toom**. Heterotopic ossification after total hip arthroplasty: clinical and pathogenetic investigation. Tartu, 2007.

141. **Lea Pehme.** Epidemiology of tuberculosis in Estonia 1991–2003 with special regard to extrapulmonary tuberculosis and delay in diagnosis of pulmonary tuberculosis. Tartu, 2007.
142. **Juri Karjagin.** The pharmacokinetics of metronidazole and meropenem in septic shock. Tartu, 2007.
143. **Inga Talvik.** Inflicted traumatic brain injury shaken baby syndrome in Estonia – epidemiology and outcome. Tartu, 2007.
144. **Tarvo Rajasalu.** Autoimmune diabetes: an immunological study of type 1 diabetes in humans and in a model of experimental diabetes (in RIP-B7.1 mice). Tartu, 2007.
145. **Inga Karu.** Ischaemia-reperfusion injury of the heart during coronary surgery: a clinical study investigating the effect of hyperoxia. Tartu, 2007.
146. **Peeter Padrik.** Renal cell carcinoma: Changes in natural history and treatment of metastatic disease. Tartu, 2007.
147. **Neve Vendt**. Iron deficiency and iron deficiency anaemia in infants aged 9 to 12 months in Estonia. Tartu, 2008.
148. **Lenne-Triin Heidmets.** The effects of neurotoxins on brain plasticity: focus on neural Cell Adhesion Molecule. Tartu, 2008.
149. **Paul Korrovits.** Asymptomatic inflammatory prostatitis: prevalence, etiological factors, diagnostic tools. Tartu, 2008.
150. **Annika Reintam.** Gastrointestinal failure in intensive care patients. Tartu, 2008.
151. **Kristiina Roots.** Cationic regulation of Na-pump in the normal, Alzheimer's and CCK_2 receptor-deficient brain. Tartu, 2008.
152. **Helen Puusepp.** The genetic causes of mental retardation in Estonia: fragile X syndrome and creatine transporter defect. Tartu, 2009.
153. **Kristiina Rull.** Human chorionic gonadotropin beta genes and recurrent miscarriage: expression and variation study. Tartu, 2009.
154. **Margus Eimre.** Organization of energy transfer and feedback regulation in oxidative muscle cells. Tartu, 2009.
155. **Maire Link.** Transcription factors FoxP3 and AIRE: autoantibody associations. Tartu, 2009.
156. **Kai Haldre.** Sexual health and behaviour of young women in Estonia. Tartu, 2009.
157. **Kaur Liivak.** Classical form of congenital adrenal hyperplasia due to 21-hydroxylase deficiency in Estonia: incidence, genotype and phenotype with special attention to short-term growth and 24-hour blood pressure. Tartu, 2009.
158. **Kersti Ehrlich.** Antioxidative glutathione analogues (UPF peptides) – molecular design, structure-activity relationships and testing the protective properties. Tartu, 2009.
159. **Anneli Rätsep.** Type 2 diabetes care in family medicine. Tartu, 2009.
160. **Silver Türk.** Etiopathogenetic aspects of chronic prostatitis: role of mycoplasmas, coryneform bacteria and oxidative stress. Tartu, 2009.

161. **Kaire Heilman.** Risk markers for cardiovascular disease and low bone mineral density in children with type 1 diabetes. Tartu, 2009.
162. **Kristi Rüütel.** HIV-epidemic in Estonia: injecting drug use and quality of life of people living with HIV. Tartu, 2009.
163. **Triin Eller.** Immune markers in major depression and in antidepressive treatment. Tartu, 2009.
164. **Siim Suutre.** The role of TGF-β isoforms and osteoprogenitor cells in the pathogenesis of heterotopic ossification. An experimental and clinical study of hip arthroplasty. Tartu, 2010.
165. **Kai Kliiman.** Highly drug-resistant tuberculosis in Estonia: Risk factors and predictors of poor treatment outcome. Tartu, 2010.
166. **Inga Villa.** Cardiovascular health-related nutrition, physical activity and fitness in Estonia. Tartu, 2010.
167. **Tõnis Org.** Molecular function of the first PHD finger domain of Autoimmune Regulator protein. Tartu, 2010.
168. **Tuuli Metsvaht.** Optimal antibacterial therapy of neonates at risk of early onset sepsis. Tartu, 2010.
169. **Jaanus Kahu.** Kidney transplantation: Studies on donor risk factors and mycophenolate mofetil. Tartu, 2010.
170. **Koit Reimand.** Autoimmunity in reproductive failure: A study on associated autoantibodies and autoantigens. Tartu, 2010.
171. **Mart Kull.** Impact of vitamin D and hypolactasia on bone mineral density: a population based study in Estonia. Tartu, 2010.
172. **Rael Laugesaar.** Stroke in children – epidemiology and risk factors. Tartu, 2010.
173. **Mark Braschinsky.** Epidemiology and quality of life issues of hereditary spastic paraplegia in Estonia and implemention of genetic analysis in everyday neurologic practice. Tartu, 2010.
174. **Kadri Suija.** Major depression in family medicine: associated factors, recurrence and possible intervention. Tartu, 2010.
175. **Jarno Habicht.** Health care utilisation in Estonia: socioeconomic determinants and financial burden of out-of-pocket payments. Tartu, 2010.
176. **Kristi Abram.** The prevalence and risk factors of rosacea. Subjective disease perception of rosacea patients. Tartu, 2010.
177. **Malle Kuum.** Mitochondrial and endoplasmic reticulum cation fluxes: Novel roles in cellular physiology. Tartu, 2010.
178. **Rita Teek.** The genetic causes of early onset hearing loss in Estonian children. Tartu, 2010.
179. **Daisy Volmer.** The development of community pharmacy services in Estonia – public and professional perceptions 1993–2006. Tartu, 2010.
180. **Jelena Lissitsina.** Cytogenetic causes in male infertility. Tartu, 2011.
181. **Delia Lepik.** Comparison of gunshot injuries caused from Tokarev, Makarov and Glock 19 pistols at different firing distances. Tartu, 2011.
182. **Ene-Renate Pähkla**. Factors related to the efficiency of treatment of advanced periodontitis. Tartu, 2011.

183. **Maarja Krass.** L-Arginine pathways and antidepressant action. Tartu, 2011.
184. **Taavi Lai.** Population health measures to support evidence-based health policy in Estonia. Tartu, 2011.
185. **Tiit Salum.** Similarity and difference of temperature-dependence of the brain sodium pump in normal, different neuropathological, and aberrant conditions and its possible reasons. Tartu, 2011.
186. **Tõnu Vooder**. Molecular differences and similarities between histological subtypes of non-small cell lung cancer. Tartu, 2011.
187. **Jelena Štšepetova.** The characterisation of intestinal lactic acid bacteria using bacteriological, biochemical and molecular approaches. Tartu, 2011.
188. **Radko Avi.** Natural polymorphisms and transmitted drug resistance in Estonian HIV-1 CRF06_cpx and its recombinant viruses. Tartu, 2011, 116 p.
189. **Edward Laane**. Multiparameter flow cytometry in haematological malignancies. Tartu, 2011, 152 p.
190. **Triin Jagomägi.** A study of the genetic etiology of nonsyndromic cleft lip and palate. Tartu, 2011, 158 p.
191. **Ivo Laidmäe.** Fibrin glue of fish (*Salmo salar*) origin: immunological study and development of new pharmaceutical preparation. Tartu, 2012, 150 p.
192. **Ülle Parm.** Early mucosal colonisation and its role in prediction of invasive infection in neonates at risk of early onset sepsis. Tartu, 2012, 168 p.
193. **Kaupo Teesalu.** Autoantibodies against desmin and transglutaminase 2 in celiac disease: diagnostic and functional significance. Tartu, 2012, 142 p.
194. **Maksim Zagura**. Biochemical, functional and structural profiling of arterial damage in atherosclerosis. Tartu, 2012, 162 p.
195. **Vivian Kont.** Autoimmune regulator: characterization of thymic gene regulation and promoter methylation. Tartu, 2012, 134 p.
196. **Pirje Hütt.** Functional properties, persistence, safety and efficacy of potential probiotic lactobacilli. Tartu, 2012, 246 p.
197. **Innar Tõru.** Serotonergic modulation of CCK-4- induced panic. Tartu, 2012, 132 p.
198. **Sigrid Vorobjov.** Drug use, related risk behaviour and harm reduction interventions utilization among injecting drug users in Estonia: implications for drug policy. Tartu, 2012, 120 p.
199. **Martin Serg.** Therapeutic aspects of central haemodynamics, arterial stiffness and oxidative stress in hypertension. Tartu, 2012, 156 p.
200. **Jaanika Kumm.** Molecular markers of articular tissues in early knee osteoarthritis: a population-based longitudinal study in middle-aged subjects. Tartu, 2012, 159 p.
201. **Kertu Rünkorg.** Functional changes of dopamine, endopioid and endocannabinoid systems in CCK2 receptor deficient mice. Tartu, 2012, 125 p.
202. **Mai Blöndal.** Changes in the baseline characteristics, management and outcomes of acute myocardial infarction in Estonia. Tartu, 2012, 127 p.

203. **Jana Lass.** Epidemiological and clinical aspects of medicines use in children in Estonia. Tartu, 2012, 170 p.
204. **Kai Truusalu.** Probiotic lactobacilli in experimental persistent *Salmonella* infection. Tartu, 2013, 139 p.
205. **Oksana Jagur.** Temporomandibular joint diagnostic imaging in relation to pain and bone characteristics. Long-term results of arthroscopic treatment. Tartu, 2013, 126 p.
206. **Katrin Sikk.** Manganese-ephedrone intoxication – pathogenesis of neurological damage and clinical symptomatology. Tartu, 2013, 125 p.
207. **Kai Blöndal.** Tuberculosis in Estonia with special emphasis on drug-resistant tuberculosis: Notification rate, disease recurrence and mortality. Tartu, 2013, 151 p.
208. **Marju Puurand.** Oxidative phosphorylation in different diseases of gastric mucosa. Tartu, 2013, 123 p.
209. **Aili Tagoma.** Immune activation in female infertility: Significance of autoantibodies and inflammatory mediators. Tartu, 2013, 135 p.
210. **Liis Sabre.** Epidemiology of traumatic spinal cord injury in Estonia. Brain activation in the acute phase of traumatic spinal cord injury. Tartu, 2013, 135 p.
211. **Merit Lamp.** Genetic susceptibility factors in endometriosis. Tartu, 2013, 125 p.
212. **Erik Salum.** Beneficial effects of vitamin D and angiotensin II receptor blocker on arterial damage. Tartu, 2013, 167 p.
213. **Maire Karelson.** Vitiligo: clinical aspects, quality of life and the role of melanocortin system in pathogenesis. Tartu, 2013, 153 p.
214. **Kuldar Kaljurand.** Prevalence of exfoliation syndrome in Estonia and its clinical significance. Tartu, 2013, 113 p.
215. **Raido Paasma.** Clinical study of methanol poisoning: handling large outbreaks, treatment with antidotes, and long-term outcomes. Tartu, 2013, 96 p.
216. **Anne Kleinberg.** Major depression in Estonia: prevalence, associated factors, and use of health services. Tartu, 2013, 129 p.
217. **Triin Eglit.** Obesity, impaired glucose regulation, metabolic syndrome and their associations with high-molecular-weight adiponectin levels. Tartu, 2014, 115 p.
218. **Kristo Ausmees.** Reproductive function in middle-aged males: Associations with prostate, lifestyle and couple infertility status. Tartu, 2014, 125 p.
219. **Kristi Huik.** The influence of host genetic factors on the susceptibility to HIV and HCV infections among intravenous drug users. Tartu, 2014, 144 p.
220. **Liina Tserel.** Epigenetic profiles of monocytes, monocyte-derived macrophages and dendritic cells. Tartu, 2014, 143 p.
221. **Irina Kerna.** The contribution of *ADAM12* and *CILP* genes to the development of knee osteoarthritis. Tartu, 2014, 152 p.

222. **Ingrit Liiv.** Autoimmune regulator protein interaction with DNA-dependent protein kinase and its role in apoptosis. Tartu, 2014, 143 p.
223. **Liivi Maddison.** Tissue perfusion and metabolism during intra-abdominal hypertension. Tartu, 2014, 103 p.
224. **Krista Ress.** Childhood coeliac disease in Estonia, prevalence in atopic dermatitis and immunological characterisation of coexistence. Tartu, 2014, 124 p.
225. **Kai Muru.** Prenatal screening strategies, long-term outcome of children with marked changes in maternal screening tests and the most common syndromic heart anomalies in Estonia. Tartu, 2014, 189 p.
226. **Kaja Rahu.** Morbidity and mortality among Baltic Chernobyl cleanup workers: a register-based cohort study. Tartu, 2014, 155 p.
227. **Klari Noormets.** The development of diabetes mellitus, fertility and energy metabolism disturbances in a Wfs1-deficient mouse model of Wolfram syndrome. Tartu, 2014, 132 p.
228. **Liis Toome.** Very low gestational age infants in Estonia. Tartu, 2014, 183 p.
229. **Ceith Nikkolo.** Impact of different mesh parameters on chronic pain and foreign body feeling after open inguinal hernia repair. Tartu, 2014, 132 p.
230. **Vadim Brjalin.** Chronic hepatitis C: predictors of treatment response in Estonian patients. Tartu, 2014, 122 p.
231. **Vahur Metsna.** Anterior knee pain in patients following total knee arthroplasty: the prevalence, correlation with patellar cartilage impairment and aspects of patellofemoral congruence. Tartu, 2014, 130 p.
232. **Marju Kase.** Glioblastoma multiforme: possibilities to improve treatment efficacy. Tartu, 2015, 137 p.
233. **Riina Runnel.** Oral health among elementary school children and the effects of polyol candies on the prevention of dental caries. Tartu, 2015, 112 p.
234. **Made Laanpere**. Factors influencing women's sexual health and reproductive choices in Estonia. Tartu, 2015, 176 p.
235. **Andres Lust.** Water mediated solid state transformations of a polymorphic drug – effect on pharmaceutical product performance. Tartu, 2015, 134 p.
236. **Anna Klugman.** Functionality related characterization of pretreated wood lignin, cellulose and polyvinylpyrrolidone for pharmaceutical applications. Tartu, 2015, 156 p.
237. **Triin Laisk-Podar**. Genetic variation as a modulator of susceptibility to female infertility and a source for potential biomarkers. Tartu, 2015, 155 p.
238. **Mailis Tõnisson.** Clinical picture and biochemical changes in blood in children with acute alcohol intoxication. Tartu, 2015, 100 p.
239. **Kadri Tamme**. High volume haemodiafiltration in treatment of severe sepsis – impact on pharmacokinetics of antibiotics and inflammatory response. Tartu, 2015, 133 p.

240. **Kai Part.** Sexual health of young people in Estonia in a social context: the role of school-based sexuality education and youth-friendly counseling services. Tartu, 2015, 203 p.